Progress in Quantum Electronics 87 (2023) 100451

Contents lists available at ScienceDirect

Progress in Quantum Electronics

journal homepage: www.elsevier.com/locate/pqe

Review

Edge emitting mode-locked quantum dot lasers

Amit Yadav [a,*], Nikolai B. Chichkov [a], Eugene A. Avrutin [b], Andrei Gorodetsky [c], Edik U. Rafailov [a]

[a] Aston Institute of Photonic Technologies (AIPT), Aston University, Birmingham, UK
[b] School of Physics, Engineering and Technology, University of York, Heslington, York, UK
[c] School of Physics and Astronomy, University of Birmingham, Birmingham, UK

ARTICLE INFO

Keywords:
Quantum dot
Mode-locking
Ultrafast lasers
Saturable absorber
Tapered lasers
Curved waveguide
Nonlinear optics
MOPA system
Bistability
Wavelength tuning

ABSTRACT

Edge-emitting mode-locked quantum-dot (QD) lasers are compact, highly efficient sources for the generation of picosecond and femtosecond pulses and/or broad frequency combs. They provide direct electrical control and footprints down to few millimeters. Their broad gain bandwidths (up to 50 nm for ground to ground state transitions as discussed below, with potential for increase to more than >200 nm by overlapping ground and excited state band transitions) allow for wavelength-tuning and generation of pico- and femtosecond laser pulses over a broad wavelength range. In the last two decades, mode-locked QD laser have become promising tools for low-power applications in ultrafast photonics.

In this article, we review the development and the state-of-the-art of edge-emitting mode-locked QD lasers. We start with a brief introduction on QD active media and their uses in lasers, amplifiers, and saturable absorbers. We further discuss the basic principles of mode-locking in QD lasers, including theory of nonlinear phenomena in QD waveguides, ultrafast carrier dynamics, and mode-locking methods. Different types of mode-locked QD laser systems, such as monolithic one- and two-section devices, external-cavity setups, two-wavelength operation, and master-oscillator power-amplifier systems, are discussed and compared. After presenting the recent trends and results in the field of mode-locked QD lasers, we briefly discuss the application areas.

1. Introduction

Pulsed semiconductor lasers are indispensable tools for modern high-speed opto-electronics, telecommunications, and ultrafast photonics. During the recent three decades, significant research efforts have been invested in particular into the development of mode-locked semiconductor lasers. The goal was the demonstration of compact, highly-efficient devices with pulse durations in the picosecond to sub-picosecond range and repetition rates of tens to hundreds of GHz, possibly even the (sub)terahertz range. These lasers would be able to address the requirements of many relatively low-power, femtosecond laser applications in biophotonics, metrology, and opto-electronics, potentially replacing more expensive and complex femtosecond solid-state and fiber laser counterparts. The multi-GHz-repetition rates would allow for speed improvements in ultrafast laser applications, including higher communication data-rates, comb generation, and high-throughput material processing.

Semiconductor laser diodes have been of interest for generating ultrashort optical pulses ever since their inception. In late 1970's and 80's nanosecond [1], picosecond [2] and sub-picosecond pulses from cw double heterostructure semiconductor diode lasers were reported. In earlier papers such as [2], mode-locking of stripe geometry double heterostructure semiconductor lasers was

* Corresponding author.
E-mail address: a.yadav1@aston.ac.uk (A. Yadav).

https://doi.org/10.1016/j.pquantelec.2022.100451

Available online 5 January 2023

primarily achieved by active mode-locking i.e. gain modulation by injection current modulation. Later on, with the advancement of semiconductor fabrication technology, proton bombarded saturable absorber sections were introduced on one of the facet of the diodes and picosecond pulses have been reported [3]. This was followed with the picosecond [4–6] and sub-picosecond [3] pulses by passive mode-locking of double heterostructure buried waveguide diodes. Picosecond and sub-picosecond pulses by hybrid modelocking have also been reported for double heterostructures laser diodes [7,8]. All this work was however restricted to external cavity designs with typical repetition rates of the order of single GHz.

In the early 90s, active and passive mode-locking of edge-emitting quantum-well (QW) lasers was demonstrated by several groups [8–13]. Delfyett et al. [13] were able to obtain output pulse durations as short as 207 fs, using an external-cavity setup with saturable absorber mirror, active laser current modulation, and dispersion compensation. Several groups have since achieved similar pulse durations with passively mode-locked two-section edge-emitters, combining gain section and saturable absorber on a single chip [14–16]. However, in terms of size and number of components, external-cavity semiconductor laser setups are not dissimilar to their solid-state counterparts, offering relatively few benefits.

First successful realization of passive ML (at about 100 GHz), in monolithic Quantum Well mode-locked lasers was reported in 1989–1990 [17,18]; through subsequent decades, the repetition rate range covered by monolithic passively, actively and hybridly mode locked QW lasers was successfully extended both downwards, towards units of GHz, and upwards, towards hundreds of GHz, by engineering cavity lengths and in the latter case employing harmonic ML techniques (see [19] for an overview).

However both theoretical analysis and practical experience show that mode-locking in two-section QW devices is highly sensitive to fabrication quality and can only be obtained in a relatively narrow range of operation parameters. This makes the development of mode-locked edge-emitting QW lasers challenging and impeded the commercialization of these devices.

Room-temperature operation of quantum-dot (QD) lasers was first demonstrated in the mid-90s. The ultrafast carrier dynamics and strong carrier confinement in QD lasers were quickly identified as highly beneficial for ultrafast laser applications. This led to rapid progress in the field of mode-locked semiconductor lasers and to the development of novel QD laser devices. Mode-locking of monolithic, two-section QD edge-emitters was first demonstrated in 2001 [20], quickly followed by the realization of compact, highly efficient femtosecond QD lasers [21–24].

In this article, we discuss the physical properties of QDs, explaining their benefits for mode-locking and femtosecond pulse generation. We present the fundamentals of mode-locking in edge-emitting QD lasers, including the influence of ultrafast carrier dynamics on saturable absorption, gain, and self-phase-modulation. We review theoretical models for the nonlinear pulse dynamics in mode-locked QD lasers, highlighting main theoretical predictions and laser design guidelines that can be derived. An overview of experimental results and performance of mode-locked edge-emitting QD lasers is then provided. Finally, we discuss applications of mode-locked QD lasers and give an outlook for future research.

2. Quantum-dots for ultrafast lasers

QD structures are clusters of semiconductor material with dimensions of a few tens of nanometers, commensurate with the de-Broglie wavelength of charge carriers in semiconductors. They provide ultrafast carrier dynamics with sub-picosecond relaxation times and, through size and composition dispersion, broad optical gain bandwidths.

These properties make them highly promising for the development of ultrafast laser devices and amplification of ultrashort pulses. In this section, we introduce the role of carrier confinement, fabrication techniques, and the carrier energy spectrum of QD materials. We discuss the optical properties most important for ultrashort pulse generation and provide a comparison between QDs and QWs.

2.1. QD lasers

2.1.1. Carrier confinement and density of states

Semiconductor lasers have advanced dramatically since lasing was first demonstrated in 1962 [25–29]. These advancements have been strongly related to improvements in fabrication techniques and the idea of carrier confinement. Early semiconductor lasers used a forward biased p–n junction as optical gain medium and suffered from inherent high electrical and optical losses, along with limited lifetime at room-temperature due to very high threshold currents. In 1963 Kromer et al. [30] and Alferov et al. [29] proposed the idea of carrier confinement using double heterostructures (DH). The DH structures consisted of a thin narrow-bandgap active layer surrounded by two cladding layers with a broader bandgap, resulting in carrier and optical mode confinement in one dimension. Soon after in 1969, the first pulsed lasers based on AlGaAs/GaAs DH were demonstrated [31–33], followed by the room temperature, continuous-wave (cw) operation of AlGaAs/GaAs lasers [34,35]. These DH lasers exhibited significantly lower threshold current densities than p–n junction (or homojunction) lasers and ushered in the era of compact laser sources that are now an integral part of modern society.

The concept of DHs has been further exploited to increase carrier confinement in one or more spatial dimensions. Confinement of carriers to quantizing dimensions comparable to their de-Broglie wavelength gives rise to new quantum mechanical effects and has profound influence on the optical and electronic characteristics of semiconductor photonic devices, including lasers. Such confinement is achieved by utilizing low-dimension semiconductor structures. A DH with the central layer of a quantizing thickness (of a few tens of nanometers or thinner) effectively confines the carriers in one (transverse) dimension. This leads to quantization of electron/hole energy states associated with transverse movement, as governed by the quantum treatment of particles in a potential well problem. Such structures are known as quantum wells (QWs). The process of quantization of states modifies the density of states

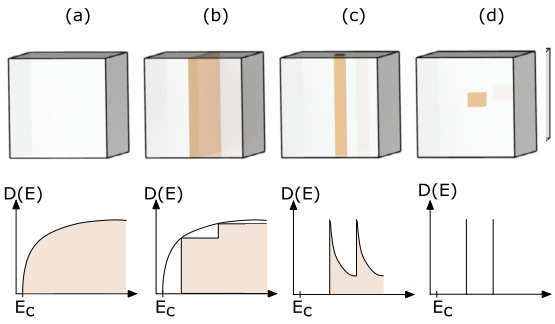

Fig. 1. Illustration of carrier confinement and density of states: (a) bulk semiconductor, (b) quantum well, (c) quantum wire, (d) quantum dot.

(DoS) of the active region in the confined spatial dimension, effectively reducing it and resulting in lower threshold current densities for population inversion and lasing. First report of state quantization and carrier confinement was made in 1974 by Dingle et al. [36]. Arakawa et al. [37] theoretically analysed the carrier confinement and state quantization in multiple dimensions, predicting further significant modifications in the DoS and lower threshold current densities. Carrier confinement in two dimensions is achieved by the 1D structures known as quantum wires (QWRs). At present, QWRs are not widely used in semiconductor photonics, partly due to the absence of efficient growth techniques (e.g. self-assembly) allowing for their fabrication with sufficiently large densities. The self-assembled structures closest to QWRs in their properties are Quantum Dashes (QDHs) - elongated nanostructures with quantization in two dimensions as in QWRs, but irregularly shaped, with strong fluctuations of transverse size and composition which mean that QDHs have a degree of three-dimensional carrier confinement. Further confinement of carriers in all three dimensions is made possible by true zero-dimension semiconductor structures — the quantum dots (QDs). QDs of the type used in active photonic devices are nanostructures of narrow-bandgap semiconductor material, with all three dimensions in the quantization range (1 nm to few 10 nm) as discussed below, buried in a host semiconductor material with a broader bandgap.

Fig. 1 shows the effect of decreasing dimensionality and increasing confinement on the DoS, as compared to the conduction band of a bulk material. It can be seen that as the free movement of carriers is spatially constrained in 1D, i.e. in the QW structure, the DoS acquires a step-like structure, with each new quantization sub-band adding a constant step contribution to the DoS, present at carrier energies greater than the quantization level (sub-band edge). Since the quantization level energies are proportional to the square of the level number, the overall DoS profile resembles a discretized version of the square root curve seen for bulk materials (if the QW thickness were to be increased, the DoS would asymptotically approach the bulk-like square root profile). The 2D confinement in QWRs results in sharp maxima in the DoS at the size quantization levels; however due to unconfined motion along the wire, the DoS is still continuous. For a single QD (or for an idealized ensemble of exactly identical uncoupled dots), the carrier confinement in all three dimensions leads to a DoS profile in the form of a discrete set of delta functions at quantization level energies [38]. However, in practice the dispersion, or wide fluctuations, of size, shape, chemical composition, and mutual location of QDs ensure an approximately Gaussian-like distribution of the DoS in a large enough ensemble of realistic dots, which results in inhomogeneous broadening [39] of optical transitions in QD photonic devices, including lasers and optical amplifiers.

2.1.2. Materials and fabrication

The material systems of III–V and II–VI constituent groups are of greatest interest for ultrafast QD lasers. These material systems together provide laser emission in the wavelength range of 0.5 μm to 1.9 μm. QD lasers based on III-V material system have shown remarkable performance over the last two decades [22]. These III–V QDs are epitaxially grown by the Stranski–Krastanov growth method on GaAs and InP substrates using standard MBE or MOCVD techniques [39,40].

It is an efficient and reproducible way of in-situ QD formation across the plane in a single step. The Stranski–Krastanov growth method allows for the spontaneous synthesis of three dimensional nanostructures during strained layer hetero-epitaxial growth. In this epitaxial process, a thin film of intended material is grown in the usual layer by layer fashion on a semiconductor substrate until a certain critical thickness is reached. Beyond this critical thickness the planar growth of the film stops and due to strain relaxation three-dimensional islands of variable size across the plane begin to form spontaneously and thus self-assembled. These three-dimensional islands become the self-organized QDs. The QDs are formed over a thin continuous film of the same semiconductor material, called the wetting layer (WL). The thickness of the WL is comparable to that of a thin QW and it is assumed to have the associated properties. The most critical requirement for QD formation by Stranski–Krastanov method is the lattice constant difference between the substrate and the material to be deposited. It requires that the deposited material has a larger lattice constant than the substrate so that build-up of strain with each monolayer leads to the formation of these islands. This condition is well satisfied for the InAs (lattice constant = 6.06 Å) QDs on GaAs (lattice constant = 5.64 Å) and on InP (lattice constant = 5.87 Å) semiconductor substrates. Furthermore, the host material can be further grown epitaxially on top of the QDs without causing any defects.

Somewhat different, though fundamentally similar, is a structure known as the dots-in-the-well [DWELL]. In such a design, rather than being positioned on top of a thin Quantum Well, each layer of QDs resides inside a thicker one, with the thickness of a well exceeding the height of the dots [41]. The as-grown QDs have a pyramidal shape, typically ∼5 nm tall and 15 nm to 20 nm at the base of the island [42]. After regrowth, the dot shape may be modified to something closer to a truncated pyramid. The distribution

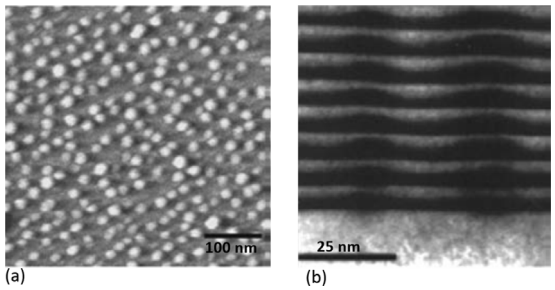

Fig. 2. SEM-image of quantum dots: (a) QD distribution across growth plane, (b) cross-section of QD layer stack. *Source:* Adapted with permission. [22] 2007, Springer Nature.

Table 1
QD semiconductor materials and corresponding laser wavelength ranges.

Materials	Wavelength range (nm)	References
(In, Al) GaN	370–600, 630	[44–46]
InGaAs/GaAs	1000–1550	[22]
InGaAs/InAs	1400–1900	[22]

of QDs across the growth plane is random and their density is relatively sparse (see Fig. 2(a)), with typical values in the range of 10^9 cm^{-2} to 10^{12} cm^{-2} [42]. A single QD layer with sparse QD distribution is unlikely to deliver the modal gain (the product of the material gain and the optical confinement factor) necessary for an optimal performance of a laser. To improve the modal gain in QD lasers, multiple stacks/layers of QDs can be grown. It has been demonstrated that multi-stacking of QD layers does not increase the internal optical loss and hence improves the net modal gain [43]. A cross-section of such a device is shown in Fig. 2(b). In the figure, the InGaAs QDs (thick dark regions) are embedded between the higher refractive index and higher bandgap energy layers of GaAs (light grey area around the dots and at the bottom). Compared to a single dot layer, this arrangement increases the modal gain by a factor only slightly smaller than the number of layers in the stack.

The emission wavelength of QD lasers is determined but the choice of semiconductor material and the size and shape of the QDs. The bandgap of the semiconductor material coarsely determines the emission wavelength of the laser, while the size, shape, and distribution of QDs can be used to tune the laser wavelength and gain bandwidth. Commonly used QD semiconductor materials their associated emission wavelength ranges are presented in the Table 1.

2.1.3. Energy level structure in QD

The energy band structure of the semiconductor is key to its optical properties, and hence to the properties of photonic devices fabricated from this semiconductor. Most fundamentally, it is well known that the emission wavelength in a semiconductor light emitter is coarsely controlled by the bandgap — the energy gap between the conduction and valence bands, determined, in a bulk material, solely by the composition of the material. The bandgap determines the fundamental absorption edge. Size quantization begins to affect the optical transitions as geometrical constraints are introduced in the form of low dimension structures i.e. QWs, QWR (or QDH) and QDs. In the case of QWs, QWRs, and QDHs, the (quasi-)continuous energy bands are still present (with the DoS modified by the sub-band structure as in Fig. 1), but the fundamental absorption edge, and hence the operating frequency of an emitter, is increased approximately by the sum of the first quantization levels of electrons and holes. In the case of QDs, due to complete size quantization as discussed above, the quasi-continuous energy bands, as seen in bulk semiconductors and QWs, collapse to discrete energy levels very similar to atomic levels.

It is thus imperative to understand the nature of the carrier energy spectrum of QDs to gain a thorough understanding of their properties and to fully exploit their potential. In 1986 Asada et al. presented a theoretical analysis of gain and threshold current for lasers with QDs as gain material. They predicted significant improvements in threshold current and gain for quantum box (QD) lasers [47]. The energy spectrum structure of InAs/GaAs based Stranski–Krastanov grown self-assembled QDs has been extensively studied both theoretically [48–56] and experimentally [57–65]. These studies demonstrated that both electrons and holes have two or more energy states [57,59]. The lowest of these states (counting the electron energy upwards and the hole energy downwards from the edge of the corresponding band in the bulk material) is referred to as the *ground state* (GS) and the others, as *excited states* (ES).

Due to the hole effective mass in III–V semiconductors being relatively large (about an order of magnitude greater than the electron mass), there are typically a large number of closely spaced hole states. *Electron* states, which are fewer and more broadly spaced, have a greater effect on the shape of optical transition (hence absorption and gain) spectra. Typically QDs present a ground electron state and 1 to 3 excited states, which are numbered as first excited state, second, and so on with increasing energy difference from the ground state.

Excited states with higher numbers have an increasingly complex state symmetry, which leads to a higher number of very closely spaced states, enhancing the optical transitions involving the excited levels [66]. Theoretical studies have shown a good overlap

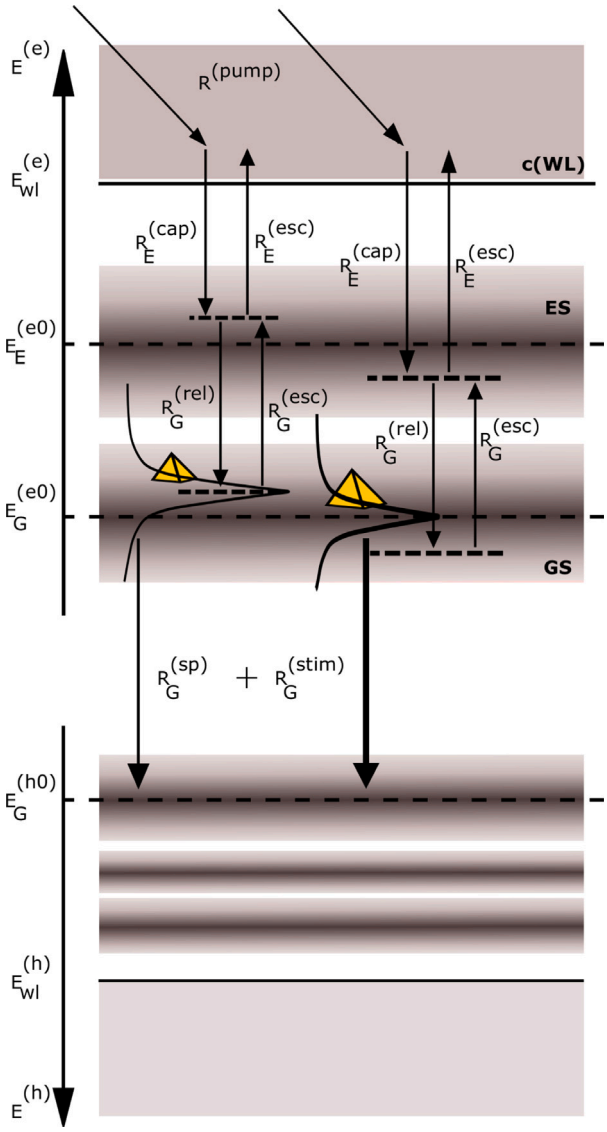

Fig. 3. Illustration of energy levels in QDs. *Source:* Adapted with permission. [42] 2011, WILEY-VCH Verlag & Co. KGaA.

between the hole and electron wave functions for the same state number [67,68]. Later, the existence of ground electron to excited hole level transitions was also identified [69].

Optical transitions between the first excited electron and hole states have been reported for mode-locked QD lasers [70], while under CW operation the ground state electron to (mainly) ground state hole transition is dominant.

A simple schematic of the energy structure of Stranski–Krastanov grown self-assembled QD is shown in Fig. 3. The discrete electron energy states, which lie below the conduction band of the reservoir (the WL for dot-on-wetting-layer structures or the QW containing the QDs in the case of a DWELL one), are identified as ground and[first] excited states in the order of increasing energy. This energy level structure is crucial for the understanding of carrier dynamics in QDs. While radiative transitions from the ground electron state are expected to be the most important due to the higher occupation factor, emission from the first excited state has also been demonstrated, meaning that the excited state, as well as the ground state, may have substantial carrier occupancy. To analyse this occupancy (probability function), the kinetics of nonradiative transitions between levels must be studied. Typically, an electron is first captured from the reservoir onto an excited state and then relaxes to the ground state. These transitions occur on sub-picosecond to picosecond time scales, which depend critically on the density of reservoir carriers N_R. At low N_R, when the electron capture and subsequent relaxation onto the ground level are both mediated by phonon emission, the characteristic time of the former process is ∼1ps and of the latter, ∼10 ps due to what is known as the phonon bottleneck. In contrast, at high N_R,

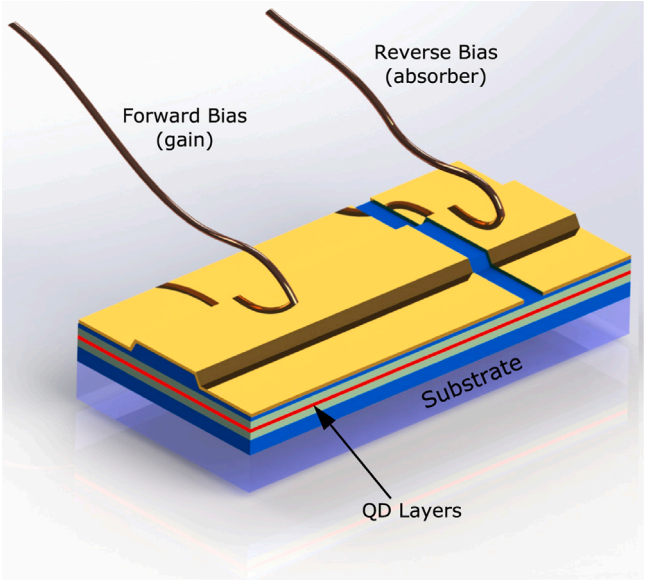

Fig. 4. Illustration of a typical two-section QD edge emitting laser. The longer section is for gain and the shorter section is the absorber.

when the relaxation of the electron from excited to ground level happens mainly by Auger type processes involving electrons in the WL, the relaxation time is reduced to a value of the order of 100 fs and becomes substantially shorter than the capture time which stays ∼1ps. At finite temperatures, the capture and relaxation processes are partly offset by the opposite processes of excitation from ground to excited level and escape from the excited level into the reservoir, which are characterized by longer kinetic times, so that at steady state and at high enough (particularly room) temperature, the energy distribution of electrons in an ensemble of QDs is close to equilibrium. These transitions and time scales critically influence the properties and parameters of a mode-locked QD laser as discussed below.

2.1.4. Edge-emitting QD lasers

Lasing action from edge emitting QD laser was first reported in 1994 by Kirstaedter et al. [71]. The strained self-organized InGaAs QDs in the shallow stripe mesa laser were grown on GaAs waveguide layer using MBE. Typically, [71] the edge emitting QD diode lasers are bottom-up epitaxially grown multi-layer structures, with designs similar to Kirstaedter et al. [71] and QW counterparts. The layer structure of a QD (or QW) edge emitter consists of n- and p-doped current spreading and cladding layers. Sandwiched between the n- and p-doped cladding layers is the waveguide core which contains the optical gain medium composed of multiple QD layers. The QD layers occupy only a small fraction of waveguide core, with total layer thicknesses in the order of 100 nm or less. All layers are epitaxially grown on top of each other either by MBE or MOCVD. Finally metal contacts for current conduction are deposited on the top and bottom layer.

A ridge waveguide is etched on the top of the layer structure to achieve strong lateral confinement of laser modes. In the transverse direction, the lasers modes are confined by the refractive index step between the waveguide region and cladding layers. The laser resonator is formed by the facets of the device, one of which, the output facet, typically has an anti-reflection (AR) coating whereas the other may have either a high-reflection (HR) coating in a monolithic design or an AR coating for an external cavity setup. In either case the length of the laser chip itself typically varies from few hundred micrometers to few millimeters.

For an ultrafast QD laser, a multisection/multicontact design is usually employed. To achieve this, electrically isolating grooves are etched through the top contact and, typically, a few μm into the waveguide to form two or more electrically isolated sections to be used as gain section(s) (forward biased) and saturable absorber(s) (reverse biased) as shown in Fig. 4. In the simplest and most common design, the edge-emitter consists of only two-sections, one for the laser gain and one for the saturable absorber. Additionally, the output gain section(s) can be laterally flared/tapered to improve the output power and reduce nonlinearity during mode-locked operation [24,72]

While most ultrafast QD lasers do employ two-section structures, single section devices have also been shown to generate stable, synchronized multimode output (frequency comb generation or self-mode-locking). The nature of modal interaction and dispersion can lead to the phase relations between the synchronized modes in the comb generated by such devices such that the temporal profile of this output is not in the form of short pulses, particularly in relatively long lasers; however sub-picosecond pulses have been observed in shorter resonators either directly or, more reliably, with the aid of external chirp compensators [73]

Table 2
Comparison of QD and QW properties for mode-locking.

	Quantum-dots	Quantum-wells
Bandwidth (nm)	up to 200	50–150
Absorber recovery time (ps)	0.7	>4
Threshold current (A/cm^2)	~20	~40
Saturation fluence (μJ/cm^2)	1.7	~10

2.2. Optical properties

2.2.1. Quantum-dots vs quantum-wells

The most important QD active medium properties for the design of passively mode-locked lasers are the gain bandwidth, the recovery time of saturable absorption, and the saturation fluence of the absorber section. In addition, as with all semiconductor lasers, a lower threshold current is a bonus. Broader gain bandwidths prevent gain narrowing effects during amplification of ultrashort pulses and enable the generation of shorter pulses from mode-locked lasers. Interestingly, simulations of mode-locked QD lasers show that the broader gain spectra help to achieve somewhat shorter pulses even when (as is usually the case in semiconductor edge emitters) the duration of the pulse is not limited by the gain spectrum. The recovery time of the saturable absorber affects the pulse dynamics and determines the maximum achievable repetition rates in passively mode-locked lasers [74]. Shorter recovery times strengthen the pulse shaping effect of the saturable absorber, improving mode-locking stability and reducing achievable output pulse durations [75–77]. Self-starting thresholds and stability of passive mode-locking benefit from lower absorber saturation fluences. Finally, lower absorber saturation energies in combination with lower threshold current densities enable self-starting mode-locking at lower laser powers and currents, improve laser efficiency, and increase the range of operating conditions (absorber voltages and gain section currents) within which mode-locking can be achieved.

The optical properties of QD active materials are compared with corresponding values for QWs in Table 2, to highlight the benefits of QDs for the design of mode-locked semiconductor lasers. QD edge-emitters provide 2–3 times broader gain bandwidths, faster sub-picosecond absorber recovery times, lower laser thresholds, and almost an order of magnitude smaller saturation fluences. These superior optical characteristics of QD edge-emitter have motivated the research in mode-locked QD lasers and will be discussed in more detail in the remainder of this section.

2.2.2. Broad gain bandwidth and lasing spectra

Originally, the discrete energy structure in QDs was expected to result in narrow-band laser emission, limited by homogeneous broadening. Instead, the broad (approximately Gaussian) size distribution of self-organized Stranski–Krastanov grown QDs, together with fluctuations in composition and, of some extent, shape (all of which affect the position of the size quantization levels) leads to substantial inhomogeneous broadening of the laser transition, as is illustrated in Fig. 5. This strong inhomogeneous broadening, and in some cases also the possibility of an overlap between the spectra of GS and ES transitions, allows for extremely broad gain bandwidths of more than 300 nm (at −10 dB) in QD active media [22,78,79], as demonstrated by the ultrabroad electroluminescence spectra of specially designed QD devices in Fig. 6.

These broad bandwidths allow for the high-gain (over 18 dB) amplification of sub-200 fs pulses [22,80] and wavelength tuning ranges of more than 202 nm in edge-emitting QD lasers [81,82]. QW-based devices can achieve comparable tuning ranges only with unpractically high current densities above 30 kA/cm^2 [83] and are otherwise limited to tuning ranges of ~100 nm (at −10 dB) [84,85]. Additional broadening of the gain spectra can be achieved by growth of *chirped* QD structures, whereby the average size of the dot (and hence the fundamental transition energy) varies gradually from layer to layer within the multilayer QD structure. As discussed below, these have proved particularly useful for mode locked operation [86,87], since broad gain spectrum helps achieve a broad lasing spectrum.

Additionally, the presence of inhomogeneous broadening results in spectral hole-burning (preferential depletion of population inversion in dots with the lasing transition resonant in frequency with the peak of the laser emission) which effectively flattens the gain profile and can be expected to counteract gain narrowing effects during amplification. The effect is stronger in QD lasers than in bulk and QW ones, since the “depth” of the spectral hole in QD lasers is governed by the characteristic time of carrier capture rather than the carrier–carrier scattering time as in bulk and QD materials. However the “width” of the hole, and thus the spectral selectivity of the hole burning, is determined by the time of quantum coherence relaxation which in QDs is broadly believed to be only slightly longer than in QWs.

A more spectrally selective effect that, together with the broad gain bandwidth and spectral hole burning, ensures the broad lasing spectra in QD lasers is the (short scale) spatial hole burning. This effect consists in preferential depletion of population inversion in the anti-nodes of the standing wave formed by the lasing light in the resonator, leading to longitudinal modulation of the optical properties of the active layer (gain/absorption and refractive index) with the spatial period of a quarter-wavelength in the laser waveguide - a self-induced Bragg grating. The effects of the spatial hole burning, like those of spectral hole burning, lead to spectral broadening and spectral shifts of lasing. In QW and bulk active materials, the nonlinear “grating” is efficiently washed out by ambipolar diffusion of carriers; in QD lasers, this process is mediated by capture and escape effects, since diffusion is possible for carriers in the reservoir but not in the dots themselves with their localized states. The grating and the effects of spatial hole burning are thus more important in QDs than in QWs.

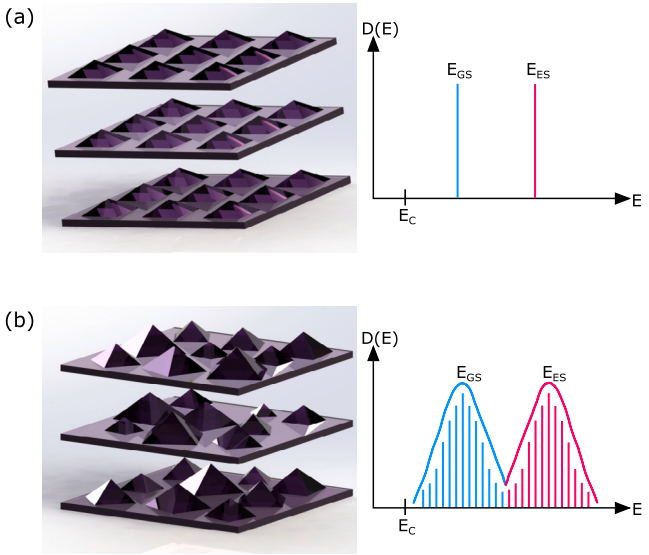

Fig. 5. Illustration of inhomogeneous broadening in QD active media: (a) density of states for QDs with constant size and (b) for QDs with random size distribution.

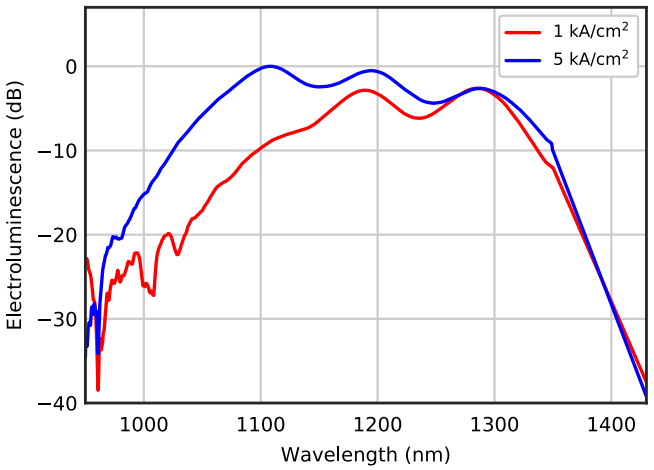

Fig. 6. Ultrabroad electroluminiscence spectra of specially designed QD device at different pump current densities.
Source: Adapted with permission. [22] 2007, Springer Nature.

2.2.3. Ultrafast carrier dynamics

The dynamics of carriers in all semiconductor nanostructures include the slow phase due to recombination and the fast/ultrafast phase associated with carrier relaxation. The energy structure of QDs, which includes multiple, discrete energy levels inside the QDs and a continuum of levels in the WL/barrier reservoir makes the ultrafast carrier dynamics in QDs very different from that in QW heterostructures [88–94]. The ultrafast dynamics are also very different in forward biased gain and reverse biased saturable absorber sections. Considering first the gain sections, we note that typical combined time of the capture times of electrons from the reservoir states onto the excited levels in the QDs and their subsequent relaxation from the excited states to the ground state are actually longer than the capture times from the barrier into the well in QW structures. Indeed at least one of the capture and relaxation times in QDs is in the picosecond rather than sub-picosecond range (as in QWs) as discussed above. The main difference between QW and QD structures however is that due to the finite DoS of the discrete levels in QDs, at high injection levels these states fill up and a substantial reservoir carrier population can build up, which is not the case in QWs. In this case, if the carriers in the QDs are depleted by, say, a short optical pulse it is the short capture time, rather than the much longer recombination time, that mainly governs the dynamics of subsequent population recovery. The fast saturation and recovery of gain (and absorption) thus becomes very important for ultrafast QD lasers, much more so than in QW counterparts.

Ultrafast gain recovery and absorber dynamics in QD structures has been studied in detail experimentally [89] Pump probe measurements have been used to characterize the relaxation time-scales in QDs. For electrically pumped QD devices, gain

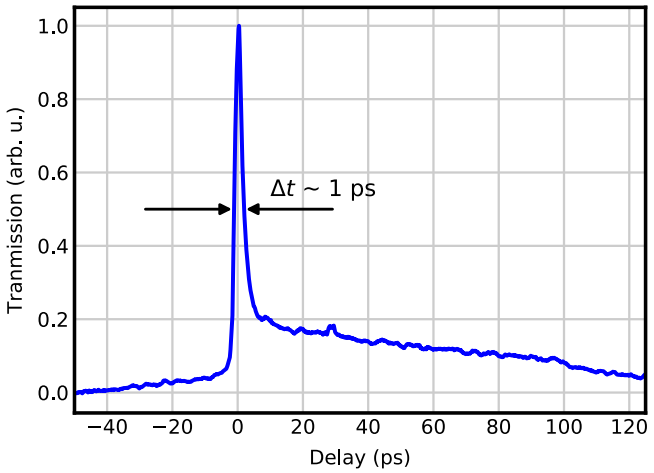

Fig. 7. Pump-probe measurement of saturable absorber relaxation in QD waveguide.
Source: Adapted and Reproduced with permission, from [91] 2004, IEEE.

compression recovery has been demonstrated to be comparable to bulk or QW devices, proving that at least at some operating conditions there was no significant bottleneck in carrier relaxation [88]. Schneider et al. [90] characterized the gain recovery time scales for excited and ground state transitions in a QD amplifier. They observed gain recovery times of 150 fs and 180 fs for the ground and excited state, respectively. These recovery times can be attributed to carrier relaxation from the excited state to the ground state and to the capture time of carriers from the WL [95]. Rafailov et al. [91] measured the absorption recovery time of the excited state transition in a QD waveguide as shown in Fig. 7. Using pump and probe wavelengths of 1050 nm, two time constants for the recovery of the probe absorption could be observed. The fast recovery time of 820 fs was attributed to carrier relaxations from the excited state to the ground state, whereas the slow relaxation time of ~100 ps was explained by carrier recombination dynamics.

Of major importance for the design of mode-locked QD devices is the dependence of absorber relaxation times on the reverse bias applied [93,94,96]. Malins et al. [92] used a pump wavelength of 1280 nm to saturate the ground state transition in a QD waveguide and measure the recovery time versus applied reverse bias. By increasing the reverse bias up to 10 V, the recovery times could be reduced by over two orders of magnitude from 62 ps down to 700 fs. The observed exponential decrease of recovery time with reverse bias in QDs is similar to the one reported in QWs [97,98], but allows for significantly shorter recovery times. In general, the recovery times demonstrated in QD waveguides are 5–10 times shorter than in QW counterparts at comparable reverse bias values. This strong dependence of absorber recovery times on reverse bias can be exploited for tuning of absorber parameters in two-section QD devices. It enables the electric control of mode-locking dynamics and optimization of output pulse parameters by variation of absorber recovery times [22,24]. Electrically controlled tuning of output pulse durations from mode-locked, two-section QD lasers over more than one order of magnitude has been demonstrated [23].

It must be noted that QD and QW-based saturable absorber mirrors can both exhibit comparable sub-picosecond recovery times, even without the presence of reverse bias, by introducing defects during growth and additional post-growth processing steps [99–101]. These defects act as recombination centers and accelerate recovery times. This type of absorbers, however, has higher unsaturable losses and cannot be easily integrated into two-section edge-emitters, rather, they can only be used as bulk components in external cavity setups.

2.2.4. Low laser threshold and saturation energy

As mentioned above, the discrete energy level structure in QDs leads to a significantly reduced DoS in comparison to QWs [37,102]. Fewer carriers are required to fill the available energy levels and to reach transparency and population inversion. Together with the high values of the radiative transition strength (matrix element), also provided by the three-dimensional confinement, this helps to achieve lower threshold currents for laser operation [102], less temperature sensitivity [103], and smaller saturation energies for absorber sections.

Room-temperature threshold current densities of ~20 A/cm^2 have been demonstrated in edge-emitting QD lasers [104–106], which are approximately two times lower than values for comparable QW lasers [102]. The saturation fluences of QD absorbers are approximately one order of magnitude lower than QW counterparts. Lorenser et al. [99] demonstrated a single layer InAs/GaAs QD absorber mirror with a saturation fluence of 1.7 μJ/cm^2, improving upon typical values of ~20 μJ/cm^2 achieved with QWs. Thompson et al. [93] compared the saturation powers of InAs/GaAs QD and GaInAsP/InP QW absorber sections in two-section edge-emitters, observing 2–5 times lower saturation powers for QDs. Viktorov et al. [94] investigated the saturation fluence of the ground state transition in a QD waveguide absorber. They used a pump-probe setup with 600 fs pulses at 1250 nm wavelength to characterize a 4 μm wide, 1 mm long waveguide with 6 stacked InAs/GaAs QD layers, measuring saturation fluences down to 10 μJ/cm^2. These fluence values correspond to saturation pulse energies of few pJ or even sub-pJ in QD waveguide absorbers, depending on waveguide design and mode-field-area.

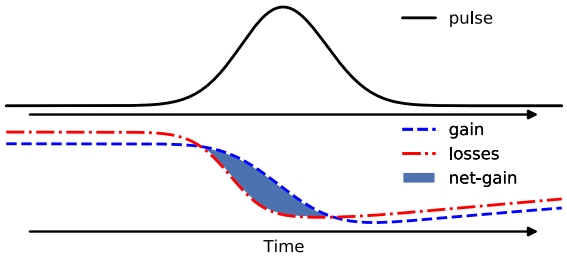

Fig. 8. Principle of passive mode-locking: absorber saturation and gain dynamics lead to short time window with net gain.

3. Mode-locking in edge-emitting QD lasers

Edge-emitting semiconductor devices were among the first laser systems in which mode-locking could be demonstrated [2,4,74]. Passively mode-locked two-section edge-emitters with integrated gain and absorber sections are now a well established technology [75], enabling the generation of high-repetition rate, ultrashort pulses from monolithic devices [8,10,22,107]. This section provides a state-of-the-art overview of the theory of mode-locked QD lasers and numerical implementations of existing models for QD laser design.

3.1. Basics of mode-locking in QD lasers

The mode-locking mechanism in semiconductor lasers is, in principle, similar to solid-state and dye laser counterparts. A short net-gain window, as shown in Fig. 8 is formed by simultaneous saturation of gain and absorber sections, suppressing cw-operation in favor of short pulses. The net-gain window leads to amplification of short optical pulses from initial cw-background and to the formation of a stable output pulse train [75].

The main difference of mode-locking dynamics in semiconductor lasers from their solid-state laser counterparts, arise from the nature of the refractive index nonlinearity [108]. In solid-state lasers the nonlinear refractive index reacts instantaneously (fs response time) to the applied electric field and is proportional to the intensity of the optical pulse. This results in nonlinear pulse broadening by self-phase-modulation (SPM) and the formation of optical solitons [75]. In semiconductor lasers the refractive index is, primarily, a function of carrier density, resulting in a delayed nonlinear response, approximately proportional to the pulse energy. The saturation of gain and absorber sections induces refractive index changes and adds a nonlinear phase-shift to the laser pulses. The phase-shifts from both sections must be exactly balanced to achieve stable mode-locking [109]. Other features of mode locking dynamics peculiar to semiconductor lasers are the absorber relaxation times that, at least in monolithic designs, tend to be of the same order as the round-trip rather than orders of magnitude shorter, and the presence of both slow (compared to the pulse) and usually weaker (ultra)fast component in both the gain and absorption dynamics; the latter is of particular importance in QD media.

The design and ongoing development of ultrafast QD lasers requires an in-depth understanding of the complex mode-locking dynamics. To this end, a large number of theoretical and numerical models have been developed to model pulse propagation and carrier distributions in QD waveguides. These models were used to investigate the multilevel carrier dynamics in inhomogeneously broadened QDs during mode-locking and to predict optimal design parameters for ultrafast QD lasers.

3.2. Theoretical analysis of mode-locked QD lasers

As mentioned above, the main differences between the QD mode locked lasers and those using QW and bulk active layers is, the complex energy structure (which in turn leads to the more complex kinetics of carrier capture and escape, to the absence, generally speaking, of equilibrium carrier distribution in energy, to a potentially complex two-peak gain spectrum, and to a more complex relation of self phase modulation than in bulk and QW materials). In addition, localization of carriers in QDs suppresses diffusion and leads to a greater prominence of short-scale spatial hole burning (self-induced gratings) than in other semiconductor lasers.

A theoretical model of a mode locked QD laser needs to a greater or lesser extent (depending on the purpose and the level of accuracy required) capture these peculiarities. Thus, all theoretical work on mode-locked QD lasers can be classified from the point of view of two main criteria: the approach to describing the laser dynamics (as with all mode-locked laser models), and the degree of detail and accuracy in describing QD physics peculiarities. To some extent, these two criteria are independent, though some dynamic approaches allow better accuracy in including QD physics than others.

As regards the approach to dynamic modelling, the three main theoretical approaches are fully time-domain approaches – lumped-element Delay-Differential models and Travelling Wave models – and mixed time–frequency domain models (dynamic modal analysis).

As regards the approach to the dot kinetics, the simplest approaches completely neglect the inhomogeneous broadening in QDs and may or may not consider the multiple quantization levels. More sophisticated ones use separate rate equations for dots of different size groups, explicitly considering inhomogeneous broadening. An intermediate approach separating the dot populations into quasi-equilibrium (slow) contribution and a non-equilibrium (fast) correction without the need to deal with different dot populations has been also proposed [42].

3.2.1. Delay-differential equation model

The first models that were used to describe passive mode locking in QD lasers were of the Delayed-Differential Equation (DDE) type. In the simplest version of the model no inhomogeneous broadening is taken into account and only the contribution of the ground level transitions to gain is included. The description of light dynamics in a model of this type follows the approach proposed in the work by Vladimirov and Turaev [110] and describes the dynamics of the light in the laser cavity by a delay-differential equation of the type:

$$Y(t) = -\gamma^{-1}\frac{\partial Y(t)}{\partial t} + \sqrt{\kappa}\exp\left[\frac{1}{2}\left(\mathrm{G(t-T_{RT})(1-i\alpha_{Hg})} - \mathrm{Q(t-T_{RT})(1-i\alpha_{Ha})}\right)\right]\cdot \mathrm{Y(t-T_{RT})}. \tag{1}$$

Here, as in the original paper dealing with a generic semiconductor laser [110] Y is the slow amplitude of the optical pulse, G and Q represent the gain and absorption integrated over the length of the corresponding sections, $\sqrt{\kappa}$ characterizes the amplitude losses, γ the gain/absorber bandwidth, α_{Hg} and α_{Ha} are the Henry linewidth enhancement factors of the gain and absorber sections, $\mathrm{T_{RT}}$ is the cavity round-trip time. The peculiarities of the QD active media dynamics are included in a model of this type by considering the dynamics of QD populations spatially averaged over the gain $\mathrm{f_G}$ and absorber $\mathrm{f_a}$ section which is described by rate equations, generically written as

$$\frac{df_g}{dt} = R_g^{(cap)} - R_g^{(esc)} - \frac{f_g}{\tau_g} - F_g\frac{P(t)}{U_g}(f_g + f_{gh} - 1) \tag{2}$$

$$\frac{df_a}{dt} = R_a^{(cap)} - R_a^{(esc)} - \frac{f_a}{\tau_a} + F_a\frac{P(t)}{U_a}(1 - f_a - f_{ah}) \tag{3}$$

Here, $R_g^{(cap)}, R_g^{(esc)}$ are the carrier (electron) capture and escape rates (which in the first approximation can be described by a phenomenological capture and escape time and statistical factors describing occulation of the initial and final levels [42]; $\tau_{g,a}$ are the "long" recovery times in the gain and absorption section, $F_{g,a}$ are the geometric averaging factors (for a unidirectional ring cavity, $F_g(t) = e^{-Q(t)}\frac{e^{G(t)}-1}{G(t)}$ and $F_a(t) = \frac{1-e^{-Q(t)}}{Q(t)}$). The parameters $U_{g,a}$ are the gain and absorption saturation energies inversely proportional to cross-sections of the corresponding transitions; it is well known that achieving $s = U_g/U_a > 1$ is a necessary condition for mode-locking. The variables f_{gh} and f_{ah} in the equations are the occupancies (probability functions) of the hole levels in the dots involved in the transitions; the gain and saturable absorption, neglecting inhomogeneous broadening, are calculated as $G = G_0(f_g + f_{gh} - 1)$; $Q = Q_0(1 - f_a - f_{ah})$ with G_0, Q_0 characteristic constants. Sometimes, particularly in early papers, the so-called excitonic approximation is used, which considers the kinetics of electron population only and effectively forces the same distribution function on the holes $f_{gh} = f_g, f_{ah} = f_a$, ensuring detailed quasineutrality in the dots. The approximation has been proven to not hold in realistic QD materials, but substantially simplifies the analysis and, strictly speaking, is a requirement for the DDE model to be self-consistent because otherwise the use of spatially averaged occupancies is not accurate. The approximation can be removed by applying the principle of detailed quasineutrality (the same total number of electrons and holes) to the whole active region (including the dots and the reservoir) rather than just the dots. It is then possible to either analyse the kinetics of electrons and holes separately, using for f_{gh} and f_{ah} equations similar to (1)–(2), or just to assume that the hole population in the dots, whose energy levels are spaced more closely than the electron ones leading to faster capture and relaxation processes, is in quasi-equilibrium with the hole population in the reservoir.

Delay-differential models, even in the case of QW and bulk materials, have certain built-in inaccuracies. They assume a hypothetical unidirectional ring cavity (as opposed to a Fabry–Perot cavity in a realistic laser), and even then can be only rigorously derived given a linear dependence of local gain and absorption in carrier population, which is not true in QDs beyond the excitonic approximation. In Quantum Dots, in addition to that, the use of a single Henry factor to describe the linewidth enhancement is also highly tenuous, and the unidirectional analysis by definition neglects the standing wave self-induced gratings which are important in QD lasers as discussed in the previous section. The analysis cannot therefore be expected to predict accurately the properties of the pulses emitted, particularly the spectra and the time–bandwidth product.

However, these limitations can be outweighed by a number of substantial advantages of DDE models if what is required is, not quantitative analysis, but qualitative understanding of the laser dynamics. Due to their mathematical simplicity (the use of only three dynamic variables), DDE models allow extremely efficient numerical analysis for a broad range of parameters, as well as some analytical insight [110]. When applied to generic (QW or bulk) semiconductor lasers, they predict the whole plethora of phenomena, including, in addition to stable mode locking at the fundamental harmonic, also the trailing-edge self-pulsing instabilities (usually at lower currents) and leading-edge chaotic instabilities [110] as well as harmonic operation at high currents. Applying the model to QD lasers shows a significantly different dynamic behaviour from QD and QW lasers, with the range of self-pulsating instabilities significantly narrower than in QW and bulk lasers (see e.g. [111]) and with some parameter values completely absent [112]. To some extent, this is due to the fast absorber relaxation in QD lasers, as discussed in the previous section, as the stability range of ML is known to benefit from fast SA relaxation (see [113] for an overview). Another effect contributing to greater stability of ML in QD lasers is that fact that, due to the presence of the reservoir carrier population, the role of fast carrier relaxation in replenishing the gain section population depleted by the ML pulse can be much greater than in bulk and QD lasers, and the role of slow recombination dynamics, correspondingly smaller [42,114]. The same effect can also be interpreted [42] as strong gain compression which is known to limit the modulation properties in QD lasers — in passive ML, in contrast, it proves beneficial by suppressing the self-pulsating instability. These conclusions agree well with the experimental observations [112]. It has to be noted however that the same effect also tends to broaden the ML pulses and contributes to the difficulties in the realization of the full potential offered the broad gain spectrum of QD lasers.

Further modifications to the DDE model may involve more sophisticated account for the nature of self-phase modulation, with separate effects of the wetting layer/QW dynamics on the QD transitions, explicit account for the inhomogeneous broadening [115], and inclusion of active modulation of laser parameters for analysis of hybrid as well as passive mode locking. In particular, the asymmetric nature of the locking range of QD hybridly mode locked lasers was successfully reproduced using bifurcation analysis involving a DDE model [116]

A particularly important application of the DDE approach is the inclusion of the dynamics of both the ground and excited state populations, for which DDE models are uniquely suited — the different round-trip times of the light resonant with ground and excited state transitions are included explicitly and simply by using different delay times for the corresponding complex amplitudes. This makes it possible to explain and analyse the experimentally observed switching of operation between ground and excited levels as well as simultaneous operation in both, depending on the recovery constants of the gain and absorber sections.

3.2.2. Travelling-wave-model

A more realistic, but also a much more computationally intensive, approach to modelling ML in QD lasers is offered by the travelling wave models. Models of this type analyse the dynamics of the slow complex amplitudes of forward- and reverse travelling electromagnetic waves $Y_{f,b}$ at each point within the laser cavity, resulting in an equation which in the most generic form can be written as:

$$\pm \frac{\partial Y_{f,b}}{\partial z} + \frac{1}{v_g}\frac{\partial Y_{f,b}}{\partial t} = iK_{bf,fb}Y_{b,f} + F_{spont}(z,t) + \left(\frac{1}{2}(\hat{g}_{\mathrm{mod}} - \alpha_{\mathrm{int}}) + ik\widehat{\Delta\eta}_{\mathrm{mod}}\right)Y_{f,b}. \tag{4}$$

Here $\hat{g}_{\mathrm{mod}} + ik\widehat{\Delta\eta}_{\mathrm{mod}}$ represents the spectrally-dependent gain and refractive index in the QD active media, implemented in time domain as a differential or integral operator (within the SA sections, if any, it represents saturable absorption rather than gain). Furthermore, v_g is the group velocity of light in the waveguide, k is the wave number in vacuum at the reference frequency used to introduce complex amplitudes. α_{int} is the internal dissipative loss, F_{spont} is the spontaneous noise source needed for self-starting of the model, and $K_{bf,fb}Y_{b,f}$ are the coupling terms between counter propagating fields representing the self-induced gratings (and built-in gratings in lasers containing DBR sections). The inclusion of these terms is a major feature of the travelling wave model, making it inherently more accurate and reliable than the DDE model, particularly as regards the spectral properties.

The "complex gain" operator $\hat{g}_{\mathrm{mod}} + ik\widehat{\Delta\eta}_{\mathrm{mod}}$ is calculated from the occupation functions f, always calculated as a function of space and time. In more advanced versions of the travelling wave models, they are also calculated as function of carrier energy in order to take into account inhomogeneous broadening and spatial hole burning. The equations used are of the same type as (1)–(2) but without the need for spatial averaging ($F_g = 1$) and with the power calculated from the local photon density $S = |Y_f|^2 + |Y_b|^2$ In a model with inhomogeneous broadening, this is modified to take into account the spectral detuning between the light and the optical transition in a given group of dots.

The coupling coefficients $K_{bf,fb}$ are calculated in the similar, though not identical, way to that used for calculation of complex gain, but from the dynamics, not of f, but of "grating populations" governed essentially by interference intensity $\mathrm{Re}(Y_b Y_f^*)$. In addition to purely optical saturation of saturable absorption by state filling, it may be necessary to include the optoelectronic effects in the model: photogenerated carriers in the SA contribute to photocurrent, which leads to voltage redistribution in the absorber circuit, affecting the electric field across the SA section which in turn affects both the absorber recovery time and, to a lesser extent, saturation energy and unsaturated absorption [42]. In principle, this can be included in a DDE type model, but so far has only been implemented, for QD lasers, in a travelling wave formalism [117]. Depending on the bias conditions (e.g. load resistance) of the absorber, the effect can have a substantial effect on the laser operation, affecting switching between ground and exciting state operation and causing bistability effects [117]. In the most straightforward numerical implementation of a TWM, the time and space steps are interrelated: $\delta z = v_g \delta t$. Thus the need to resolve the dot populations in space, time, and energy makes the travelling wave models inherently time-consuming. The computational efficiency can however be substantially increased by using the decimation technique [76,113] which makes use of the fact that, although the variation of fields in space and time can be fast, their variation along the travelling coordinate typically remains much slower. This allows the use of δz an integer number of times greater than $v_g \delta t$, with corresponding significant computational time saving.

TWMs have been used since the 1990s [118] to analyse the properties of active, hybrid, and passive mode locking in "generic" ML lasers; a recent overview is available in [113]. The application specifically to Quantum Dot lasers required the inclusion of rate equations describing interlevel relaxation dynamics [111,119,120]. More sophisticated versions of the models benefitted from the account of the effects of inhomogeneous broadening [121,122], with populations of the corresponding population groups determining gain and refractive index variation.

TWMs (and also, in principle, DDE models) of QD lasers can benefit also from using microscopic calculation of transition rates (which in the simpler model versions are characterized phenomenologically), as in [123], reducing the number of unknown/fitting parameters and increasing the reliability of the model.

Like the DDE models, TWMs can be used to predict the current and reverse bias dependence of the onset of leading and trailing edge instabilities in ML QD lasers, [111,117,121,122,124,125], and can, with accurate definition of parameters, perform this task more accurately than the DDE models, with quantitative as well as qualitative agreement with experiment possible.

TWMs with inhomogeneous broadening included are successful in describing many properties of the pulse as functions of operating parameters [117,121,122,124], e.g. predicting (in a version of the model including the inhomogeneous broadening) an increase in the pulse duration with current [123] and decrease with the increased absorber bias/absorber recovery rate (the latter also predicted by DDE models [115]). Even without the account for asymmetric broadening, they reproduce well the extremely asymmetric pulse shapes, typical for strong modification of the pulse shape per round trip and particularly prominent in Quantum Dot lasers [119].

Like the DDE model, the TWM can be extended to cover the operating regime when both ground and excited state transitions are present in the laser spectrum. In this case, either an ultra-broadband model considering both levels can be implemented, at the expense of using very short time steps, or, in principle, different reference frequencies can be introduced for ground and excited state transitions [42]. By carefully treating the dynamics of various populations (reservoir carriers, excited and ground state populations), the ultra-broadband model with a single reference frequency was capable of explaining the switching of operation with increase in current both from GS to ES (more common in experiment) and from ES to GS transitions (seen in some designs and operating conditions) [117,122].

In addition to providing more accurate and more reliable results than the DDE models, travelling wave models can also address problems that cannot be tackled by the DDE approach at all due to the nature of the model formalism.

One such class of problems is the effect of absorber position and geometry, and/or the presence of multiple absorbers, on the ML dynamics. In [126], a TWM was used to analyse a performance of a Quantum Dot ML laser with one absorber placed at the high reflective facet and an additional second one at 1/3 of the total cavity length (the rest of the cavity length was occupied by gain sections). Simulations showed transitions from fundamental harmonic mode-locking (n=1; 10 GHz) to higher harmonic mode-locking (n=3; 30 GHz) by increasing the injected current density, a regime known as Asymmetric Colliding Pulse ML [19]. Associated with that transition was a drastic (by a factor of 333) improvement in the timing stability (jitter), in very good agreement with experiment.

At the expense of some further computational load, TWMs can be extended to cover lasers with a flared/tapered geometry, which is particularly useful in Quantum Dots due to the limited value of the parameter $s = U_g/U_a > 1$ afforded by straight waveguide geometries [124,127]. In the simple form of the model [124], this can be achieved by simply scaling the amplitude of light along the cavity; more sophisticated approaches can include explicitly two-dimensionally spatially resolved carrier populations. In a recent study [123,127], travelling wave modelling was used to assist a design of a laser combining a tapered amplifier and ACPM type geometry (with the saturable absorber offset by about 1/3 of the 3 mm length from the facet) to achieve pulse generation at the fundamental harmonic with a peak power of over 9 W and a duration of about 0.5 ps; good agreement was obtained between experiment and theory.

Travelling wave modelling was also applied to establish detailed theoretical understanding of self mode locking in single section lasers [128]. It was shown that, essentially, the broad, frequency locked spectrum of laser operation in this case is due to a combination of two effects. Firstly, the fast optical nonlinearities in the active media (corresponding to four-wave mixing between longitudinal modes in modal language) establish a constant phase relation between modes (in the absence of saturable absorbers, the phases are not necessarily close to each other so the temporal outcome need not be in the form of short pulses). The effect can be present in non-QD lasers, and some theoretical analysis of it was published previously (see e.g. [129]). Secondly, and uniquely to QD lasers, the strong spectral and particularly spatial hole burning (the self-induced grating caused by the standing wave profiles of the modes and included in the coupling coefficients $K_{bf,fb}$) broadens the spectrum and stabilizes the self-mode locked regime [125,128]. Spatial hole burning is substantially stronger in QD land QDH lasers than in Quantum Well materials due to the fact that carriers localised in dots or dashes do not experience diffusion which smoothes down spatial nonuniformities in the Quantum Wells (though carriers in the reservoir do). It is impossible to include spatial hole burning effects consistently in DDE models which assume unidirectional propagation. The threshold current for mode locking in single section devices was analysed using a travelling wave model with spatial hole burning included [130], with good agreement with experiment.

3.2.3. Static and dynamic modal analysis

Mode-locking in QD lasers, including self ML in single section lasers, can be also analysed using the formalism completely alternative to both DDE and Travelling Wave models, namely the Dynamic Modal Analysis. Instead of following dynamics of spatially resolved fields at "fast" time scales (shorter than the round-trip) as both DDE and Travelling Wave models, this approach represents the shape of the optical field in the form

$$Y(z,t) = \sum_k E_k(t) u_k(z) \exp\left[i\left(\omega_k t + \varphi_k(t)\right)\right]$$

where E_k, u_k, ω_k and ϕ_k are respectively the amplitude, mode profile, frequency and phase of the longitudinal mode k. The fast laser dynamics (of the order of, and shorter than, round-trip, that is, on the pulse scale) is then contained in the instantaneous values of amplitudes and phases, whereas the slow dynamics (on the scale longer than round-trip) is determined by the dynamics of complex mode amplitudes

$$Y_k = E_k(t) \exp\left(i\varphi_k(t)\right)$$

which satisfy complex rate equations describing amplitude and phase dynamics. In a somewhat simplified form, these equations can be expressed as [19,131]

$$\frac{\partial}{\partial t} Y_k = \left[\frac{1}{2} g_k^{net} + i(\Omega_k - \omega_k)\right] Y_k + \sum_m \Delta g_m^{coupl} Y_{k+m} + F_k^{(spont)}(t) \tag{5}$$

where g_k and Ω_k are the gain and notional (unlocked) frequency of each longitudinal mode (in a microscopic approach, they are calculated together and are related to the real and imaginary part of the same variable); Δg_m^{coupl} are the (complex) mode coupling parameters . They include a contribution due to four-wave mixing (FWM) in gain and (in the case of passive or hybrid ML) SA sections (this contribution is proportional to the intensity of light oscillating at m intermodal intervals $\sum_k Y_k Y_{k+m}^*$), and in the case of active or hybrid ML, also a separate contribution due to resonant modulation. A more accurate, though much more computationally intensive,

version of the model [132] takes into account dispersion of nonlinear (FWM) as well as linear gain, leading to triple summation in each of the Eqs. (5), but still no need for spatially resolved modelling. The dynamics of gain and SA carrier populations are also described by lumped rate equations, as opposed to distributed ones in TWM.

The logical advantage of such an approach is that steady-state ML, as well as single-mode operation, are the steady-state, stationary solutions of the model. If only this steady state is sought (static modal analysis) then the derivatives in the rhs of (5) can be omitted from the start, and the model can be solved as a system of nonlinear algebraic (rather than differential) equations.

In the case of active or passive short-pulse mode locking the modal analysis approach is somewhat limited by the fact that, like all frequency-domain analysis methods, it is limited to weak to moderate nonlinearities, an approximation that becomes tenuous in the presence of short intense pulses and makes it impossible to predict accurately the onset of ML instabilities at high current — however in QD lasers, where such instabilities are less prominent than in QW media, and particularly for single-section designs, this limitation is arguably somewhat less significant than in QW lasers. In the context of double-section short-pulse mode-locking of QD lasers, with microscopic calculation of both linear gain and coupling, the dynamic modal analysis approach was used to analyse the potential effect of spectral hole burning on the laser spectrum [133]. More sophisticated models, some with self-induced gratings taken into account, have been employed for the analysis of single-section lasers, helping explicitly identify the significance of both spectral and spatial effects in the laser operation [134] and, with a somewhat different formalism, in [132,135]. Good agreement with experiments was reached [132,135]. The importance of the group velocity dispersion, arising to a substantial extent from the QD (rather than passive material) contributions to the unlocked mode frequencies Ω_k, as a limiting factor for mode locking stability and quality was stressed, and it was pointed out that both the GVD and self phase modulation could be minimised with correct design of the QD active layer.

4. Ultrafast QD lasers

The promise of low-threshold current and tolerance to temperature provided the initial impetus to pursue research on QD lasers. The first reports of lasing from such devices were published in 1994 by Kirstaedter [71]. Since then these devices have shown improved gain saturation, high differential and internal efficiencies, low threshold and room temperature CW output power up to 4 W [136–138]. Soon after single mode operation from QD edge emitting lasers was achieved [139].

Ultrashort pulses from mode-locked QD lasers were first demonstrated in 2001 by Huang et al. [20]. The authors used a two-section QD edge-emitter with separate gain and absorber sections (see Section 2.1.4) to generate output pulses with durations of 17 ps at a laser wavelength of 1278 nm. Since then different mode-locking techniques, waveguide designs, and cavity setups have been used to generate ultrashort pulses from single- and two-section QD lasers.

In this section the state-of-the-art for mode-locked edge-emitting QD lasers is presented. The overview will include both straight and tapered QD waveguides, monolithic and external-cavity (EC) setups, and master-oscillator power-amplifier (MOPA) systems. These designs are discussed in with focus on key parameters such as pulse width, repetition rate, peak power, average output powers, and wavelength tunability.

4.1. Monolithic QD lasers

Monolithic, passively mode-locked QD lasers are fully-integrated, compact semiconductor devices with footprints of few millimeters. The compact design enables the generation of high-repetition (up to hundreds of GHz) ultrashort pulses with pulse durations in the femtosecond and picosecond range. Previously demonstrated devices can be categorized in two types, based on their waveguide design. The most widespread type are single- and two-section devices with straight waveguides, which have constant width along the entire length of the device. The second type, tapered waveguide QD lasers, use waveguides with increasing ridge-widths (see Fig. 9) to reduce nonlinearity and enable higher pulse energies.

4.1.1. Straight waveguide QD lasers

Passively mode-locked, straight waveguide QD lasers with monolithic cavity setups produce ultrafast pulses with varying repetition rates depending on the length of the laser cavity. Such lasers allow for electrical control of pulse width and peak/average power. In the picosecond range, output pulse durations from 1 ps to few 10 ps, pulse energies above 20 pJ, and peak powers of several Watts have been demonstrated [140,141]. Additionally, the inhomogeneous gain broadening in QD active media and fast recovery times of QD absorbers have allowed for the generation of sub-picosecond pulses directly from monolithic single- and two-sections devices.

The first demonstration of picosecond pulses from QD lasers 2001 generated a lot of interest is two-section QD lasers. The focus of this interest entailed both the ultrashort pulses and high repetition rate which are desirable for high-speed communication and opto-electronics. In 2003, Thompson et al. demonstrated 14.2 ps ML QD lasers with 10 GHz hybrid modelocking [142]. Around the same time, Tan et al. reported ∼5 ps pulses from a passively ML QD laser at a repetition rate of 18 GHz [143]. Such high repetition rates and short pulses were very promising even though the peak optical power is still limited to few mW. In 2004, Gubenko et al. demonstrated the shortest pulse of 1.7 ps from a two-section passively ML QD laser with a repetition rate of 9.7 GHz lasing at 1.28 μm [144]. Soon after 10 ps Fourier transform limited pulses at a high repetition rate of 18 GHz were demonstrated from passively ML QD lasers. In the same year Kuntz et al. published results highlighting 35 GHz passively ML 7 ps lasers [145] and repetition rates up to 50 GHz from passively ML QD lasers generating 3 ps pulses. By this time it was clearly established that two-section QD

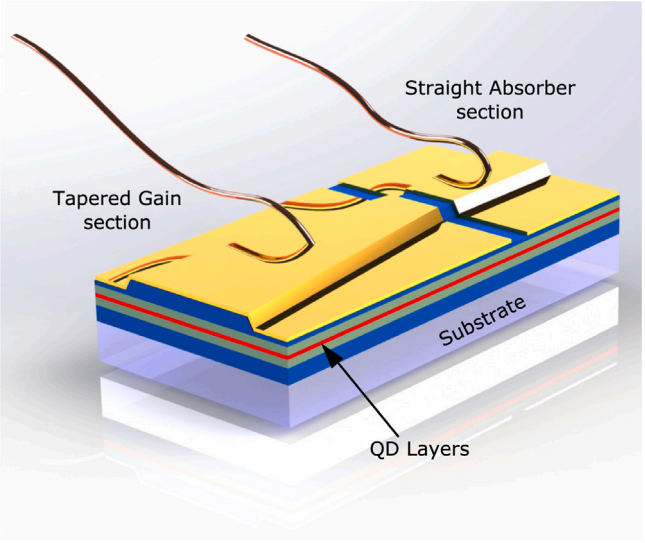

Fig. 9. An illustration of tapered, index-guided, two-section mode-locked QD laser. For tapered lasers the gain section increases in width along the length of the laser.

lasers can produce ultrashort pulses at high repetition rate. However, shorter pulses were expected from such devices especially due to short absorber recovery times.

In 2005, the first demonstration of sub-picosecond pulses from a straight waveguide, passively mode-locked, two-section QD laser was made by Rafailov et al. [21,22]. The generated pulses had a duration of 390 fs and peak power of 3 W. The laser operated at a repetition rate of 21 GHz with a laser wavelength of 1260 nm. In the subsequent year a other research groups also demonstrated sub-picosecond pulse generation from passively mode-locked two-section lasers [23,146]. Laemmlin et al. demonstrated 710 fs pulses from a two-section QD laser [146], Thompson et al. demonstrated 780 fs from a two-section flared waveguide laser diode [23]. Sub-picosecond pulses from InAs QDs and quantum dash (similar to elongated QDs, as discussed above) based monolithic laser diodes with a single-section have also been demonstrated [147,148].

Using InAs/InP based QD active media, Lu et al. in 2008 and 2009 demonstrated 312 fs and 445 fs pulses at laser wavelengths of 1530 nm and 1590 nm, targeting the C- and L- communication bands [149,150]. Finch et al. have reported the shortest optical pulses of 290 fs from monolithic QD devices [151], so far. Their results were achieved at cryogenic temperatures of 20 K, and by use of a proton bombarded absorber section with reduced recovery times.

One of the key advantages of monolithic mode-locked laser diodes, including QD ones, are their intrinsically high repetition rates. Typical repetition rates for fundamental mode-locking are in the GHz (1–100 GHz) range for such lasers. A maximum fundamental repetition rate of 80 GHz from a 500 μm passively mode-locked two-section QD laser with straight waveguide has been demonstrated [146]. Even higher repetition rates can be achieved by use of harmonic mode-locking. One technique to increase the repetition rates of mode-locked QD lasers by a factor of two is the colliding pulse mode locking. This technique still uses a passive saturable absorber but unlike the two-section devices it is placed in the middle of the gain section (resulting in three separate sections) [152]. This allows simultaneous bleaching of the absorber by two counter-propagating pulses and leads to second order harmonic mode-locking. The geometry of such lasers allows for twice the repetition rate from the same cavity length. Following the same principle, asymmetric absorber placement (i.e. not in the middle) can be used to achieve stable higher-order harmonic mode-locking with multiple counter-propagating pulses colliding in the absorber section. With this method repetition rates as high as 238 GHz have been demonstrated [153].

Nikitichev et al. [154] demonstrated electronically controlled wavelength tuning in a monolithic, mode-locked QD laser. They presented a two-section QD laser with picosecond pulse durations (4–8 ps) and a wavelength tuning range of 50 nm from 1245 nm to 1295 nm at a repetition rate of 10 GHz [154]. The wavelength tuning was achieved by variation of reverse bias in the absorber section. The observed wavelength shift towards longer wavelengths with increasing reverse bias was explained by the shifting of absorption spectra towards longer wavelengths for InAs QD lasers at higher electrical fields [155]. More recently, the high stacking growth techniques to compensate for strain used in [156] produced 464 fs pulses at a repetition rate of 81 GHz from a 0.5 mm two section laser. Further progress on the topic is discussed in the application (Section 4.4) section of ML QD lasers below.

4.1.2. Tapered QD lasers

Edge emitting QD lasers with tapered waveguides have also been explored over the years to improve peak and average output powers [24] of mode-locked QD lasers. Typically, a tapered, two-section QD laser, as shown in Fig. 9, has a straight absorber section and a gain section of increasing width towards the end facet of the device. The taper design increases the saturation energy of the gain section due to increased average modal area. At the same time spatial mode filtering is provided by the narrower waveguide in

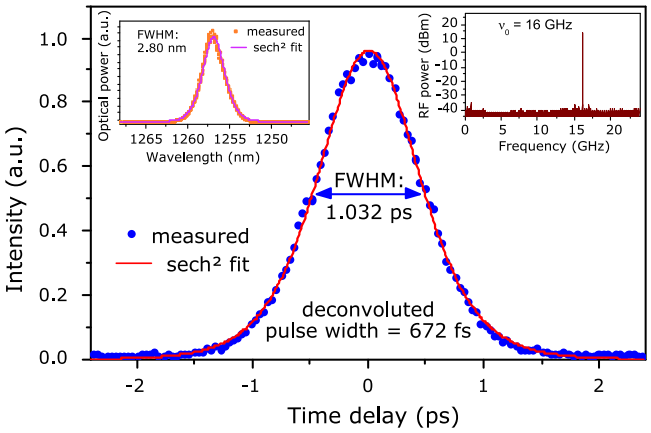

Fig. 10. Typical characteristics of a tapered two-section mode-locked QD laser. Inset (left) spectra and (right) RF spectrum under mode-locked operation. *Source:* Adapted and Reproduced with permission, from [124] 2012, Pleiades Publishing, Ltd. (Springer: Laser Physics).

the absorber section, ensuring single lateral mode operation. Thus, this combination of coupled straight and tapered sections holds enables the generation of higher pulse energies and peak powers, while simultaneously preserving single mode operation [157]. Fig. 10 depicts typical pulse shapes for ps pulses generated from such gain-guided two-section QD lasers. A wide spectral width and neat RF spectrum of −40 dBm at fundamental frequency demonstrates provision of utility for such lasers.

Pulse durations of 360 fs with peak power of 2.25 W have been reported from tapered, two-section QD lasers by Thompson et al. [24]. Nikitichev et al. [124] investigated the influence of taper- and absorber-length ratios on laser performance. For taper and absorber lengths of 2.14 mm and 0.4, they obtained pulse durations of 672 fs, pulse energy of 2.55 pJ, and peak powers of 3.8 W. Using a taper length of 3.2mm and absorber length of 0.8 mm, resulted in 1.26 ps pulse durations, pulse energy of 22.3 pJ, and record high peak powers of 17.7 W. These measurements underlines the influence and importance of gain to absorber section ratio for optimization of pulse parameters in mode-locked, two-section QD lasers. More recently, tapered design in a 3-section configuration has been demonstrated to generate 500 fs pulses with 10 W of peak power while working in a fundamental mode-locking regime [123] with a reverse bias of −6 V. The relative position of absorber between 2 gain sections (straight and tapered) at approximately 1/3 of cavity length from the facet. The laser produced pulses within the range of 500–600 fs in a give current range. This demonstrates that the pulse shortening in the QD lasers is a subject of more rigorous investigation factors such as facet quality and reflectivity, length and position of absorber, design of gain section significantly contributes towards pulse shortening.

4.1.3. Excited state mode-locking in QD lasers

The discrete energy levels in QDs offer access to different emission bands from the same QD laser. The ES and GS transitions, as discussed earlier, are two independent spectral bands that are easier to access in QDs as compared to QWs. Markus et al. achieved simultaneous lasing from ES and GS, demonstrating the possibility for a ES or dual-state (i.e. ES and GS) mode-locked QD laser [158]. The ES transition is particularly interesting for the design of mode-locked QD lasers, due to the faster gain recovery times of the order of few hundred femtosecond [90] and potentially negative LEFs for the ES transition. In this context, the first demonstration of pulsed operation in an optically-pumped QD laser, emitting at 1160 nm, resulted in output pulses with durations of 20 ps [159].

In 2006, the first demonstration of a passively mode-locked InAs QD laser operating at the ES transition (wavelength 1190 nm) by Cataluna et al. [70] resulted in the generation of output pulses with durations of 7 ps. They also reported similar pulse durations for GS transitions at 1260 nm from the same device. The ES mode-locking also generated average powers of 23 mW. Repetition rates of 20.5 GHz for ES mode-locking and 21 GHz for GS mode-locking were recorded. In this work, the authors also demonstrated that switching between GS and ES mode-locking is electronically controllable by changing bias conditions. Kim et al. also demonstrated GS and ES mode-locking with similarly controlled switching in an external cavity configuration [160]. In this regime of operation, typically GS mode-locking dominates before switching to ES mode-locking as the gain current is increased. This happens due to filling of GS electron levels at higher currents, which paves the way for lasing at the ES transitions. However, reverse state switching has also been observed by Breuer et al. and was attributed to small net modal gain due to broad gain spectrum for the chirped QD layers in the active region [161,162]. At the same time they also demonstrate a transition from ES mode-locking to simultaneous dual state mode-locking with ES pulses longer than GS pulses at a fixed current [163].

Dual state mode-locking with simultaneous pulse generation via GS and ES transitions has also been reported and further adds to the versatility to QD lasers [115,164]. In this work, the authors demonstrated a two-section QD laser with spectral separation of 83 nm between GS (at 1263 nm) and ES (at 1180 nm) with simultaneous passive mode-locking from both transitions. Pulse durations of 5.9 ps from GS and 7 ps from ES mode-locking are the shortest reported from a QD laser operating in such a regime. However, this dual state mode-locking regime occurs only over a small range of gain currents for 6 V or more reverse bias to the saturable absorber. It has been argued that carrier intra-band escape and capture processes among the two states allow a stable operation only for a narrow range of gain currents. As expected, a lower repetition rate of 19.6 GHz (ES) compared to 20.1 GHz for

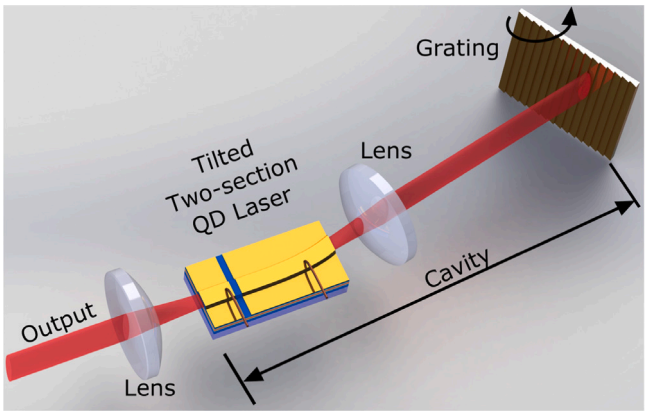

Fig. 11. A typical External-cavity (index-guided) QD laser setup. The QD laser has a curved gain section with anti-reflection coating. A grating or a mirror is added to form a cavity.

GS is observed due to higher refractive index seen by shorter wavelengths. Furthermore, this regime of operation is in agreement with Delay-Differential Equation simulations [114].

It can be seen from the results discussed above that ES and dual-state mode-locking regimes can provide stable ultrafast pulses and add versatility to the QD lasers. Moreover, ES mode-locking in QD lasers merits further investigations due to improved characteristics i.e. higher optical feedback tolerance [165] and reduced chirp as compared to GS mode-locked regime [166].

4.2. External-cavity mode-locked QD lasers

QD external-cavity mode-locked lasers (QD-ECMLL) are an interesting prospect from the perspective of tunability of pulse repetition rate and wavelength. A typical external cavity configuration for a semiconductor laser, mode-locked or otherwise, consists of a gain medium i.e. a diode laser with one facet coated with anti-reflection (AR) coating, a mirror or a grating or an output coupler, and collimating optics. A schematic of such an arrangement is shown in Fig. 11. The external grating can be mounted on a moving stage to achieve variable repetition rates. The first demonstration of a tunable QD-ECMLL was done by Choi et al. in 2005 [167]. The InAs QD laser operated at a repetition rate of 5 GHz generating 1.2 ps pulses with 1.22 W peak power after post-amplification and pulse compression. A QD-ECMLL with tunable repetition rate is demonstrated by McRobbie et al. in 2006 [168]. They demonstrated mode-locking with tunable repetition rates from as low as 350 MHz to up to 1.5 GHz. To mode-lock the QD laser, they used a QD semiconductor saturable absorber mirror (SESAM) for saturable absorption. Soon after, Xia et al. demonstrated broad repetition rate tuning from 310 MHz to 1 GHz in a two-section QD-ECMLL [169]. The laser produced 2.15 ps pulses with 150 mW peak power. They also reported a pulse energies of around 0.45 pJ at varying repetition rates. The pulse characteristics were further improved to 980 fs pulse durations with 0.5 pJ of energy and peak power of 410 mW by introducing an intracavity etalon (150 μm thickness) [170]. Around the same time Ding et al. demonstrated 44 ps pulses with 25 pJ pulse energy from a QD-ECMLL [171]. A record high peak power of 1.5 W is also demonstrated by the same laser for an operation state with 13.6 ps pulses at 1.14 GHz repetition rate with an average power of 23.2 mW, corresponding to 20 pJ pulse energy. Later, the same group of authors, with a slight modification to the EC setup, demonstrated a record low repetition rate of 191 MHz from a QD-ECMLL [172]. A 53% output coupler was used as one of the end facet of the QD-ECMLL setup to achieve stable fundamental mode-locking by providing stronger optical feedback to the QD laser. The output coupler was kept on an adjustable translation stage (with 0.1 μm step) to continuously change cavity length and achieve broad repetition rate tuning. With this arrangement they were able to tune the cavity length in the range of 15 cm to 78.5 cm, demonstrating repetition rates from 191 MHz to 1 GHz. The output pulses had durations between 9.3 ps to 12 ps over the full range of tunable repetition rates.

Wavelength tunable QD-ECMLLs have been shown to produce picosecond pulses over a broad range of wavelengths. Delfyett's group demonstrated wavelength tuning ranges of 30 nm and 50 nm from GS and ES, respectively, in a two-section QD-ECMLL with Littrow configuration [173]. For GS mode-locking a wavelength range of 1265 nm to 1295 nm was realized, whereas ES mode-locking allowed for wavelength tuning between 1170 nm to 1220 nm.

In 2012, broad wavelength tunability of 137 nm was demonstrated by Nikitichev et al. [174] from a 10 layer non-identical InAs QD gain medium. The QD-ECMLL laser operated, with a repetition rate of 740 MHz, under passive mode-locked regime over a broad range of wavelengths from 1183 nm to 1319 nm. The tuning range for the QD-ECMLL was reported to be gain current dependent and increased from 70 nm to 137 nm as the gain current is increased from 0.5 A to 1 A. The pulse width for the longest tuning range varied in the range of 12.8 ps to 39 ps, with the maximum peak power of 532 mW reported for 15.3 ps pulses at 1226 nm.

With spectrally selective elements in the external cavity, ECMLLs can used to obtain, not just low, but also ultrahigh repetition rates; for example the use of several highly selective Fiber Bragg Gratings in an external cavity allowed generation of pulses at up to 437 GHz, with a relatively high power (up to 50 mW) [175] which is difficult to achieve from a very short laser that would generate such a high repetition frequency directly.

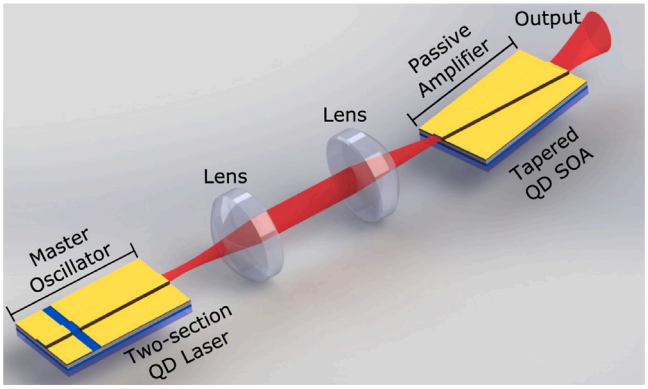

Fig. 12. Master Oscillator and Power Amplifier (MOPA) QD laser setup. The master oscillator is a pulsed two-section monolithic (or external cavity) QD laser, its output is them amplified with a tapered QD amplifier. This configuration is flexible to accommodate external cavity configuration of master oscillator with (a) mirror/grading at the far end or (b) an out-coupler after the first lens.

4.3. Master oscillator power amplifier systems

Master oscillator and power amplifier (MOPA) systems as the name suggests are designed to improve the optical power generated by the monolithic diode lasers in external cavity or otherwise. This is a very application specific requirement for example multi-photon absorption is a non-linear process and favours high optical power. Typically, in an all-semiconductor device setup, such systems incorporates a pulsed laser source as a master oscillator and a forward biased passive semiconductor optical amplifier (SOA) as shown in Fig. 12. The experimental setup further includes either a grating or an output coupler depending on the reflectivity coatings of the facet. Typical mode-locked characteristics are depicted in Fig. 13. The pulsed laser sources utilizing different pulse generation techniques such as passive mode-locking citeUlm2008,Balzer2013, colliding pulse mode-locking [176,177], Q-switching [178] and gain switching [179] has been used to achieve Watt and kW levels of peak power. The kW power levels of 1.4 kW (λ = 975 nm) [177], 2.5 kW (λ = 830 nm) [180] and 6.5 kW (λ = 850 nm) [181] have been achieved by explicitly using pulse compression techniques while these techniques have also been used to generate peak powers of few hundred watts [176,182].

It is understandable that without pulse compression the power levels from these systems will be comparatively low. Nonetheless, MOPA systems without pulse compression optical elements have demonstrated ps pulses with several watts of peak power in an all-semiconductor QD system. Weber et al. have demonstrated a high peak power of 42 W from a QD MOPA system with a pulse width of 1.37 ps post amplification [72]. They have realized an all QD MOPA system with a tapered master oscillator (MO) and a tapered amplifier. The MO is passively mode-locked and generated pulses with width as small as 1.2 ps (deconvoluted). A small TBP of 0.88 for highest peak power pulses leaves little scope for pulse compression and thus demonstrating generation of nearly transform limited high power ps pulses from an all semiconductor QD MOPA systems. The footprint of the system can be reduced further by integrating the SOA and the MO as demonstrated by Riecke et al. for QW MOPA systems [184]. QD MOPA systems in an external cavity configuration with an addition advantage of tunability has also been reported [185]. The authors have demonstrated ps pulses in the wavelength range of 1187–1283 nm using a two section QD (tilted gain section and straight absorber section) laser and a tapered QD SOA. The peak power varies in the range of ≈2.7–4.3 W over the range of achievable emission wavelength. A maximum peak power of 4.39 W at 1.226 μm is achieved by the authors. MOPA setup with a QD-ECMLL has also been investigated by Ding et al. [183]. They used a chirped volume Bragg grating (CBG) at a centre wavelength of around 1262 nm as an output coupler for the curved waveguide two-section QD laser. The grating is mounted on a movable stage to achieve variable repetition rates. Under such an arrangement they have achieved ∼1 W peak power for 9 ps pulses, from QD-ECMLL, at two different repetition rates of 1.1 GHz and 648 MHz. However, high peak power and pulse energy is achieved at both the repetition rates post amplification at high SOA current in the range of 2 to 3 A. At 1.1 GHz repetition rate peak power of 26.3 W and pulse energy of 267 pJ is demonstrated. A record high 30.3 W peak power and pulse energy of 321 pJ is reported for 648 MHz repetition rate. The pulse duration increase is minimal, from ∼9 ps to ∼10.18 ps and 10.6 ps, for 1.1 GHz and 648 MHz repetition rate respectively.

In all the configurations discussed in this section the design choice of SOA has been mostly tapered. The choice is non trivial considering the effect of such a design on saturation energy (discussed in Section 4.1.2) that determines the amplification strength or the maximum achievable output power from the amplifier. To summarize, all semiconductor MOPA systems are compact, ultrafast, high peak power systems that can used for applications that rely on high optical power to exploit non-linear response from its samples.

4.4. Applications

Mode-locked edge-emitting QD lasers are of great interest for applications such as optical communications, optical clock generation and recovery, optical comb generation, microwave over fibre applications, and biomedical/biophotonics applications.

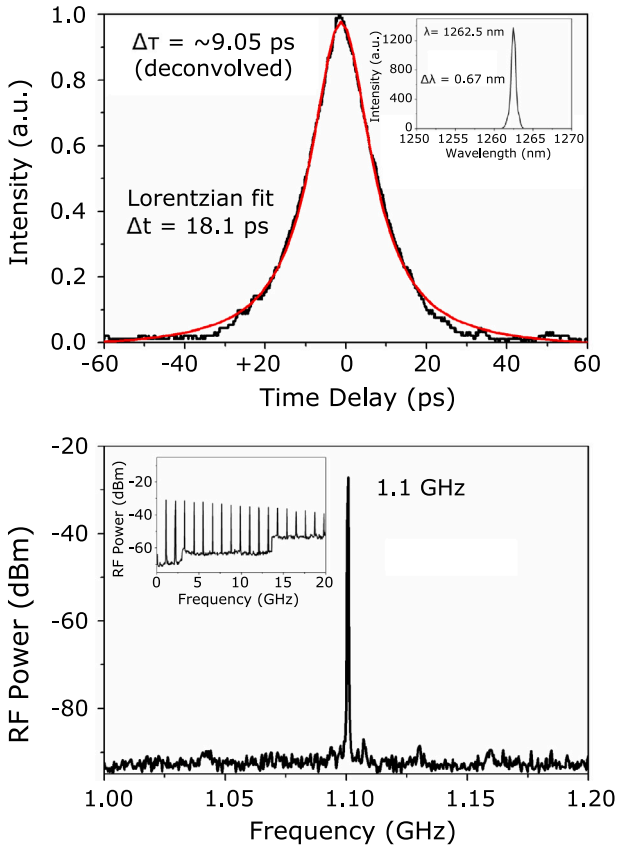

Fig. 13. Typical characteristics of a mode-locked QD laser in MOPA configuration. Top: Typical pulse shape and durations conveniently obtained with such configuration, inset: corresponding optical spectrum. Bottom:RF spectrum under mode-locked operation at 1 GHz repetition rate, inset: RF spectrum depicting higher harmonics over a 20 GHz span.
Source: Adapted and Reproduced with permission, from [183] 2012, Optical Society of America.

The state-of-the-art mode-locked QD edge emitters emitting in the low dispersion O-band wavelength region of optical fibers can potentially be used as sources for metropolitan area optical networks. Return-to-zero digital modulation at 40 GBit/s using QD MLLs was demonstrated in some of the first experiments on high repetition rate ML in QD lasers [140]. High repetition rate sub-picosecond sources with relatively low timing jitter are of particular interest for optical time-division multiplexing systems (OTDMs). Hybridly mode-locked QD laser operating at the wavelength of 1300 nm, at a repetition rate of 40 GBit/s, have been demonstrated to be suitable for OFDM links at transmission rates up to 160 Gb/s by interleaving up to 4 pulse streams [186]. For this purpose, laser pulses, originally highly chirped and with length in picosecond range, were characterized using Frequency Resolved Optical Gating (FROG) technique, which allowed the intensity and phase profile to be retrieved, in turn allowing for an optimized dispersion compensation scheme using a free space dispersion compensator to be designed, bringing the pulse durations down to 0.7 ps in a broad range of parameters. A similar procedure of dispersion compensation (in this case, using a stretch of SMF-28 fiber) informed by detailed FROG characterization allowed the pulses generated by single-section QDH ML lases at 1570 nm (repetition rate 48 GHz) to be compressed down to 374 fs [187], showing the possibility of even higher aggregate bit rates in a potential OFDM system.

QD mode-locked sources also exhibit better tolerance towards defect related efficiency degradation as compared to QW devices along with broad temperature resilience [188,189]. These attributes are highly desirable for space based communication applications.

Design and fabrication flexibility of QDMLLs also makes them suitable for low-repetition rate applications. One such application is optical clocks for computers [190]. The low-repetition rate on-board mode-locked laser can help avoid cross-talk among electrical (data and clock) signals [191].

As well as clock generation, burst mode clock recovery from has also been demonstrated by injecting data packets at 40 GBit/s, deteriorated by propagation through 52 km of fiber, into mode locked Quantum Dash lasers [192] the locking time was 25 ns, substantially shorter than the packet length used (286 ns).

For a number of applications, e.g. radio over fibre, it is not the short pulses as such that are required but a stable optoelectronically generated radio frequency signal — the intermodal separation frequency or its harmonic. The potential of QD mode-locked lasers to be used as a compact RF source has been demonstrated in a number of papers, see e.g. [141,193], in which a 10 GHz signal was generated directly from the saturable absorber of a passively mode-locked laser, without the need for a fast photodetector.

Electric signal at higher frequencies can also be generated using mode locked QD lasers. For example, THz beat signals tunable between 1 and 2.1 THz have been generated using a single section C-band (1550 nm) InAs/InP QD mode-locked laser operated in an external cavity containing two Bragg gratings each selecting one of the lines from the ML spectrum. With one grating having a fixed reflectance peak and the other a tunable one, it was possible to tune their frequency separation in increments of an intermodal separation of the laser, while the ML process ensured phase locking of the modes so that a narrow THz line could be expected [194]. A similar approach was followed later using a tunable optical filter in the external cavity, resulting in the beat frequency tuning from 1 to 2.9 THz [195]. Interestingly, THz photomixers can also be designed using a QD material [196–198], opening a path to an all-QD integrated system for THz signal generation.

In frequency domain, the output of any mode locked laser is a comb of narrow, frequency-synchronized equidistant lines. Optical combs can find use as compact, cost-effective sources for Wavelength Division Multiplexed (WDM) optical communications, as well as in a number of applications in metrology. Quantum Dot and Quantum Dash lasers are natural candidates for such applications due to robust mode locked operation with wide emission spectra. Importantly, the frequency chirp properties of the laser emission, which in frequency domain manifest themselves in nontrivial phase relations between different modes in the comb but do not affect the frequency interval between them, are not important for this range of applications. Thus single- and double-section mode locked 1.55 μm Quantum Dot and Quantum Dash lasers, which may be not ideal for use as short pulse sources due to their strongly chirped emission, have found their natural application in comb generation. Choosing the laser length such that the spectral spacing between modes is near the channel separation in a WDM system, each line in the comb can be used to carry a WDM channel. The spectral efficiency of the channel, and hence the channel bit rate, is defined by the modulation methods. In addition to simple on–off keying (OOK), modulation methods ranging from Manchester encoding and 4-level pulse amplitude modulation (4-PAM) [199–202] and Differential Quaternary Phase-Shift Keying (DQPSK) [203], to Quadrature Amplitude Modulation (16-QAM) [204–206] have been realized successfully. The latter technique allowed record aggregate transmission rates of more than 12 TBit/s to be transmitted [204,206]. The specific implementations included (16-QAM 47 × 32 GBaud PDM) from a single laser with 47 individual modes spanning the spectral range of 1531.60 nm to 1544.20 nm [204] and 16QAM 56 × 28-GBd PDM [206,207] in a laser with 56 modes. In the latter case, transmission over 100 km of standard single-mode fibre was demonstrated.

Optical combs emitted by single-section ML QD and QDash lasers have been used for efficient, low-noise and low-cost Wavelength Division Multiplexed Passive Optical Networks (PONs), both as direct multiwavelength sources [208]and by each of the ML laser lines locking a specially designed polarization insensitive Fabry–Perot laser source directly modulated at a required rate (2.5 GHz) [208,209] Mode locked single-section Quantum Dash lasers were also used for Orthogonal Frequency Division Multiplexing (OFDM) in a single sideband direct detection OFDM transmission experiments [210]. The single-subband OFDM signal consisting of 74 subcarriers each encoded with 16QAM was modulated onto 33 significant modes of a laser with a 48 GHz intermodal interference.

Double-section mode locked lasers can also be used for comb generation [211,212]. A highly stable comb of more than 60 modes/lines with an intermodal distance of 4.5 GHz was realized using InAs/InP (100) QD passively and hybridly mode locked lasers. The exact spectral position of the comb in that work was determined by CW light injection significantly (20 nm) detuned from the peak of free running laser spectrum, so the nature of the comb modes was identified as modulation side bands superimposed on the injection line by the absorber section of the laser working as an electro-optic modulator, rather than mode locking spectrum modes as such [211]. In addition to being used as carriers for WDM transmission of channels using coherent modulation formats (different types of PSK or QAM), ML QD lasers can also provide a set of optical local oscillators (LO) for each channel at the receiving end. In [213], transmission of an aggregate net data rate of 3.9 Tbit/s (23 × 45 GBd QPSK with Polarization Division Multiplexing) over 75 km standard single-mode fiber was achieved with using two single-section QD ML lasers at the transmitting end (to generate carriers) and at the receiving end (to generate LO signals). The two ML lasers did not have to be synchronized with each other and had slightly different (by 4 MHz) free spectral ranges. Detailed examples of the design and use of QD and QDash (QDH) lasers for comb generation and WDM communications, as well as some techniques of their stabilization (see below) are given in [214]

The use of QD/QDH lasers as both sources and LOs has been shown to be particularly attractive for cost-sensitive applications such as a proposed coherent Passive Optical Networks (PON); the use of same QDH based comb source as a modulated signal source for the downstream link and a local oscillator for a number of upstream signals received at the Optical Line Terminal has been demonstrated [215]

Optical combs emitted by mode-locked Quantum Dot or Dash lasers can also find applications in microwave photonics. By modulating all the lines in the comb emitted by a single-section QDH laser by the same microwave signal, temporally separating the lines using a length of fibre, shaping the OFC spectrum using a programmable optical filter, and then detecting the signal to convert to microwave, a microwave photonic filter has been demonstrated, widely tunable from 0.1 to 7.5 GHz [216]. The performance of the filter was reported to improve with the number of lines in the comb.

Biophotonics is another niche area that can immensely benefit from mechanically rugged, compact and low maintenance QDMLLs. By exploiting non-linear response of biological samples to a short intense pulse of radiation internal organs can be imaged non-invasively with different level of details using different imaging techniques such as single-, two- and multi-photon fluorescence imaging. The wavelength window for these imaging techniques to be most effective is between 600 nm and 1.3 μm. It corresponds to maximum transmission through the tissue thus allowing greater penetration for better in-depth images. Non-linear bio-imaging using all semiconductor mode-locked laser setup has been demonstrated with tens of watts of peak power [217,218]. A MOPA system with 30.3 W peak power at 1.26 μm has been used to image 15 μm crimson micro-spheres using two-photon fluorescence imaging [183].

Recently the operating range of ML QD lasers has been extended from the relatively long wavelengths of 1.2–1.3 and 1.5 μm to the red side of the visible spectrum (730 nm) by using InP dots grown on InGaAsP substrate. 6 ps long pulses at a repetition rate of 12.6 GHz were achieved [219]. This design is promising for applications such as high-resolution biomedical fluorescence imaging, targeted cell transfection and biological nanosurgery [219].

Due to the limited power from stripe edge-emitting lasers, particularly Quantum Dot ones, MOPA systems are likely to remain the design of choice for this group of applications. More detail on the use of picosecond semiconductor lasers, including Quantum Dot ones, for biophotonics related applications may be found in [220].

5. Stabilisation of mode-locked quantum dot and dash lasers

A significant limitation to the operation of mode-locked lasers as either sources of short pulse stream or a frequency comb for WDM applications is posed by their noise properties. These include, firstly, the amplitude noise (of particular importance to WDM applications is Mode Partition Noise, which is always present in the emission of a selected mode of a multimode source, even if the amplitude noise of total emission is relatively low), and, secondly, the phase noise which is the main limitation to the pulse jitter (when the laser is used as a short pulse source), the individual mode linewidth (for comb applications), and the RF or terahertz beat frequency linewidth (for microwave over fiber and THz applications) [221]. Some ML QD and QDH laser designs show remarkably good noise performance under free-running operation [207,222], with free-running modal linewidth below 1 kHz achieved in a recent study [207]. Moreover, in some communication applications as described above, the use of optimized modulation and (balanced) detection methods can be used for overcoming Mode Partition Noise [199,200].

More often though, some laser stabilization technique is required, particularly if low noise is needed within a reasonable range of parameters rather than in a narrow "sweet spot". The reported methods of stabilizing QD and QDH ML lasers, suppressing both amplitude and phase noise, included active/hybrid mode locking [116,223,224], injection of external optical signal either within or outside the mode locked spectrum, on its own [211,225–228] or combined with electrical modulation [224], and external cavity self-injection systems [204,226,228–233] including specialized dual-cavity self-injection schemes [232,234].

The former three methods have been compared in [224], and it was shown that combination of hybrid mode locking with side band injection seeding provided the narrowest jitter (121 fs), with in-band injection locking resulting in a jitter of 240 fs, and conventional hybrid mode locking, of about 620 fs, in the same laser.

The additional advantage of external injection locking is that it allows the laser comb to be anchored to a stabilized optical frequency, which may be useful for some WDM applications where the grid of carrier frequencies is standardized. It is also possible to tune the wavelength of the stabilized pulse train, e.g. simultaneous coherent optical injection into two nearest modes of a QD laser mode-locked at 10 GHz allowed the tuning of the laser emission over about 10 nm (the width of the spectrum of the free-running laser; the spectrum of the injected laser was narrowed to approximately 2 nm) [225].

An alternative method of stabilising the absolute frequency/wavelength of a comb generator [235] involves using (electrically) active wavelength locking with a stabilised narrowband optical filter (etalon) used to determine the desired optical frequency of one of the modes.

The use of external cavity designs/external optical feedback, on the other hand, has the advantage of being a passive technique, requiring neither an external electrical nor optical signal. With this technique, the optical mode linewidth can be narrowed by a factor of the order of the ratio of the optical lengths of the external cavity and the intrinsic laser cavity. With a very long (~8 m, corresponding to a round-trip of >50 ns) external cavity, a laser stabilized with this technique allowed record WDM signal transmission rate as described in the previous section [204].

The use of some of the stabilization methods above allows, in addition to frequency stabilization, also some control over the wavelength separation between the lines in the comb (thus the repetition frequency of pulses, or microwave frequency of the generated signal). For instance, in the analysis of [224], the conventional hybrid mode locking allowed tuning of the repetition frequency of about 10 MHz, hybrid modulation with in-band injection locking, of 167 MHz, and with side-band injection, of 342 MHz, in the range of frequencies of 39.7–40 GHz. This may be related to the spectral narrowing under injection operation.

In the case of (dual-cavity) external feedback [232], the variation of the round-trip times of one of the cavities (which was in the range of ~100 ns) by approximately 40 ps allowed the mode-locking frequency to be tuned by about 70 MGz around a 40.6 GHz mean value, i.e. comparable to hybrid mode locking.

Finally, it may be noted that the narrowing of ML spectrum under external injection locking culminates, at sufficiently high injection light intensity, in complete suppression of ML pulsations and switching to CW operation. Thus by switching the injecting light on and off (or from low to high intensity), it is possible to trigger the ML regime correspondingly off and on, which was recently demonstrated in a 2-section 1.3 μm QD ML operating at the repetition frequency of 5 GHz, with subnanosecond on–off transient times and, correspondingly, subnanosecond durations of on and off intervals [236].

6. Mode-locked QD lasers on silicon; the integration prospects

The optical setups for applications and laser stabilization considered in the previous sections involve fibre of free-space elements.

One of the major advantages of QD lasers in general is their amenability to on-chip integration with passive waveguides and, potentially, integrated circuits, either by means of hybrid (bonding) techniques, or by monolithic integration, including direct growth on silicon substrates [237]. The latter option stems from the relative resilience of QD active layers to dislocations that are formed when a III-V compound is grown on a silicon substrate. Integrating QD lasers with silicon photonics has attracted considerable

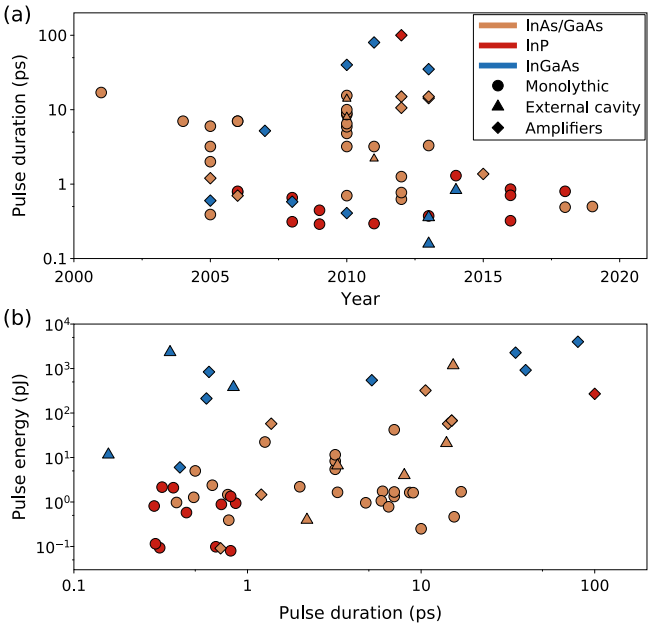

Fig. 14. QD MLL in this review. (a) pulse duration vs year, (b) pulse energy vs pulse duration.

attention, which recently included specifically mode-locked lasers, a trend which is likely to continue in the future. Recent reviews of the performance and promise of QD lasers on Si [238,239] highlight mode-locked operation as one of the drivers of integration on silicon as well as an enabling technology for important potential applications.

A double-section colliding-pulse mode-locked QD ML laser hybridly integrated by bonding to a silicon stripe waveguide showed error-free NRZ amplitude modulated transmission at 10 GBit/s on three frequency channels selected from the laser comb, without any external stabilization (though the authors noted that not all ML modes had low enough noise to be used as transmission channels). [212]. A single-section passively mode-locked QD laser was grown directly on on-axis (001) GaP/Si substrate, demonstrating a low threshold current of 34 mA and stable emission of 490 fs pulses at a repetition rate of 31 GHz, with the spectral width of more than 5 nm [222,240]. This was followed by a double-section ML QD laser being grown directly on a similar Si substrate, generating slightly longer pulses (1.7 ps) at a lower repetition rate (9 GHz), with over 100 lines (5.5 nm comb width at −3 dB) and an extremely narrow width of individual line, down to just 400 Hz (pulse jitter of 9 fs) at the optimal performance conditions, despite no specific stabilization scheme present [41,222]. A similar design, with a shorter cavity to give a mode spacing of 20 GHz and with chirped dot design in order to increase the gain bandwidth and hence the width of the ML spectrum, produced 5-ps pulses with a record-low values of the integrated timing jitter of 82.7 fs from 4 to 80 MHz of the ITU-T specified range and of pulse to pulse jitter of 6fs. The wide gain bandwidth allowed a very broad ML spectrum, with a 3 dB bandwidth of 6.1 nm in wavelength or about 1.2 THz in frequency, which is very promising for optical combs applications including but not restricted to TBit/s WDM transmission [87,222]

From the ML functionality perspective, integration with silicon photonics opens a path to robust, compact realization of elements such as on-chip optical feedback and spectrum shaping elements to stabilize the laser performance in a broad operating range, improve and tailor the ML parameters, as well as directly enabling application-specific photonic integrated circuits including ML lasers, as discussed for a generic ML semiconductor laser in [241]. In addition to advantages considered in previous sections, we note that it was mentioned [241] that QD based on-chip laser sources can offer advantage in pulse energy over QW active media in some future integrated circuits due to the lower confinement factor of the QD active medium.

Successful stabilisation of double-section [233] and single-section [242] on-Si QD/QDH lasers using off-chip external feedback has been reported. An on-chip realisation of a feedback scheme for a broadband ML semiconductor laser is likely to be less straightforward due to the possible effect of the waveguide dispersion on the phases of reflected modes [243]; a solution proposed in [243] involves frequency selective, phase-controlled feedback for just two of modes in the comb.

Extending the spectral width of a comb generated by a hybrid silicon/QD double-section passively mode locked laser by optical injection through a grating coupler realized in the silicon waveguide has been demonstrated recently [244].

7. Conclusion and future perspectives

Passively mode-locked edge-emitting QD lasers have advanced significantly since their first demonstration almost two decades ago. Ultrafast QD lasers have matured from early laboratory setups to practical and potentially fully integrable laser sources for pico- and femtosecond pulses. The unique properties of QD active media, namely, the broad gain bandwidths, ultrafast recovery

Table 3
QD MLLs in this review. (Mono: Monolithic Lasers, External: EC Lasers, Amp: MOPA setups).

Year	Laser type	Pulse duration,ps	Peak Power, W	λ, nm	Rep rate, MHz	Ref.
2001	Mono	17	0.1	1278	7400	[20]
2004	Mono	7	6	1300	35000	[145]
2005	Mono	3.2	1.7	1260	5000	[190]
2005	Mono	0.39	2.5	1255	21000	[21]
2005	Mono	2	1.1	1255	21000	[21]
2005	Mono	6	0.29	1250	5000	[191]
2006	Mono	7	0.19	1190	20500	[70]
2006	Mono	7	0.24	1260	21000	[70]
2006	Mono	0.8	0.1	1567	42200	[148]
2006	Mono	0.78	0.5	1300	24000	[23]
2008	Mono	0.657	0.15	1555	92500	[245]
2008	Mono	0.312	0.3	1540	92000	[149]
2009	Mono	0.445	1.3	1580	46000	[150]
2009	Mono	0.29	2.8	1560	50000	[246]
2010	Mono	10	0.025	1220	12100	[163]
2010	Mono	15.5	0.03	1290	12300	[163]
2010	Mono	5.9	0.18	1260	20100	[115]
2010	Mono	6.5	0.12	1263	20000	[115]
2010	Mono	8.6	0.19	1190	19600	[115]
2010	Mono	9	0.18	1180	20000	[115]
2010	Mono	4.8	0.2	1295	10000	[225]
2010	Mono	3.2	2.6	1250	14650	[247]
2010	Mono	0.7	0.006	1310	40000	[186]
2011	Mono	0.295	0.39	1540	437000	[175]
2011	Mono	3.2	3.6	1250	14650	[248]
2012	Mono	0.627	3.8	1260	10000	[124]
2012	Mono	1.26	17.7	1260	10000	[124]
2012	Mono	0.77	1.9	1340	45000	[73]
2013	Mono	0.374	5.6	1583	48000	[187]
2013	Mono	3.3	0.5	1250	10000	[154]
2014	Mono	1.3		1570	47500	[221]
2016	Mono	0.322	6.7	1560	45500	[86]
2016	Mono	0.855	1.10	1580	29800	[249]
2016	Mono	0.707	1.25	1580	55600	[249]
2018	Mono	0.49	2.6	1318	30700	[240]
2018	Mono	0.8	1.67	1540	34462	[231]
2019	Mono	0.5	10	1300	13240	[127]
2019	Mono	1.7	0.028	1310	9400	[41]
2020	Mono	6	0.023	735	12550	[219]
2021	Mono	0.464	0.03	1570	81000	[156]
1995	External	3.3	2			[157]
2010	External	8	0.5	1274	1140	[171]
2010	External	14	1.5	1274	1140	[171]
2011	External	2.2	0.18	1288	1000	[170]
2012	External	15.3	77	1226	740	[174]
2013	External	0.158	73.4	835	1035	[181]
2013	External	0.358	6500	835	345	[181]
2014	External	0.83	460	1040	1500	[250]
2005	Amp	1.2	1.22	1265	5000	[167]
2005	Amp	0.6	1400	975	95	[177]
2006	Amp	0.7	0.13	1230	20000	[251]
2007	Amp	5.2	105	783	500	[217]
2008	Amp	0.58	366	922	4000	[182]
2010	Amp	40	23	1063	80	[184]
2010	Amp	0.408	14.7	920	3326	[176]
2011	Amp	80	50	1066	1.25	[178]
2012	Amp	100	2.7	1546.9	1000	[252]
2012	Amp	10.6	30.3	1262	648	[183]
2012	Amp	15	4.5	1225	1316	[185]
2013	Amp	14.3	4	1230		[253]
2013	Amp	15	4.5	1225		[253]
2013	Amp	35	65	1063	1	[179]
2015	Amp	1.37	42	1260	1.76E−02	[72]

times, and low saturation fluences, have enabled the demonstration of compact ultrafast semiconductor lasers with repetition rates up to 238 GHz, pulse durations as short as 312 fs, and pulse energies of 321 pJ (in MOPA configuration). Despite these breakthrough results, further progress is necessary to improve QD lasers performance and to open new application areas.

Above, we put together all the main results achieved during development of mode-locked semiconductor lasers and amplifiers These data are presented in Table 3. Moreover, the two main trends of pulse duration shortening with the year of laser appearance and pulse energy vs pulse duration trade-off are reflected additionally in Fig. 14.

Looking forward at further developments, it would appear that monolithic integration and on-silicon growth may be the main area of development. With good performance QD mode-locked lasers already realised as discussed above, the natural next step appears to be the use of integration with passive silicon optics to increase functionality, with on-chip solutions for feedback stabilisation and spectral shaping/dispersion compensation looking like the natural first candidates. Reports of successful stabilisation of on-Si QD lasers using off-chip external feedback of a double-section [233] and single-section [242] laser devices inspire some optimism that on-chip realisation may follow soon.

As regards applications, at this point it looks as if, while historically mode-locked lasers including QD ones have been seen first and foremost as sources of short pulses, currently the applications involving optical comb generation, from metrology to WDM tele- and datacommunication links, are the more immediately promising. However high-peak power short pulses may also find their use eventually, e.g. in nonlinear applications and possibly some return-to-zero communication links

The majority of mode-locked QD lasers have been based on the InGaAs/GaAs material system, providing laser emission in the wavelength range from 1100 nm to 1300 nm. Further development of QD active media and the use of other material systems is expected to extend the wavelength range of mode-locked QD lasers in the future. Mode-locked lasers based on InAs/InP QDs have already been demonstrated, resulting in the generation of femtosecond pulses at wavelengths from 1530 nm to 1590 nm and potentially allowing for laser operation at wavelengths up to 1900 nm. At shorter wavelengths, the InGaN material system may enable the realization of ultrafast QD devices with laser emission in the visible part of the optical spectrum.

Finally, mode-locked QD lasers would significantly benefit from further increases in output pulse energies and shorter pulse durations. Current designs are limited, according to both experimental results and theoretical predictions, to pulse energies of few pJ and pulse durations of several hundred femtosecond. However, the coherent combination of the full gain bandwidth of QD active media would allow for the generation of sub-100 fs pulse durations with peak powers in the kW range. Thus, mode-locked QD lasers have substantial potential for further improvements and progress will depend on the investigation of novel QD structure layouts and edge-emitter designs.

Declaration of competing interest

The authors declare that they have no known competing financial interests or personal relationships that could have appeared to influence the work reported in this paper.

Acknowledgements

The authors acknowledge financial support from Engineering and Physical Sciences Research Council (EPSRC) (Grant no. - EP/R024898/1, EP/W002868/1, and EP/S018395/1) and European Union's Horizon 2020 program (decision No. 824996). N. B. Chichkov acknowledges funding from the European Union Horizon 2020 research and innovation programme under the Marie Skłodowska-Curie Actions grant agreement No 843801. A. Gorodetsky thanks MagicPlot LLC for providing a copy of MagicPlot Pro used for preparation of Fig. 14.

References

[1] E.P. Harris, Spiking in current-modulated cw GaAs external cavity lasers, J. Appl. Phys. 42 (2) (1971) 892–893, http://dx.doi.org/10.1063/1.1660125, http://aip.scitation.org/doi/10.1063/1.1660125.

[2] P.T. Ho, L.A. Glasser, E.P. Ippen, H.A. Haus, Picosecond pulse generation with a cw GaAlAs laser diode, Appl. Phys. Lett. 33 (3) (1978) 241–242, http://dx.doi.org/10.1063/1.90312.

[3] J.P. van der Ziel, Active mode locking of double heterostructure lasers in an external cavity, J. Appl. Phys. 52 (7) (1981) 4435–4446, http://dx.doi.org/10.1063/1.329358, http://aip.scitation.org/doi/10.1063/1.329358.

[4] E.P. Ippen, D.J. Eilenberger, R.W. Dixon, Picosecond pulse generation by passive mode locking of diode lasers, Appl. Phys. Lett. 37 (3) (1980) 267–269, http://dx.doi.org/10.1063/1.91902.

[5] H.-F. Liu, M. Fukazawa, Y. Kawai, T. Kamiya, Gain-switched picosecond pulse (<10 ps) generation from 1.3 mu m InGaAsP laser diodes, IEEE J. Quantum Electron. 25 (6) (1989) 1417–1425, http://dx.doi.org/10.1109/3.29277, http://ieeexplore.ieee.org/document/29277.

[6] D. Bimberg K. Ketterer, E.H. Böttchër, E. Scöll, Gain modulation of unbiased semiconductor lasers: ultrashort light-pulse generation in the 0.8 μm–1.3 μm wavelength range, Int. J. Electron. 60 (1) (1986) 23–45, http://dx.doi.org/10.1080/00207218608920760, http://www.tandfonline.com/doi/abs/10.1080/00207218608920760.

[7] A. Weber, M. Schell, G. Fischbeck, D. Bimberg, Generation of single femtosecond pulses by hybrid mode-locking of a semiconductor laser, IEEE J. Quantum Electron. 28 (10) (1992) 2220–2229, http://dx.doi.org/10.1109/3.159529, http://ieeexplore.ieee.org/document/159529.

[8] P.A. Morton, J.E. Bowers, L.A. Koszi, M. Soler, J. Lopata, D.P. Wilt, Monolithic hybrid mode-locked 1.3 μm semiconductor lasers, Appl. Phys. Lett. 56 (2) (1990) 111–113, http://dx.doi.org/10.1063/1.103046.

[9] J.E. Bowers, P.A. Morton, S.W. Corzine, A. Mar, Actively mode-locked semiconductor lasers, IEEE J. Quantum Electron. 25 (6) (1989) 1426–1439.

[10] M.C. Wu, Y.K. Chen, T. Tanbun-Ek, R.A. Logan, M.A. Chin, G. Raybon, Transform-limited, 1.4 ps optical pulses from a monolithic colliding-pulse mode-locked quantum well laser, Appl. Phys. Lett. 57 (8) (1990) 759–761, http://dx.doi.org/10.1063/1.103413.

[11] P.J. Delfyett, C.-H. Lee, L.T. Florez, N.G. Stoffel, N.C. Andreadakis, T.J. Gmitter, G.A. Alphonse, J.C. Connolly, Generation of sub-picosecond high-power optical pulses from a hybrid mode-locked semiconductor laser system, Opt. Lett. 15 (23) (1990) 1371–1373, http://link.springer.com/chapter/10.1007/978-3-642-84269-6_25%5Cnhttp://link.springer.com/chapter/10.1007/978-3-642-84269-6_25#page-1.

[12] P.J. Delfyett, Y. Silberberg, G.A. Alphonse, Hot-carrier thermalization induced self-phase modulation in semiconductor traveling wave amplifiers, Appl. Phys. Lett. 59 (1) (1991) 10–12, http://dx.doi.org/10.1063/1.105561.

[13] P.J. Delfyett, L. Florez, N. Stoffel, T. Gmitter, N. Andreadakis, G. Alphonse, W. Ceislik, 200-Fs optical pulse generation and intracavity pulse evolution in a hybrid mode-locked semiconductor diode-laser/amplifier system., Opt. Lett. 17 (9) (1992) 670–672, http://dx.doi.org/10.1364/OL.17.000670, http://www.ncbi.nlm.nih.gov/pubmed/19794593.

[14] S. Kono, H. Watanabe, R. Koda, T. Miyajima, M. Kuramoto, 200-Fs pulse generation from a gainn semiconductor laser diode passively mode-locked in a dispersion-compensated external cavity, Appl. Phys. Lett. 101 (8) (2012) http://dx.doi.org/10.1063/1.4747808.

[15] T. Schlauch, J.C. Balzer, A. Klehr, G. Erbert, G. Tränkle, M.R. Hofmann, Femtosecond passively modelocked diode laser with intracavity dispersion management, Opt. Express 18 (23) (2010) 24316–24324, http://dx.doi.org/10.1364/OE.18.024316s, http://www.opticsexpress.org/abstract.cfm?URI=oe-18-23-24316%5Cnhttp://www.opticsinfobase.org/DirectPDFAccess/B0FC9003-0F33-13B1-FEF1129FC022A4E2_207117/oe-18-23-24316.pdf?da=1&id=207117&seq=0&mobile=no%5Cnhttp://www.opticsinfobase.org/oe/abstract.cfm?uri.

[16] B. Döpke, R.H. Pilny, C. Brenner, A. Klehr, G. Erbert, G. Tränkle, J.C. Balzer, M.R. Hofmann, Self-optimizing femtosecond semiconductor laser, Opt. Express 23 (8) (2015) 9710, http://dx.doi.org/10.1364/OE.23.009710, https://www.osapublishing.org/abstract.cfm?URI=oe-23-8-9710.

[17] P.P. Vasil'ev, A.B. Sergeev, Generation of bandwidth-limited 2 ps pulses with 100 ghz repetition rate from multisegmented injection laser, Electron. Lett. 25 (16) (1989) 1049–1050.

[18] Steve Sanders, Lars Eng, Joel Paslaski, Amnon Yariv, 108 Ghz passive mode locking of a multiple quantum well semiconductor laser with an intracavity absorber, Appl. Phys. Lett. 56 (4) (1990) 310–311, http://dx.doi.org/10.1063/1.103187.

[19] E.A. Avrutin, J.H. Marsh, E.L. Portnoi, Monolithic and multi-GigaHertz mode-locked semiconductor lasers: Constructions, experiments, models and applications, IEE Proc.-Optoelectronics 147 (4) (2000) 251–278, 10.1049/ip-opt http://ieeexplore.ieee.org/stampPDF/getPDF.jsp?arnumber=1404613&isnumber=30468.

[20] X. Huang, A. Stintz, H. Li, L.F. Lester, J. Cheng, K.J. Malloy, Passive mode-locking in 1.3 μm two-section InAs quantum dot lasers, Appl. Phys. Lett. 78 (19) (2001) 2825–2827, http://dx.doi.org/10.1063/1.1371244.

[21] E.U. Rafailov, M.A. Cataluna, W. Sibbett, N.D. Il'Inskaya, Y.M. Zadiranov, A.E. Zhukov, V.M. Ustinov, D.A. Livshits, A.R. Kovsh, N.N. Ledentsov, High-power picosecond and femtosecond pulse generation from a two-section mode-locked quantum-dot laser, Appl. Phys. Lett. 87 (2005) 081107, http://dx.doi.org/10.1063/1.2032608.

[22] E.U. Rafailov, M.A. Cataluna, W. Sibbett, Mode-locked quantum-dot lasers, Nat. Photonics 1 (7) (2007) 395–401, http://dx.doi.org/10.1038/nphoton.2007.120, http://ieeexplore.ieee.org/document/5730035/ http://www.nature.com/articles/nphoton.2007.120.

[23] M.G. Thompson, A. Rae, R.L. Sellin, C. Marinelli, R.V. Penty, I.H. White, A.R. Kovsh, S.S. Mikhrin, D.A. Livshits, I.L. Krestnikov, Subpicosecond high-power mode locking using flared waveguide monolithic quantum-dot lasers, Appl. Phys. Lett. 88 (2006) 133119, http://dx.doi.org/10.1063/1.2186110.

[24] M.G. Thompson, A.R. Rae, M. Xia, R.V. Penty, I.H. White, InGaAs Quantum-Dot Mode-Locked Laser Diodes, IEEE J. Sel. Top. Quantum Electron. 15 (3) (2009) 661–672.

[25] R.N. Hall, G.E. Fenner, J.D. Kingsley, T.J. Soltys, R.O. Carlson, Coherent light emission form GaAs junctions, Phys. Rev. Lett. 9 (9) (1962) 366–369.

[26] T.M. Quist, R.H. Rediker, R.J. Keyes, W.E. Krag, B. Lax, A.L. McWhorter, H.J. Zeigler, Semiconductor maser of GaAs, Appl. Phys. Lett. 1 (4) (1962) 91–92, http://dx.doi.org/10.1063/1.1753710.

[27] M.I. Nathan, W.P. Dumke, G. Burns, F.H. Dill, G. Lasher, Stimulated emission of radiation from GaAs p-n junctions, Appl. Phys. Lett. 1 (3) (1962) 62–64, http://dx.doi.org/10.1063/1.1777371.

[28] N. Holonyak, S.F. Bevacqua, Coherent (visible) light emission from ga(as1-xpx) junctions, Appl. Phys. Lett. 1 (4) (1962) 82–83, http://dx.doi.org/10.1063/1.1753706, arXiv:0003-6951.

[29] Z.I. Alferov, R.F. Kazarinov, Semiconductor laser with electric pumping, 1963.

[30] H. Kroemer, A proposed class of hetero-junction injection lasers, in: Proceedings of the IEEE, Vol.51, 1963, pp. 1782–1783.

[31] H. Kressel, H. Nelson, Close-confinement gallium arsenide pn junction lasers with reduced optical loss at room temperature, RCA Rev. 30 (1969) 106–113.

[32] I. Hayashi, M.B. Panish, P.W. Foy, A Low-Threshold Room-Temperature Injection Laser, IEEE J. Quantum Electron. 5 (1969) 211.

[33] Z.I. Alferov, V.M. Andreev, E.L. Portnoi, M.K. Trukan, Injection lasers based on heterojunctions of the AlAs-GaAs system having a low emission threshold at room temperature, Fizika I Tekhnika Poluprovodnikov 3 (1969) 1328–1332.

[34] I. Hayashi, M.B. Panish, P.W. Foy, S. Sumski, Junction lasers which operate continuously at room temperature, Appl. Phys. Lett. 17 (3) (1970) 109–111.

[35] Z.I. Alferov, V.M. Andreev, D.Z. Garbuzov, Y.V. Zhilyaev, E.P. Morozov, E.L. Portnoi, V.G. Trofim, Investigation of the influence of the AlAs–GaAs heterostructure parameters on the laser threshold current and the realization of continuous emission at room temperature, Sov. Phys.-Semicond. 4 (9) (1971) 1573–15775.

[36] R. Dingle, W. Wiegmann, C.H. Henry, Quantum states of confined carriers in very thin $Al_xGa_{1-x}As$-gaas-$Al_xGa_{1-x}As$ heterostructures, Phys. Rev. Lett. 33 (14) (1974) 827–830, http://dx.doi.org/10.1103/PhysRevLett.33.827, https://link.aps.org/doi/10.1103/PhysRevLett.33.827.

[37] Y. Arakawa, H. Sakaki, Multidimensional quantum well laser and temperature dependence of its threshold current, Appl. Phys. Lett. 40 (1982) 939, http://dx.doi.org/10.1063/1.92959.

[38] M. Grundmann, J. Christen, N.N. Ledentsov, J. Böhrer, D. Bimberg, S.S. Ruvimov, P. Werner, U. Richter, U. Gösele, J. Heydenreich, V.M. Ustinov, A.Y. Egorov, A.E. Zhukov, P.S. Kop'ev, Z.I. Alferov, Ultranarrow Luminescence Lines from Single Quantum Dots, Phys. Rev. Lett. 74 (20) (1995) 4043.

[39] V.M. Ustinov, A.E. Zhukov, A.Y. Egorov, N.A. Maleev, Quantum Dot Lasers, Oxford University Press, New York, 2003.

[40] V.A. Shchukin, N.N. Ledentsov, D. Bimberg, Epitaxy of nanostructures, in: NanoScience and Technology, Springer Berlin Heidelberg, Berlin, Heidelberg, 2004, http://dx.doi.org/10.1007/978-3-662-07066-6, http://link.springer.com/10.1007/978-3-662-07066-6.

[41] D. Auth, S. Liu, J. Norman, J. Edward Bowers, S. Breuer, Passively mode-locked semiconductor quantum dot on silicon laser with 400 hz rf line width, Opt. Express 27 (19) (2019) 27256, http://dx.doi.org/10.1364/OE.27.027256, https://www.osapublishing.org/abstract.cfm?URI=oe-27-19-27256.

[42] E.U. Rafailov, M.A. Cataluna, E.A. Avrutin, Ultrafast Lasers Based on Quantum Dot Structures, WILEY-VCH Verlag & Co. KGaA, Weinheim, Germany, 2011.

[43] P.M. Smowton, E. Herrmann, Y. Ning, H.D. Summers, P. Blood, M. Hopkinson, Optical mode loss and gain of multiple-layer quantum-dot lasers, Appl. Phys. Lett. 78 (18) (2001) 2629–2631, http://dx.doi.org/10.1063/1.1366652.

[44] M. Pristovsek, Wavelength limits for InGaN quantum wells on GaN, Appl. Phys. Lett. 102 (24) (2013) 242105, http://dx.doi.org/10.1063/1.4811560, http://aip.scitation.org/doi/10.1063/1.4811560.

[45] T. Frost, A. Hazari, A. Aiello, M. Zunaid Baten, L. Yan, J. Mirecki-Millunchick, P. Bhattacharya, High performance red-emitting multiple layer InGaN/GaN quantum dot lasers, Japan. J. Appl. Phys. 55 (2016) 032101, http://dx.doi.org/10.7567/JJAP.55.032101.

[46] M. Zhang, A. Banerjee, C.-S. Lee, J.M. Hinckley, P. Bhattacharya, A InGaN/GaN quantum dot green (λ=524 nm) laser, Appl. Phys. Lett. 98 (22) (2011) 221104, http://dx.doi.org/10.1063/1.3596436, http://aip.scitation.org/doi/10.1063/1.3596436.

[47] M. Asada, Y. Miyamoto, Y. Suematsu, Gain and the threshold of three-dimensional quantum-box lasers, IEEE J. Quantum Electron. 22 (9) (1986) 1915–1921, http://dx.doi.org/10.1109/JQE.1986.1073149, http://ieeexplore.ieee.org/document/1073149.

[48] J.Y. Marzin, G. Bastard, Calculation of the energy levels in InAs GaAs quantum dots, Solid State Commun. 92 (5) (1994) 437–442, http://dx.doi.org/10.1016/0038-1098(94)90524-X.

[49] M. Grundmann, O. Stier, D. Bimberg, InAs/GaAs pyramidal quantum dots: Strain distribution optical phonons, and electronic structure, Phys. Rev. B 52 (16) (1995) 11969–11981, http://dx.doi.org/10.1103/PhysRevB.52.11969.

[50] A. Wojs, P. Hawrylak, Charging and infrared spectroscopy of self-assembled quantum dots in a magnetic field, Phys. Rev. B 53 (16) (1996) 10841–10845, http://dx.doi.org/10.1103/PhysRevB.53.10841.

[51] M.A. Cusack, P.R. Briddon, M. Jaros, Electronic structure of InAs/GaAsself-assembled quantum dots, Phys. Rev. B 54 (4) (1996) R2300—R2303, http://dx.doi.org/10.1103/PhysRevB.54.R2300, http://link.aps.org/doi/10.1103/PhysRevB.54.R2300.

[52] M.A. Cusack, P.R. Briddon, M. Jaros, Absorption spectra and optical transitions in InAs/GaAsself-assembled quantum dots, Phys. Rev. B 56 (7) (1997) 4047–4050, http://dx.doi.org/10.1103/PhysRevB.56.4047, http://dreamtalk.hypermart.net/international/chile_english.htm.

[53] H. Jiang, J. Singh, Strain distribution and electronic spectra of InAs/GaAsself-assembled dots: An eight-band study, Phys. Rev. B 56 (8) (1997) 4696–4701, http://dx.doi.org/10.1103/PhysRevB.56.4696.

[54] L. Fonseca, J. Jimenez, J. Leburton, Self-consistent calculation of the electronic structure and electron-electron interaction in self-assembled InAs-GaAs quantum dot structures, Phys. Rev. B 57 (7) (1998) 4017–4026, http://dx.doi.org/10.1103/PhysRevB.57.4017.

[55] C. Pryor, Eight-band calculations of strained InAs/GaAsquantum dots compared with one-four-, and six-band approximations, Phys. Rev. B 57 (12) (1998) 7190–7195, http://dx.doi.org/10.1103/PhysRevB.57.7190, arXiv:9710304.

[56] J. Kim, L.-W. Wang, A. Zunger, Comparison of the electronic structure of InAs/GaAspyramidal quantum dots with different facet orientations, Phys. Rev. B 57 (16) (1998) 9408–9411, http://dx.doi.org/10.1016/j.actbio.2013.11.021.

[57] G. Medeiros-Ribeiro, D. Leonard, P.M. Petroff, Electron and hole energy levels in InAs self-assembled quantum dots, Appl. Phys. Lett. 66 (14) (1995) 1767–1769, http://dx.doi.org/10.1063/1.113361, http://aip.scitation.org/doi/10.1063/1.113361.

[58] M. Grundmann, N. Ledentsov, O. Stier, J. Böhrer, D. Bimberg, V. Ustinov, P. Kopşev, Z.I. Alferov, Nature of optical transitions in self-organized InAs/GaAsquantum dots, Phys. Rev. B 53 (16) (1996) R10509–R10511, http://dx.doi.org/10.1103/PhysRevB.53.R10509.

[59] R. Heitz, M. Veit, N.N. Ledentsov, A. Hoffmann, D. Bimberg, V.M. Ustinov, P.S. Kop'ev, Z.I. Alferov, Energy relaxation by multiphonon process in InAs/GaAsquantum dots, Phys. Rev. B 56 (16) (1997) 10435–10445.

[60] F. Adler, M. Geiger, A. Bauknecht, F. Scholz, H. Schweizer, M.H. Pilkuhn, B. Ohnesorge, A. Forchel, Optical transitions and carrier relaxation in self assembled InAs/GaAsquantum dots, J. Appl. Phys. 80 (7) (1996) 4019–4026, http://dx.doi.org/10.1063/1.363361, http://aip.scitation.org/doi/10.1063/1.363361.

[61] K.H. Schmidt, M. Oestreich, P.M. Petroff, G.H. Döhler, Carrier relaxation and electronic structure in InAs self-assembled quantum dots, Phys. Rev. B 54 (16) (1996) 11346–11353, http://dx.doi.org/10.1093/humrep/27.s2.69.

[62] M. Fricke, A. Lorke, J.P. Kotthaus, G. Medeiros-Ribeiro, P.M. Petroff, Shell structure and electron-electron interaction in self-assembled inas quantum dots, Europhysics Letters 36 (3) (1996) 197–202, http://dx.doi.org/10.1209/epl/i1996-00210-x, arXiv:9609270.

[63] M. Steer, D. Mowbray, W. Tribe, M. Skolnick, M. Sturge, M. Hopkinson, A. Cullis, C. Whitehouse, Electronic energy levels and energy relaxation mechanisms in self-organized InAs/GaAsquantum dots, Phys. Rev. B 54 (24) (1996) 17738–17744, http://dx.doi.org/10.1103/PhysRevB.54.17738.

[64] K.H. Schmidt, G. Medeiros-Ribeiro, J. Garcia, P.M. Petroff, Size quantization effects in InAs self-assembled quantum dots, Appl. Phys. Lett. 70 (13) (1997) 1727–1729, http://dx.doi.org/10.1063/1.118682.

[65] S. Sauvage, P. Boucaud, F.H. Julien, J.M. Gérard, J.Y. Marzin, Infrared spectroscopy of intraband transitions in self-organized InAs/GaAsquantum dots, J. Appl. Phys. 82 (7) (1997) 3396–3401, http://dx.doi.org/10.1063/1.365654.

[66] D.W. Reschner, E. Gehrig, O. Hess, Pulse Amplification and Spatio-Spectral Hole-Burning in Inhomogeneously Broadened Quantum-Dot Semiconductor Optical Amplifiers, IEEE J. Quantum Electron. 45 (1) (2009) 21–33.

[67] O. Stier, M. Grundmann, D. Bimberg, Electronic and optical properties of strained quantum dots modeled by 8-band kp theory, Phys. Rev. B 59 (8) (1999) 5688–5701, http://dx.doi.org/10.1103/PhysRevB.59.5688.

[68] M. Grundmann, The present status of quantum dot lasers, Physica E 5 (2000) 167–184.

[69] M.T. Crowley, A.D. Andreev, T. Piwonski, J. Houlihan, E.P. O'Reilly, G. Huyet, Interconnection between ground state and excited state gain in InAs/GaAsquantum dot semiconductor optical amplifiers, Physica Status Solidi (B) 246 (4) (2009) 868–871, http://dx.doi.org/10.1002/pssb.200880631, http://doi.wiley.com/10.1002/pssb.200880631.

[70] M.A. Cataluna, W. Sibbett, D.A. Livshits, J. Weimert, A.R. Kovsh, E.U. Rafailov, Stable mode locking via ground- or excited-state transitions in a two-section quantum- dot laser Stable mode locking via ground- or excited-state transitions in a two-section quantum-dot laser, Appl. Phys. Lett. 89 (2006) 081124, http://dx.doi.org/10.1063/1.2338767.

[71] N. Kirstaedter, N. Ledentsov, M. Grundmann, D. Bimberg, V. Ustinov, S. Ruvimov, M. Maximov, P. Kop'ev, Z. Alferov, U. Richter, P. Werner, U. Gösele, J. Heydenreich, Low threshold large to injection laser emission from (InGa)As quantum dots, Electron. Lett. 30 (17) (1994) 1416–1417, http://dx.doi.org/10.1049/el:19940939, https://digital-library.theiet.org/content/journals/10.1049/el_19940939.

[72] C. Weber, L. Drzewietzki, M. Rossetti, T. Xu, P. Bardella, H. Simos, C. Mesaritakis, M. Ruiz, I. Krestnikov, D. Livshits, M. Krakowski, D. Syvridis, I. Montrosset, E.U. Rafailov, W. Els, S. Breuer, Picosecond pulse amplification of up to 42 W peak power using a tapered optical amplifier and a monolithic quantum-dot tapered mode-locked laser, Opt. Lett. 40 (3) (2015) 395–398, http://dx.doi.org/10.1364/OL.40.000395.

[73] R. Rosales, K. Merghem, C. Calo, G. Bouwmans, I. Krestnikov, A. Martinez, A. Ramdane, Optical pulse generation in single section InAs/GaAs quantum dot edge emitting lasers under continuous wave operation, Appl. Phys. Lett. 101 (22) (2012) 221113, http://dx.doi.org/10.1063/1.4768946.

[74] H.A. Haus, Invited paper: modelocking of semiconductor laser diodes, 1981, http://dx.doi.org/10.1143/JJAP.20.1007.

[75] H.A. Haus, Mode-locking of lasers, IEEE J. Sel. Top. Quantum Electron. 6 (6) (2000) 1173–1185, http://dx.doi.org/10.1109/2944.902165.

[76] J. Javaloyes, S. Balle, Quasiequilibrium time-domain susceptibility of semiconductor quantum wells, Phys. Rev. A 81 (6) (2010) 062505, http://dx.doi.org/10.1103/PhysRevA.81.062505, https://link.aps.org/doi/10.1103/PhysRevA.81.062505.

[77] E.P. Ippen, Principles of passive mode locking, Appl. Phys. B Laser Opt. 58 (3) (1994) 159–170, http://dx.doi.org/10.1007/BF01081309.

[78] M. Rossetti, L. Li, A. Fiore, L. Occhi, C. Élez, S. Mikhrin, A. Kovsh, High-power quantum-dot superluminescent diodes with p-Doped active region, IEEE Photonics Technol. Lett. 18 (18) (2006) 1946–1948, http://dx.doi.org/10.1109/LPT.2006.882303.

[79] S.K. Ray, K.M. Groom, H.Y. Liu, M. Hopkinson, R.A. Hogg, Broad-band superluminescent light emitting diodes incorporating quantum dots in compositionally modulated quantum wells, in: Device Research Conference - Conference Digest, DRC 2005 (1), 2005, pp. 71–72, http://dx.doi.org/10.1109/DRC.2005.1553060.

[80] E.U. Rafailov, P. Loza-Alvarez, W. Sibbett, G.S. Sokolovskii, D.A. Livshits, A.E. Zhukov, V.M. Ustinov, Amplification of femtosecond pulses over by 18 dB in a quantum-dot semiconductor optical amplifier, IEEE Photonics Technol. Lett. 15 (8) (2003) 1023–1025, http://dx.doi.org/10.1109/LPT.2003.815362.

[81] K.A. Fedorova, M.A. Cataluna, I. Krestnikov, D. Livshits, E.U. Rafailov, Broadly tunable high-power InAs/GaAs quantum-dot external cavity diode lasers, Opt. Express 18 (18) (2010) 19438, http://dx.doi.org/10.1364/OE.18.019438.

[82] H. Li, G.T. Liu, P.M. Varangis, T.C. Newell, A. Stintz, B. Fuchs, K.J. Malloy, L.F. Lester, 150-nm Tuning Range in a Grating-Coupled External Cavity Quantum-Dot Laser, IEEE Photonics Technol. Lett. 12 (7) (2000) 759–761, http://dx.doi.org/10.1109/68.853491.

[83] H. Tabuchi, H. Ishikawa, External grating tunable MQW laser with wide tuning range of 240 nm, Electron. Lett. 26 (11) (1990) 742–743.

[84] H.S. Gingrich, D.R. Chumney, S.Z. Sun, S.D. Hersee, L.F. Lester, S.R. Brueck, Broadly tunable external cavity laser diodes with staggered thickness multiple quantum wells, IEEE Photonics Technol. Lett. 9 (2) (1997) 155–157, http://dx.doi.org/10.1109/68.553070.

[85] X. Zhu, D.T. Cassidy, M.J. Hamp, D.A. Thompson, B.J. Robinson, Q.C. Zhao, M. Davies, 1.4-μM InGaAsP-InP strained multiple-quantum-well laser for broad-wavelength tunability, IEEE Photonics Technol. Lett. 9 (9) (1997) 1202–1204.

[86] F. Gao, S. Luo, H.-M. Ji, S.-T. Liu, F. Xu, Z.-R. Lv, D. Lu, C. Ji, T. Yang, Ultrashort pulse and high power mode-locked laser with chirped InAs/InP quantum dot active layers, IEEE Photonics Technol. Lett. 28 (13) (2016) 1481–1484, http://dx.doi.org/10.1109/LPT.2016.2561302, http://ieeexplore.ieee.org/document/7463548.

[87] S. Liu, X. Wu, D. Jung, J.C. Norman, M.J. Kennedy, H.K. Tsang, A.C. Gossard, J.E. Bowers, High-channel-count 20 ghz passively mode-locked quantum dot laser directly grown on si with 4.1 tbit/s transmission capacity, Optica 6 (2) (2009) 128–134, http://dx.doi.org/10.1364/OPTICA.6.000128, https://opg.optica.org/optica/abstract.cfm?URI=optica-6-2-128.

[88] P. Borri, W. Langbein, J.M. Hvam, F. Heinrichsdorff, M. Mao, D. Bimberg, Spectral Hole-Burning and Carrier-Heating Dynamics in InGaAs Quantum-Dot Amplifiers, IEEE J. Sel. Top. Quantum Electron. 6 (3) (2000) 544–551.

[89] P. Borri, S. Schneider, W. Langbein, D. Bimberg, Ultrafast carrier dynamics in ingaas quantum dot materials and devices*, J. Opt. A 8 (2006) 33–46, http://dx.doi.org/10.1088/1464-4258/8/4/S03.

[90] S. Schneider, P. Borri, W. Langbein, U. Woggon, R.L. Sellin, D. Ouyang, D. Bimberg, Excited-state gain dynamics in InGaAs quantum-dot amplifiers, IEEE Photonics Technol. Lett. 17 (10) (2005) 2014–2016, http://dx.doi.org/10.1109/LPT.2005.856446, http://ovidsp.ovid.com/ovidweb.cgi?T=JS&CSC=Y&NEWS=N&PAGE=fulltext&D=psyn&AN=0268939%0A.

[91] E. Rafailov, S. White, A. Lagatsky, A. Miller, W. Sibbett, D. Livshits, A. Zhukov, V. Ustinov, Fast quantum-dot saturable absorber for passive mode-locking of solid-state lasers, IEEE Photonics Technol. Lett. 16 (11) (2004) 2439–2441, http://dx.doi.org/10.1109/LPT.2004.835648, http://ieeexplore.ieee.org/document/1344060.

[92] D.B. Malins, S.J. White, W. Sibbett, A. Miller, E.U. Rafailov, Ultrafast electroabsorption dynamics in an InAs quantum dot saturable, Appl. Phys. Lett. 89 (2006) 171111, http://dx.doi.org/10.1063/1.2369818.

[93] M.G. Thompson, Y. Chu, R.L. Sellin, R.V. Pentyl, D. Birkedal, P.S. Group, T. Street, Properties of ingaas quantum dot saturable absorbers in monolithic mode-locked lasers, in: IEEE 19th International Semiconductor Laser Conference, 2004, p. ThB2, Conference Digest. 2004.

[94] E.A. Viktorov, T. Erneux, P. Mandel, T. Piwonski, G. Madden, J. Pulka, G. Huyet, J. Houlihan, E.A. Viktorov, T. Erneux, P. Mandel, T. Piwonski, G. Madden, J. Pulka, G. Huyet, J. Houlihan, Recovery time scales in a reversed-biased quantum dot absorber recovery time scales in a reversed-biased quantum dot absorber, Appl. Phys. Lett. 94 (2009) 263502, http://dx.doi.org/10.1063/1.3159838.

[95] T.W. Berg, S. Bischoff, I. Magnusdottir, J. Moørk, Ultrafast gain recovery and modulation limitations in self-assembled quantum-dot devices, IEEE Photonics Technol. Lett. 13 (6) (2001) 541–543, http://dx.doi.org/10.1109/68.924013.

[96] T. Piwonski, J. Pulka, G. Madden, G. Huyet, J. Houlihan, E.A. Viktorov, T. Erneux, P. Mandel, Intradot dynamics of InAs quantum dot based electroabsorbers, Appl. Phys. Lett. 94 (12) (2009) 1–4, http://dx.doi.org/10.1063/1.3106633.

[97] V.V. Nikolaev, E.A. Avrutin, Quantum-Well Design for Monolithic Optical Devices With Gain and Saturable Absorber Sections, IEEE Photonics Technol. Lett. 16 (1) (2004) 24–26.

[98] J.R. Karin, R.J. Helkey, D.J. Derickson, R. Nagarajan, D.S. Allin, J.E. Bowers, R.L. Thornton, D.S. Allin, Ultrafast dynamics in field-enhanced saturable absorbers, Appl. Phys. Lett. 64 (1994) (1994) 676, http://dx.doi.org/10.1063/1.111058.

[99] D. Lorenser, H.J. Unold, D.J. Maas, A. Aschwanden, R. Grange, R. Paschotta, D. Ebling, E. Gini, U. Keller, Towards wafer-scale integration of high repetition rate passively mode-locked surface-emitting semiconductor lasers, Appl. Phys. B 79 (8 SPEC.) (2004) 927–932, http://dx.doi.org/10.1007/s00340-004-1675-3.

[100] D.J.H.C. Maas, A. Bellancourt, M. Hoffmann, B. Rudin, Y. Barbarin, M. Golling, T. Südmeyer, U. Keller, Growth parameter optimization for fast quantum dot SESAMs, Opt. Express 16 (23) (2008) 18646–18656.

[101] U. Keller, K.J. Weingarten, F.X. Kärtner, D. Kopf, B. Braun, I.D. Jung, R. Fluck, C. Hönninger, N. Matuschek, J. Aus Der Au, Semiconductor saturable absorber mirrors (SESAM's) for femtosecond to nanosecond pulse generation in solid-state lasers, IEEE J. Sel. Top. Quantum Electron. 2 (3) (1996) 435–451, http://dx.doi.org/10.1109/2944.571743.

[102] N.N. Ledentsov, M. Grundmann, F. Heinrichsdorff, D. Bimberg, V.M. Ustinov, A.E. Zhukov, M.V. Maximov, Z.I. Alferov, J.A. Lott, Quantum-Dot Heterostructure Lasers, IEEE J. Sel. Top. Quantum Electron. 6 (3) (2000) 439–451.

[103] S.S. Mikhrin, A.R. Kovsh, I.L. Krestnikov, A.V. Kozhukhov, D.A. Livshits, N.N. Ledentsov, Y.M. Shernyakov, I.I. Novikov, M.V. Maximov, V.M. Ustinov, Z.I. Alferov, High power temperature-insensitive 1 . 3 μm InAs / InGaAs / GaAs quantum dot lasers, Semiconductor Sci. Technol. 20 (2005) 340–342, http://dx.doi.org/10.1088/0268-1242/20/5/002.

[104] G.T. Liu, A. Stintz, H. Li, K.J. Malloy, L.F. Lester, Low threshold current density 1.3 μm metamorphic InGaAs/GaAs quantum well laser diodes, Electron. Lett. 35 (14) (1999) 1163–1164, 10.1049/el.

[105] H.Y. Liu, D.T. Childs, T.J. Badcock, K.M. Groom, I.R. Sellers, M. Hopkinson, R.A. Hogg, D.J. Robbins, D.J. Mowbray, M.S. Skolnick, High-performance three-layer 1.3-μm InAs-GaAs quantum-dot lasers with very low continuous-wave room-temperature threshold currents, IEEE Photonics Technol. Lett. 17 (6) (2005) 1139–1141, http://dx.doi.org/10.1109/LPT.2005.846948.

[106] I.R. Sellers, H.Y. Liu, K.M. Groom, D.T. Childs, D. Robbins, T.J. Badcock, M. Hopkinson, D.J. Mowbray, M.S. Skolnick, 1.3 μM InGaAs/GaAs multilayer quantum-dot laser with extremely low room-temperature threshold current density, Electron. Lett. 40 (22) (2004) 1412–1413, 10.1049/el.

[107] S. Sanders, A. Yariv, J. Paslaski, J.E. Ungar, H.A. Zarem, S. Sanders, A. Yariv, J. Paslaski, J.E. Ungar, H.A. Zarem, Passive mode locking of a two-section multiple quantum well laser at harmonics of the cavity round-trip frequency Passive mode locking of a two-section multiple quantum well laser at harmonics of the cavity round-trip frequency, Appl. Phys. Lett. 58 (1991) 681–683, http://dx.doi.org/10.1063/1.104567.

[108] R.W. Boyd, Nonlinear optics, Academic Press, San Diego, 2008.

[109] R. Paschotta, R. Häring, A. Garnache, S. Hoogland, A.C. Tropper, U. Keller, Soliton-like pulse shaping mechanism in passively mode-locked urface-emitting semiconductor lasers, Appl. Phys. B 75 (2002) 445–451, http://dx.doi.org/10.1109/CLEOE.2003.1312191.

[110] A.G. Vladimirov, Model for passive mode locking in semiconductor lasers, Phys. Rev. A 72 (2005) 033808, http://dx.doi.org/10.1103/PhysRevA.72.033808.

[111] A.G. Vladimirov, U. Bandelow, G. Fiol, D. Arsenijevic, M. Kleinert, D. Bimberg, A. Pimenov, D. Rachinskii, D. Arsenijević, M. Kleinert, D. Bimberg, A. Pimenov, D. Rachinskii, Dynamical regimes in a monolithic passively mode-locked quantum dot laser, Journal of the Optical Society of America B 27 (10) (2010) 2102, http://dx.doi.org/10.1364/JOSAB.27.002102, https://www.osapublishing.org/abstract.cfm?URI=josab-27-10-2102.

[112] E.A. Viktorov, P. Mandel, M. Kuntz, G. Fiol, D. Bimberg, A.G. Vladimirov, M. Wolfrum, Stability of the mode-locked regime in quantum dot lasers, Appl. Phys. Lett. 91 (23) (2007) 2005–2008, http://dx.doi.org/10.1063/1.2822808.

[113] E.A. Avrutin, J. Javaloyes, Mode-locked semiconductor lasers, in: J. Piprek (Ed.), Handbook of optoelectronic device modeling and simulation, 1st Edition, CRC Press, 2017, Ch.32.

[114] E.A. Viktorov, P. Mandel, A.G. Vladimirov, U. Bandelow, Model for mode locking in quantum dot lasers, Appl. Phys. Lett. 88 (2006) 201102, http://dx.doi.org/10.1063/1.2203937.

[115] M.A. Cataluna, D.I. Nikitichev, S. Mikroulis, H. Simos, C. Simos, C. Mesaritakis, D. Syvridis, I. Krestnikov, D. Livshits, E.U. Rafailov, Dual-wavelength mode-locked quantum-dot laser, via ground and excited state transitions: experimental and theoretical investigation, Opt. Express 18 (12) (2010) 12832, http://dx.doi.org/10.1364/OE.18.012832, https://www.osapublishing.org/oe/abstract.cfm?uri=oe-18-12-12832.

[116] G. Fiol, D. Arsenijević, D. Bimberg, A.G. Vladimirov, M. Wolfrum, E.A. Viktorov, P. Mandel, Hybrid mode-locking in a 40 GHz monolithic quantum dot laser, Appl. Phys. Lett. 96 (1) (2010) 011104, http://dx.doi.org/10.1063/1.3279136, http://aip.scitation.org/doi/10.1063/1.3279136.

[117] S. Breuer, M. Rossetti, L. Drzewietzki, I. Montrosset, M. Krakowski, M. Hopkinson, W. Elsäßsser, Dual-state absorber-photocurrent characteristics and bistability of two-section quantum-dot lasers, IEEE J. Sel. Top. Quantum Electron. 19 (5) (2013) 1901609, http://dx.doi.org/10.1109/JSTQE.2013.2255264.

[118] M. Schell, A. Weber, E. Scholl, D. Bimberg, Fundamental limits of sub-ps pulse generation by active mode locking of semiconductor lasers: the spectral gain width and the facet reflectivities, IEEE J. Quantum Electron. 27 (6) (1991) 1661–1668, http://dx.doi.org/10.1109/3.89937, http://ieeexplore.ieee.org/document/89937.

[119] M. Radziunas, A.G. Vladimirov, E.A. Viktorov, G. Fiol, H. Schmeckebier, D. Bimberg, Strong pulse asymmetry in quantum-dot mode-locked semiconductor lasers, Appl. Phys. Lett. 98 (3) http://dx.doi.org/10.1063/1.3544579.

[120] M. Radziunas, E.A. A.G. Vladimirovand Viktorov, G. Fiol, H. Schmeckebier, D. Bimberg, Pulse broadening in quantum-dot mode-locked semiconductor lasers: Simulation analysis, and experiments, IEEE J. Quantum Electron. 47 (7) (2011) 935–943.

[121] M. Rossetti, P. Bardella, I. Montrosset, Time-Domain Travelling-Wave Model for Quantum Dot Passively Mode-Locked Lasers, IEEE J. Quantum Electron. 47 (2) (2011) 139–150.

[122] S. Breuer, M. Rossetti, L. Drzewietzki, P. Bardella, I. Montrosset, W. Elsaser, Joint experimental and theoretical investigations of two-state mode locking in a strongly chirped reverse-biased monolithic quantum dot laser, IEEE J. Quantum Electron. 47 (10) (2011) 1320–1329, http://dx.doi.org/10.1109/JQE.2011.2165834.

[123] S. Meinecke, L. Drzewietzki, C. Weber, B. Lingnau, M. Krakowski, I. Krestnikov, K. Lüdge, S. Breuer, 492 Fs short optical pulse generation with 9 . 2 w peak power by a monolithic edge-emitting quantum dot laser, in: Proc. IEEE Semiconductor Laser conference, 2018, pp. 65–66.

[124] D.I. Nikitichev, Y. Ding, M.a. Cataluna, E.U. Rafailov, L. Drzewietzki, S. Breuer, W. Elsaesser, M. Rossetti, P. Bardella, T. Xu, I. Montrosset, I. Krestnikov, D. Livshits, M. Ruiz, M. Tran, Y. Robert, M. Krakowski, High peak power and sub-picosecond Fourier-limited pulse generation from passively mode-locked monolithic two-section gain-guided tapered InGaAs quantum-dot lasers, Laser Phys. 22 (4) (2012) 715–724, http://dx.doi.org/10.1134/S1054660X12040147.

[125] P. Bardella, C. Weber, L. Columbo, L.F. Lester, M. Gioannini, S. Breuer, Rf line width and integrated rin study of a single-section quantum dot comb laser, in: Proc. SPIE, Vol. 10682, 2018, p. 1068223, http://dx.doi.org/10.1117/12.2307553.

[126] M. Birkholz, J. Javaloyes, O. Nikiforov, C. Weber, S. Breuer, Numerical modeling of mode-locking repetition rate transitions in monolithic multi-section semiconductor lasers, in: Proc. SPIE, Vol. 10682, 2018, p. 106821Y, http://dx.doi.org/10.1117/12.2307353.

[127] S. Meinecke, L. Drzewietzki, C. Weber, B. Lingnau, S. Breuer, K. Lüdge, Ultra-short pulse generation in a three section tapered passively mode-locked quantum-dot semiconductor laser, Scientific Reports 9 (1) (2019) 1783, http://dx.doi.org/10.1038/s41598-018-38183-1, http://www.nature.com/articles/s41598-018-38183-1.

[128] P. Bardella, L.L. Columbo, M. Gioannini, Self-generation of optical frequency comb in single section quantum dot Fabry-Perot lasers: a theoretical study, Opt. Express 25 (21) (2017) 26234–26252, http://dx.doi.org/10.1364/OE.25.026234, http://arxiv.org/abs/1707.06561%0A.

[129] W. Yee, K. Shore, Multimode analysis of self locked FM operation in laser diodes, IEE Proc. J. Optoelectron. 140 (1) (1993) 21, http://dx.doi.org/10.1049/ip-j.1993.0004, http://digital-library.theiet.org/content/journals/10.1049/ip-j.1993.0004.

[130] C. Weber, L.L. Columbo, M. Gioannini, S. Breuer, P. Bardella, Threshold behavior of optical frequency comb self-generation in an inas/ingaas quantum dot laser, Opt. Lett. 44 (14) (2019) 3478–3481, http://dx.doi.org/10.1364/OL.44.003478, https://opg.optica.org/ol/abstract.cfm?URI=ol-44-14-3478.

[131] E. Avrutin, J. Arnold, J. Marsh, Dynamic modal analysis of monolithic mode-locked semiconductor lasers, IEEE J. Sel. Top. Quantum Electron. 9 (3) (2003) 844–856, http://dx.doi.org/10.1109/JSTQE.2003.818845.

[132] F. Grillot, W.W. Chow, B. Dong, S. Ding, H. Huang, J. Bowers, Multimode physics in the mode locking of semiconductor quantum dot lasers, Applied Sciences 12 (7) http://dx.doi.org/10.3390/app12073504, https://www.mdpi.com/2076-3417/12/7/3504.

[133] C. Xing, E.A. Avrutin, Multimode spectra and active mode locking potential of quantum dot lasers, J. Appl. Phys. 97 (2005) 104301, http://dx.doi.org/10.1063/1.1894601.

[134] P. Bardella, L. Columbo, J. Rahimi, M. Gioannini, Self-generation of optical frequency combs in single section qd lasers: theory and numerical modelling, in: Proc. SPIE, Vol. 10682, 2018, p. 106820G.

[135] W.W. Chow, S. Liu, Z. Zhang, J.E. Bowers, M. Sargent, Multimode description of self-mode locking in a single-section quantum-dot laser, Opt. Express 28 (4) (2020) 5317–5330, http://dx.doi.org/10.1364/OE.382821, https://opg.optica.org/oe/abstract.cfm?URI=oe-28-4-5317.

[136] A. Zhukov, A. Kovsh, S. Mikhrin, N. Maleev, V. Ustinov, D. Livshits, I. Tarasov, D. Bedarev, M. Maximov, A. Tsatsul'nikov, I. Soshnikov, P. Kop'ev, Z. Alferov, N. Ledentsov, D. Bimberg, 3.9 W CW power from sub-monolayer quantum dot diode laser, Electron. Lett. 35 (21) (1999) 1845, http://dx.doi.org/10.1049/el:19991264, https://digital-library.theiet.org/content/journals/10.1049/el_19991264.

[137] R. Mirin, A. Gossard, J. Bowers, Room temperature lasing from InGaAs quantum dots, Electron. Lett. 32 (18) (1996) 1732, http://dx.doi.org/10.1049/el:19961147, https://digital-library.theiet.org/content/journals/10.1049/el_19961147.

[138] D. Bimberg, M. Grundmann, N. Ledentsov, M. Mao, C. Ribbat, R. Sellin, V. Ustinov, A. Zhukov, Z. Alferov, J. Lott, Novel infrared quantum dot lasers: theory and reality, physica status solidi (b) 224 (3) (2001) 787–796, http://dx.doi.org/10.1002/(SICI)1521-3951(200104)224:3<787::AID-PSSB787>3.0.CO;2-M, http://doi.wiley.com/10.1002/%28SICI%291521-3951%28200104%29224%3A3%3C787%3A%3AAID-PSSB787%3E3.0.CO%3B2-M.

[139] V. Ustinov, A. Zhukov, N. Maleev, A. Kovsh, S. Mikhrin, B. Volovik, Y. Musikhin, Y. Shernyakov, M. Maximov, A. Tsatsul'nikov, N. Ledentsov, Z. Alferov, J. Lott, D. Bimberg, 1.3μM InAs/GaAs quantum dot lasers and VCSELs grown by molecular beam epitaxy, J. Crystal Growth 227-228 (2001) 1155–1161, http://dx.doi.org/10.1016/S0022-0248(01)01006-5, https://linkinghub.elsevier.com/retrieve/pii/S0022024801010065.

[140] G. Fiol, C. Meuer, H. Schmeckebier, D. Arsenijević, S. Liebich, M. Laemmlin, M. Kuntz, D. Bimberg, D. Arsenijevic, S. Liebich, M. Laemmlin, M. Kuntz, D. Bimberg, Quantum-dot semiconductor mode-locked lasers and amplifiers at 40 GHz, IEEE J. Quantum Electron. 45 (11) (2009) 1429–1435, http://dx.doi.org/10.1109/JQE.2009.2027718, http://ieeexplore.ieee.org/document/5308735.

[141] C.Y. Lin, Y.C. Xin, J.H. Kim, C.G. Christodoulou, L.F. Lester, Compact optical generation of microwave signals using a monolithic quantum dot passively mode-locked laser, IEEE Photonics J. 1 (4) (2009) 236–244, http://dx.doi.org/10.1109/JPHOT.2009.2035523.

[142] M. Thompson, C. Marinelli, K. Tan, K. Williams, R. Penty, I. White, I. Kaiander, R. Sellin, D. Bimberg, D.-J. Kang, M. Blamire, F. Visinka, S. Jochum, S. Hansmann, 10 GHz hybrid modelocking of monolithic InGaAs quantum dot lasers, Electron. Lett. 39 (15) (2003) 1121, http://dx.doi.org/10.1049/el:20030734, https://digital-library.theiet.org/content/journals/10.1049/el_20030734.

[143] K. Tan, M. Thompson, C. Marinelli, K. Williams, R. Penty, I. White, I. Kaiander, R. Sellin, D. Bimberg, D.-J. Kang, M. Blamire, F. Visinka, S. Jochum, S. Hansmann, Investigation of high repetition rate mode-locked quantum dot lasers, in: The 16th Annual Meeting of the IEEE Lasers and Electro-Optics Society, 2003. LEOS 2003., Vol.2, IEEE, 2003, pp. 826–827, http://dx.doi.org/10.1109/LEOS.2003.1253055, http://ieeexplore.ieee.org/document/1253055/.

[144] A. Gubenko, L. Gadjiev, N. Il'inskaya, Y. Zadiranov, A. Zhukov, V. Ustinov, Z. Alferov, E. Portnoi, A. Kovsh, D. Livshits, N. Ledentsov, Mode locking at 9.7 GHz repetition rate with, 1.7 Ps pulse duration in two-section QD lasers, in: IEEE 19th International Semiconductor Laser Conference 2004 Conference Digest, IEEE, 2004, pp. 51–52, http://dx.doi.org/10.1109/ISLC.2004.1382750, http://ieeexplore.ieee.org/document/1382750.

[145] M. Kuntz, G. Fiol, M. Lämmlin, D. Bimberg, M.G. Thompson, K.T. Tan, C. Marinelli, R.V. Penty, I.H. White, V.M. Ustinov, A.E. Zhukov, Y.M. Shernyakov, A.R. Kovsh, 35Ghz mode-locking of 1.3μm quantum dot lasers, Appl. Phys. Lett. 85 (5) (2004) 843–845, http://dx.doi.org/10.1063/1.1776340, http://aip.scitation.org/doi/10.1063/1.1776340.

[146] M. Laemmlin, G. Fiol, M. Kuntz, F. Hopfer, A. Mutig, N.N. Ledentsov, A.R. Kovsh, C. Schubert, A. Jacob, A. Umbach, D. Bimberg, Quantum-dot-based photonic devices photonic devices at 1.3 μm: Direct modulation mode-locking, SOAs and VECSELs, phys. stat. sol. (c) 3 (3) (2006) 391–394, http://dx.doi.org/10.1002/pssc.200564142.

[147] J. Renaudier, R. Brenot, B. Dagens, F. Lelarge, B. Rousseau, F. Poingt, O. Legouezigou, F. Pommereau, A. Accard, P. Gallion, G.-H. Duan, 45 Ghz self-pulsation with narrow linewidth in quantum dot Fabry-Perot semiconductor lasers 1.5 μm, Electron. Lett. 41 (18) (2005) 1007–1008, 10.1049/el.

[148] C. Gosset, K. Merghem, A. Martinez, G. Moreau, G. Patriarche, G. Aubin, A. Ramdane, J. Landreau, F. Lelarge, Subpicosecond pulse generation at 134 GHz using a quantum-dash-based Fabry-Perot laser emitting at 1.56 μm, Appl. Phys. Lett. 88 (24) (2006) 10–13, http://dx.doi.org/10.1063/1.2213007.

[149] Z.G. Lu, J.R. Liu, S. Raymond, P.J. Poole, P.J. Barrios, D. Poitras, 312-Fs pulse generation from a passive c-band inas/inp quantum dot mode-locked laser, Opt. Express 16 (14) (2008) 10835, http://dx.doi.org/10.1364/OE.16.010835, https://www.osapublishing.org/oe/abstract.cfm?uri=oe-16-14-10835 http://www.scopus.com/record/display.url?eid=2-s2.0-47249123688&origin=inward&txGid=D4FEB70D7D2A9C4446074257216469C3.y7ESLndDIsN8cE7qwvy6w%3A1.

[150] Z.G. Lu, J.R. Liu, P.J. Poole, S. Raymond, P.J. Barrios, D. Poitras, G. Pakulski, P. Grant, D. Roy-Guay, An L-band monolithic InAs/InP quantum dot mode-locked laser with femtosecond pulses, Opt. Express 17 (16) (2009) 13609–13614, http://dx.doi.org/10.1364/OE.17.013609, http://www.scopus.com/record/display.url?eid=2-s2.0-68349141504&origin=inward&txGid=D4FEB70D7D2A9C4446074257216469C3.y7ESLndDIsN8cE7qwvy6w%3A9.

[151] P. Finch, P. Blood, P.M. Smowton, A. Sobiesierski, R.M. Gwilliam, I. O'Driscoll, Femtosecond pulse generation from a two-section mode-locked quantum-dot laser using random population, in: Proc. SPIE, Vol. 9002, 2014, p. 90020E, http://dx.doi.org/10.1117/12.2039130, http://proceedings.spiedigitallibrary.org/proceeding.aspx?doi=10.1117/12.2039130.

[152] M. Thompson, C. Marinelli, X. Zhao, R. Sellin, R. Penty, I. White, I. Kaiander, D. Bimberg, D.-J. Kang, M. Blamire, Colliding-pulse modelocked quantum dot lasers, Electron. Lett. 41 (5) (2005) 248, http://dx.doi.org/10.1049/el:20047868, https://digital-library.theiet.org/content/journals/10.1049/el_20047868.

[153] A.R. Rae, M.G. Thompson, R.V. Penty, I.H. White, A.R. Kovsh, S.S. Mikhrin, D.A. Livshits, I.L. Krestnikov, Harmonic mode-locking of a quantum-dot laser diode, in: Conference Proceedings - Lasers and Electro-Optics Society Annual Meeting-LEOS, 2006, pp. 874–875, http://dx.doi.org/10.1109/LEOS.2006.279085.

[154] D.I. Nikitichev, M.A. Cataluna, K.A. Fedorova, Y. Ding, S.S. Mikhrin, I.L. Krestnikov, D.A. Livshits, E.U. Rafailov, High-power wavelength bistability and tunability in passively mode-locked quantum-dot laser, IEEE J. Sel. Top. Quantum Electron. 19 (4) (2013) 1100907, http://dx.doi.org/10.1109/JSTQE.2013.2239610.

[155] I.B. Akca, A. Dâna, A. Aydinli, M. Rossetti, L. Li, A. Fiore, N. Dagli, Electro-optic and electro-absorption characterization of InAs quantum dot waveguides, Opt. Express 16 (5) (2008) 3439–3444, http://dx.doi.org/10.1364/OE.16.003439.

[156] K. Akahane, A. Matsumoto, T. Umezawa, N. Yamamoto, High-frequency short-pulse generation with a highly stacked inas quantum dot mode-locked laser diode, Japanese Journal of Applied Physics 60 (SB) (2021) SBBH02, http://dx.doi.org/10.35848/1347-4065/abd2a1, https://iopscience.iop.org/article/10.35848/1347-4065/abd2a1.

[157] A. Mar, R. Helkey, W.X. Zou, D.B. Young, J.E. Bowers, High-power mode-locked semiconductor lasers using flared waveguides, Appl. Phys. Lett. 66 (26) (1995) 3558–3560, http://dx.doi.org/10.1063/1.113786.

[158] A. Markus, J.X. Chen, C. Paranthoën, A. Fiore, C. Platz, O. Gauthier-Lafaye, Simultaneous two-state lasing in quantum-dot lasers, Appl. Phys. Lett. 82 (12) (2003) 1818–1820, http://dx.doi.org/10.1063/1.1563742.

[159] E.U. Rafailov, A.D. McRobbie, M.A. Cataluna, L. O'Faolain, W. Sibbett, D.A. Livshits, Investigation of transition dynamics in a quantum-dot laser optically pumped by femtosecond pulses, Appl. Phys. Lett. 88 (2006) 041101, http://dx.doi.org/10.1109/LEOS.2005.1548264.

[160] J. Kim, M.T. Choi, P.J. Delfyett, Pulse generation and compression via ground and excited states from a grating coupled passively mode-locked quantum dot two-section diode laser, Appl. Phys. Lett. 89 (26) (2006) 87–90, http://dx.doi.org/10.1063/1.2410217.

[161] S. Breuer, W. Elsässer, M. Hopkinson, State-switched modelocking of two-segment quantum dot laser via self-electro-optical quantum dot absorber, Electron. Lett. 46 (2) (2010) 161, http://dx.doi.org/10.1049/el.2010.3360, http://digital-library.theiet.org/content/journals/10.1049/el.2010.3360.

[162] S. Breuer, M. Rossetti, W. Elsässer, L. Drzewietzki, P. Bardella, I. Montrosset, M. Krakowski, M. Hopkinson, Reverse ground-state excited-state transition dynamics in two-section quantum dot semiconductor lasers: mode-locking and state-switching, in: Proc. SPIE, Vol. 7720, 2010, p. 772011, http://dx.doi.org/10.1117/12.854418, http://proceedings.spiedigitallibrary.org/proceeding.aspx?doi=10.1117/12.854418.

[163] S. Breuer, M. Rossetti, W. Elsässer, L. Drzewietzki, P. Bardella, I. Montrosset, M. Krakowski, M. Hopkinson, Reverse-emission-state-transition mode locking of a two-section InAs/InGaAs quantum dot laser, Appl. Phys. Lett. 97 (7) (2010) 1–4, http://dx.doi.org/10.1063/1.3480405.

[164] M.A. Cataluna, D. I, I. Krestnikov, D.A. Livshits, A.R. Kovsh, E.U. Rafailov, Dual-wavelength mode-locked gaas-based quantum-dot laser, in: CLEO/Europe and EQEC 2009 Conference Digest, 2009, pp. CB4–CB6.

[165] C. Mesaritakis, C. Simos, H. Simos, S. Mikroulis, I. Krestnikov, E. Roditi, D. Syvridis, Effect of optical feedback to the ground and excited state emission of a passively mode locked quantum dot laser, Appl. Phys. Lett. 97 (2010) 061114, http://dx.doi.org/10.1063/1.3477955.

[166] M. Gioannini, I. Montrosset, Numerical analysis of the frequency chirp in quantum-dot semiconductor lasers, IEEE J. Quantum Electron. 43 (10) (2007) 941–949, http://dx.doi.org/10.1109/JQE.2007.904306.

[167] M.T. Choi, W. Lee, J.M. Kim, P.J. Delfyett, Ultrashort, high-power pulse generation from a master oscillator power amplifier based on external cavity mode locking of a quantum-dot two-section diode laser, Appl. Phys. Lett. 87 (22) (2005) 1–3, http://dx.doi.org/10.1063/1.2137309.

[168] A.D. McRobbie, M.A. Cataluna, D.A. Livshits, W. Sibbett, E. Rafailov, High power all-quantum-dot based external cavity mode-locked laser, in: LEOS-19th Annual Meeting of the IEEE Lasers and Electro-Optics Society Vol. 2006, 2006, pp. 796–797, http://dx.doi.org/10.1109/LEOS.2006.279008.

[169] M. Xia, M.G. Thompson, R.V. Penty, I.H. White, External-cavity mode-locked quantum-dot lasers for low repetition rate, sub-picosecond pulse generation, in: 2008 Conference on Lasers and Electro-Optics, Vol.17, IEEE, 2008, pp. 1–2, http://dx.doi.org/10.1109/CLEO.2008.4551504, http://ieeexplore.ieee.org/document/5892873/http://ieeexplore.ieee.org/document/4571754.

[170] M. Xia, M.G. Thompson, R.V. Penty, I.H. White, External-cavity mode-locked quantum-dot laser diodes for low repetition rate sub-picosecond pulse generation, IEEE J. Sel. Top. Quantum Electron. 17 (5) (2011) 1264–1271, http://dx.doi.org/10.1109/JSTQE.2011.2159828, http://ieeexplore.ieee.org/document/5892873.

[171] Y. Ding, D.I. Nikitichev, I. Krestnikov, D. Livshits, M.A. Cataluna, E.U. Rafailov, Quantum-dot external-cavity passively modelocked laser with high peak power and pulse energy, Electron. Lett. 46 (22) (2010) 1516–1518, http://dx.doi.org/10.1049/el.2010.2336.

[172] Y. Ding, M.A. Cataluna, D. Nikitichev, I. Krestnikov, D. Livshits, E. Rafailov, Broad repetition-rate tunable quantum-dot external-cavity passively mode-locked laser with extremely narrow radio frequency linewidth, Appl. Phys. Express 4 (6) (2011) 2–4, http://dx.doi.org/10.1143/APEX.4.062703.

[173] J. Kim, M.-T. Choi, W. Lee, P.J. Delfyett Jr., Wavelength tunable mode-locked quantum-dot laser, in: Proc. SPIE, Vol. 6243, 2006, p. 62430M, http://dx.doi.org/10.1117/12.673753, http://proceedings.spiedigitallibrary.org/proceeding.aspx?doi=10.1117/12.673753.

[174] D.I. Nikitichev, K.A. Fedorova, Y. Ding, A. Alhazime, A. Able, W. Kaenders, I. Krestnikov, D. Livshits, E.U. Rafailov, Broad wavelength tunability from external cavity quantum-dot mode-locked laser, Appl. Phys. Lett. 101 (12) http://dx.doi.org/10.1063/1.4751034.

[175] Z.G. Lu, J.R. Liu, P.J. Poole, Z.J. Jiao, P.J. Barrios, D. Poitras, J. Caballero, X.P. Zhang, Ultra-high repetition rate InAs/InP quantum dot mode-locked lasers, Opt. Commun. 284 (9) (2011) 2323–2326, http://dx.doi.org/10.1016/j.optcom.2010.11.083, https://linkinghub.elsevier.com/retrieve/pii/S0030401810013301.

[176] T. Ulm, A. Klehr, G. Erbert, F. Harth, J.A. L'Huillier, Femtosecond diode laser MOPA system at 920 nm based on asymmetric colliding pulse mode-locking, Appl. Phys. B 99 (3) (2010) 409–414, http://dx.doi.org/10.1007/s00340-010-3963-4.

[177] K. Kim, S. Lee, P. Delfyett, 1.4Kw high peak power generation from an all semiconductor mode-locked master oscillator power amplifier system based on extreme chirped pulse amplification(x-CPA)., Opt. Express 13 (12) (2005) 4600–4606, http://dx.doi.org/10.1364/OPEX.13.004600, http://www.ncbi.nlm.nih.gov/pubmed/19495375.

[178] S. Schwertfeger, A. Klehr, T. Hoffmann, A. Liero, H. Wenzel, G. Erbert, Picosecond pulses with 50 w peak power and reduced ase background from an all-semiconductor mopa system, Appl. Phys. B 103 (3) (2011) 603–607, http://dx.doi.org/10.1007/s00340-011-4481-8.

[179] S. Schwertfeger, A. Klehr, T. Hoffmann, A. Liero, H. Wenzel, G. Erbert, Generation of sub-100 ps pulses with a peak power of 65 W by gain switching, pulse shortening, and pulse amplification using a semiconductor-based master oscillator-power amplifier system, Appl. Opt. 52 (14) (2013) 3364, http://dx.doi.org/10.1364/AO.52.003364, https://www.osapublishing.org/abstract.cfm?URI=ao-52-14-3364.

[180] C. Jördens, T. Schlauch, M. Li, M.R. Hofmann, M. Bieler, M. Koch, All-semiconductor laser driven terahertz time-domain spectrometer, Appl. Phys. B 93 (2-3) (2008) 515–520, http://dx.doi.org/10.1007/s00340-008-3210-4.

[181] J. Balzer, T. Schlauch, A. Klehr, G. Erbert, G. Tränkle, M. Hofmann, High peak power pulses from dispersion optimised modelocked semiconductor laser, Electron. Lett. 49 (13) (2013) 838–839, http://dx.doi.org/10.1049/el.2013.1447, http://ieeexplore.ieee.org/Xplore/defdeny.jsp?url=http%3A%2F%2Fieeexplore.ieee.org%2Fstamp%2Fstamp.jsp%3Ftp%3D%26arnumber%3D6553049%26userType%3Dinst&denyReason=-134&arnumber=6553049&productsMatched=null&userType=inst https://digital-library.theiet.org/co.

[182] T. Ulm, F. Harth, H. Fuchs, J.A. L'Huillier, R. Wallenstein, InGaAs diode laser system generating pulses of 580 fs duration and 366 W peak power, Appl. Phys. B 92 (4) (2008) 481–485, http://dx.doi.org/10.1007/s00340-008-3121-4.

[183] Y. Ding, M.A. Cataluna, D. Nikitichev, M. Ruiz, M. Tran, Y. Robert, A. Kapsalis, H. Simos, C. Mesaritakis, T. Xu, P. Bardella, M. Rossetti, I. Krestnikov, D. Livshits, I. Montrosset, D. Syvridis, M. Krakowski, P. Loza-Alvarez, E. Rafailov, High peak-power picosecond pulse generation at 1.26 μm using a quantum-dot-based external-cavity mode-locked laser and tapered optical amplifier, Opt. Express 20 (13) (2012) 14308–14320.

[184] S. Riecke, S. Schwertfeger, K. Lauritsen, K. Paschke, R. Erdmann, G. Tränkle, 23W peak power picosecond pulses from a single-stage all-semiconductor master oscillator power amplifier, Appl. Phys. B Lasers Opt. 98 (2-3) (2010) 295–299, http://dx.doi.org/10.1007/s00340-009-3672-z.

[185] Y. Ding, A. Alhazime, D. Nikitichev, K. Fedorova, M. Ruiz, M. Tran, Y. Robert, A. Kapsalis, H. Simos, C. Mesaritakis, T. Xu, P. Bardella, M. Rossetti, I. Krestnikov, D. Livshits, I. Montrosset, D. Syvridis, M.A. Cataluna, M. Krakowski, E. Rafailov, Tunable master-oscillator power-amplifier based on chirped quantum-dot structures, IEEE Photonics Technol. Lett. 24 (20) (2012) 1841–1844, http://dx.doi.org/10.1109/LPT.2012.2216516.

[186] H. Schmeckebier, G. Fiol, C. Meuer, D. Arsenijević, D. Bimberg, Complete pulse characterization of quantum dot mode-locked lasers suitable for optical communication up to 160 Gbit/s, Opt. Express 18 (4) (2010) 3415, http://dx.doi.org/10.1364/oe.18.003415.

[187] C. Calò, H. Schmeckebier, K. Merghem, R. Rosales, F. Lelarge, A. Martinez, D. Bimberg, A. Ramdane, Frequency resolved optical gating characterization of sub-ps pulses from single-section InAs/InP quantum dash based mode-locked lasers, Opt. Express 22 (2) (2014) 1742, http://dx.doi.org/10.1364/OE.22.001742, https://www.osapublishing.org/oe/abstract.cfm?uri=oe-22-2-1742.

[188] F. Guffarth, R. Heitz, M. Geller, C. Kapteyn, H. Born, R. Sellin, A. Hoffmann, D. Bimberg, N.A. Sobolev, M.C. Carmo, Radiation hardness of InGaAs/GaAs quantum dots, Appl. Phys. Lett. 82 (12) (2003) 1941–1943, http://dx.doi.org/10.1063/1.1561165.

[189] S. Marcinkevičius, J. Siegert, R. Leon, B. Čechavičius, B. Magness, W. Taylor, C. Lobo, Changes in luminescence intensities and carrier dynamics induced by proton irradiation in (formula presented) quantum dots, Phys. Rev. B 66 (23) (2002) 1–6, http://dx.doi.org/10.1103/PhysRevB.66.235314.

[190] A. Gubenko, D. Livshits, I. Krestnikov, S. Mikhrin, A. Kozhukhov, A. Kovsh, N. Ledentsov, A. Zhukov, E. Portnoi, High-power monolithic passively modelocked quantum-dot laser, Electron. Lett. 41 (20) (2005) 1124–1125, http://dx.doi.org/10.1049/el.

[191] L. Zhang, L. Cheng, a.L. Gray, S. Luong, J. Nagyvary, F. Nabulsi, L. Olona, K. Sun, T. Tumolillo, R. Wang, C. Wiggins, J. Zilko, Z. Zou, P.M. Varangis, Low timing jitter, 5 GHz optical pulses from monolithic two-section passively mode-locked 1250 / 1310 nm quantum dot lasers for high speed optical interconnects, in: Optical Fiber Communication Conference, 2005, OWM4.

[192] J. Luo, J. Parra-Cetina, P. Landais, H.J.S. Dorren, N. Calabretta, Performance assessment of 40 gb/s burst optical clock recovery based on quantum dash laser, IEEE Photonics Technol. Lett. 25 (22) (2013) 2221–2224, http://dx.doi.org/10.1109/LPT.2013.2284529, http://ieeexplore.ieee.org/document/6623112.

[193] J. Kim, C.G. Christodoulou, Z. Ku, C.Y. Lin, Y. Xin, N.A. Naderi, L.F. Lester, Hybrid integration of a bowtie slot antenna and a quantum dot mode-locked laser, IEEE Antennas Wirel. Propag. Lett. 8 (2009) 1337–1340, http://dx.doi.org/10.1109/LAWP.2009.2038345.

[194] Z. Jiao, J. Liu, Z. Lu, X. Zhang, P.J. Poole, P.J. Barrios, D. Poitras, J. Caballero, Tunable terahertz beat signal generation from an InAs/InP quantum-dot mode-locked laser combined with external-cavity, IEEE Photonics Technol. Lett. 24 (6) (2012) 518–520, http://dx.doi.org/10.1109/LPT.2011.2182642.

[195] Y. Ding, F. Gao, H. Yuan, Z. Lv, T. Yang, 1–2.9-Thz tunable terahertz beat signal generation based on inas/inp quantum-dot mode-locked laser, IEEE Photonics Technol. Lett. 30 (13) (2018) 1234–1237.

[196] R.R. Leyman, A. Gorodetsky, N. Bazieva, G. Molis, A. Krotkus, E. Clarke, E.U. Rafailov, Quantum dot materials for terahertz generation applications, Laser Photonics Rev. 10 (5) (2016) 772–779, http://dx.doi.org/10.1002/lpor.201500176, http://doi.wiley.com/10.1002/lpor.201500176.

[197] K.A. Fedorova, A. Gorodetsky, E.U. Rafailov, Compact all-quantum-dot-based tunable THz laser source, IEEE J. Sel. Top. Quantum Electron. 23 (4) (2017) 1–5, http://dx.doi.org/10.1109/JSTQE.2016.2633870, http://ieeexplore.ieee.org/document/7762827.

[198] A. Gorodetsky, A. Yadav, E. Avrutin, K.A. Fedorova, E.U. Rafailov, Photoelectric properties of InAs/GaAs quantum dot photoconductive antenna wafers, IEEE J. Sel. Top. Quantum Electron. 24 (2) (2018) 1–5.

[199] V. Vujicic, A.P. Anthur, A. Saljoghei, V. Panapakkam, R. Zhou, Q. Gaimard, K. Merghem, F. Lelarge, A. Ramdane, L.P. Barry, Mitigation of relative intensity noise of quantum dash mode-locked lasers for pam4 based optical interconnects using encoding techniques, Opt. Express 25 (1) (2017) 20–29, http://dx.doi.org/10.1364/OE.25.000020, http://www.opticsexpress.org/abstract.cfm?URI=oe-25-1-20.

[200] M.E. Chaibi, L. Bramerie, S. Lobo, C. Peucheret, Mitigation of mode partition noise in quantum-dash fabry-perot mode-locked lasers using Manchester encoding, Euro. Conf. Opt. Commun., ECOC 25 (14) (2016) 319–321.

[201] Z. Lu, J. Liu, L. Mao, C.-Y. Song, J. Weber, D. Poitras, P. Poole, 2.24 Tbit/s PAM-4 transmission by an InAs/InP quantum dot mode-locked laser, in: M. Glick, A.K. Srivastava, Y. Akasaka (Eds.), Metro and Data Center Optical Networks and Short-Reach Links II, no. February 2019, SPIE, 2019, http://dx.doi.org/10.1117/12.2507949, https://www.spiedigitallibrary.org/conference-proceedings-of-spie/10946/2507949/224-Tbit-s-PAM-4-transmission-by-an-InAs-InP/10.1117/12.2507949.full.

[202] J.-Z. Huang, Z.-T. Ji, J.-J. Chen, W.-Q. Wei, J.-L. Qin, Z.-H. Wang, Z.-Y. Li, T. Wang, X. Xiao, J.-J. Zhang, Ultra-broadband flat-top quantum dot comb lasers, Photonics Research 10 (5) (2022) 1308, http://dx.doi.org/10.1364/PRJ.446349, https://opg.optica.org/abstract.cfm?URI=prj-10-5-1308.

[203] Y. Ben M'Sallem, Q.T. Le, L. Bramerie, Q.-T. Nguyen, E. Borgne, P. Besnard, A. Shen, F. Lelarge, S. LaRochelle, L.A. Rusch, J.-C. Simon, Quantum-dash mode-locked laser as a source for 56-Gb/s DQPSK modulation in WDM multicast applications, IEEE Photonics Technol. Lett. 23 (7) (2011) 453–455, http://dx.doi.org/10.1109/LPT.2011.2106116, http://ieeexplore.ieee.org/document/5688220.

[204] Z. Lu, J. Liu, L. Mao, C.-Y. Song, J. Weber, P. Poole, 12.032 Tbit/s coherent transmission using an ultra-narrow linewidth qantum dot 34.46-ghz c-band coherent comb laser, in: X.Zhou G.Li (Ed.), Next-Generation Optical Communication: Components, Sub-Systems, and Systems VIII, Vol. 10947, International Society for Optics and Photonics, SPIE, 2019, pp. 116–122, http://dx.doi.org/10.1117/12.2507504.

[205] Y. Mao, J. Liu, Z. Lu, C. Song, P.J. Poole, Ultra-low timing jitter of quantum dash semiconductor comb lasers with self-injection feedback locking, IEEE J. Sel. Top. Quantum Electron. 25 (6) (2019) 1–7.

[206] G. Liu, P.J. Poole, Z. Lu, J. Liu, Y. Mao, M. Vachon, P. Barrios, InAs/InP quantum dot mode-locked laser with an aggregate 12.544 tbit/s transmission capacity, Opt. Express 30 (3) (2022) 3205, http://dx.doi.org/10.1364/OE.441820.

[207] Y. Mao, G. Liu, K. Zeb, Z. Lu, J. Liu, P.J. Poole, C.-Y. Song, P. Barrios, Ultralow noise and timing jitter semiconductor quantum-dot passively mode-locked laser for terabit/s optical networks, Photonics 9 (10) (2022) 695, http://dx.doi.org/10.3390/Photonics9100695, https://www.mdpi.com/2304-6732/9/10/695.

[208] Q. Nguyen, L. Bramerie, P. Besnard, A. Shen, A. Garreau, C. Kazmierski, G. Duan, J. Simon, 24 Channels colorless WDM-PON with l-band 10Gb/s downstream and C-band 2.5Gb/s upstream using multiple- wavelengths seeding sources based on mode-locked lasers, in: Optical Fiber Communication Conference, Vol. 2010, OSA, Washington, D.C, 2010, p. OThG6, http://dx.doi.org/10.1364/OFC.2010.OThG6, https://www.osapublishing.org/abstract.cfm?URI=OFC-2010-OThG6.

[209] Quoc Thai Nguyen, P. Besnard, L. Bramerie, A. Shen, C. Kazmierski, P. Chanlou, Guang-Hua Duan, J.-C. Simon, Bidirectional 2.5-Gb/s WDM-PON using FP-LDs wavelength-locked by a multiple-wavelength seeding source based on a mode-locked lasers, IEEE Photonics Technol. Lett. 22 (11) (2010) 733–735, http://dx.doi.org/10.1109/LPT.2010.2044569, http://ieeexplore.ieee.org/document/5430923.

[210] A. Martinez, C. Calò, R. Rosales, R.T. Watts, K. Merghem, A. Accard, F. Lelarge, L.P. Barry, A. Ramdane, Quantum dot mode locked lasers for coherent frequency comb generation, in: M. Razeghi, E. Tournié, G.J. Brown (Eds.), Quantum Sensing and Nanophotonic Devices XI, Vol. 8993, 2014, p. 89930A, http://dx.doi.org/10.1117/12.2036278, http://proceedings.spiedigitallibrary.org/proceeding.aspx?doi=10.1117/12.2036278.

[211] T.J. Pinkert, E.J. Salumbides, M.S. Tahvili, W. Ubachs, E.A.J.M. Bente, K.S.E. Eikema, Frequency comb generation by CW laser injection into a quantum-dot mode-locked laser, Opt. Express 20 (19) (2012) 21357–21381, http://dx.doi.org/10.1364/OE.20.021357.

[212] G. Kurczveil, M.A. Seyedi, D. Liang, M. Fiorentino, R.G. Beausoleil, Error-free operation in a hybrid-silicon quantum dot comb laser, IEEE Photonics Technol. Lett. 30 (1) (2018) 71–74, http://dx.doi.org/10.1109/LPT.2017.2775145, http://ieeexplore.ieee.org/document/8114222.

[213] J.N. Kemal, P. Marin-Palomo, V. Panapakkam, P. Trocha, S. Wolf, K. Merghem, F. Lelarge, A. Ramdane, S. Randel, W. Freude, C. Koos, Coherent wdm transmission using quantum-dash mode-locked laser diodes as multi-wavelength source and local oscillator, Opt. Express 27 (22) (2019) 31164–31175, http://dx.doi.org/10.1364/OE.27.031164, http://www.opticsexpress.org/abstract.cfm?URI=oe-27-22-31164.

[214] Dejan Arsenijević, Dieter Bimberg, Quantum-dot mode-locked lasers: sources for tunable optical and electrical pulse combs, in: G. Eisenstein, D. Bimberg (Eds.), Green Photonics and Electronics, Springer International Publishing, Cham, 2017.

[215] M.M.H. Adib, C. Füllner, J.N. Kemal, P. Marin-Palomo, A. Ramdane, C. Koos, W. Freude, S. Randel, Colorless coherent tdm-pon based on a frequency-comb laser, J. Lightwave Technol. 40 (13) (2022) 4287–4299, http://dx.doi.org/10.1109/JLT.2022.3164168.

[216] H. Sun, M. Khalil, D.V. Plant, L.R. Chen, J. Liu, Z. Lu, P.J. Poole, J. Weber, Reconfigurable microwave photonic filter enabled by a quantum dash mode-locked laser, in: 2021 IEEE Photonics Conference (IPC), IEEE, 2021, pp. 1–2, http://dx.doi.org/10.1109/IPC48725.2021.9592840.

[217] M. Kuramoto, Two-photon fluorescence bioimaging with an all-semiconductor laser picosecond pulse source, Opt. Lett. 32 (18) (2007) 2726, http://dx.doi.org/10.1364/OL.32.002726.

[218] H. Yokoyama, A. Sato, H.C. Guo, K. Sato, M. Mure, H. Tsubokawa, Nonlinear-microscopy optical-pulse sources based on mode-locked semiconductor lasers, Opt. Express 16 (22) (2008) 17752, http://dx.doi.org/10.1364/OE.16.017752, https://www.osapublishing.org/oe/abstract.cfm?uri=oe-16-22-17752.

[219] Z. Li, C.P. Allford, S. Shutts, A.F. Forrest, R. Alharbi, A.B. Krysa, M.A. Cataluna, P.M. Smowton, Monolithic InP quantum dot mode-locked lasers emitting at 730 nm, IEEE Photonics Technol. Lett. 32 (17) (2020) 1073–1076, http://dx.doi.org/10.1109/LPT.2020.3012568, https://ieeexplore.ieee.org/document/9151243.

[220] E.U. Rafailov, E.A. Avrutin, Q-switched and mode-locked lasers for biophotonic applications, healthcare technologies, Inst. Eng. Technol. (2018) http://dx.doi.org/10.1049/PBHE007E_ch3, https://digital-library.theiet.org/content/books/10.1049/pbhe007e_ch3.

[221] K. Merghem, C. Calo, R. Rosales, X. Lafosse, G. Aubin, A. Martinez, F. Lelarge, A. Ramdane, Stability of optical frequency comb generated with InAs/InP quantum-dash-based passive mode-locked lasers, IEEE J. Quantum Electron. 50 (4) (2014) 275–280, http://dx.doi.org/10.1109/JQE.2014.2308323, http://ieeexplore.ieee.org/document/6750711.

[222] S. Liu, X. Wu, J.C. Norman, D. Jung, M. Dumont, C. Shang, Y. Wan, M.J. Kennedy, B. Dong, D. Auth, S. Breuer, F. Grillot, W.W. Chow, A.C. Gossard, J.E. Bowers, High-performance mode-locked lasers on silicon, in: M. Osiński, Y. Arakawa, B. Witzigmann (Eds.), Physics and Simulation of Optoelectronic Devices XXVIII, no. March 2020, SPIE, 2020, p. 55, http://dx.doi.org/10.1117/12.2552224, https://www.spiedigitallibrary.org/conference-proceedings-of-spie/11274/2552224/High-performance-mode-locked-lasers-on-silicon/10.1117/12.2552224.full.

[223] T. Sadeev, D. Arsenijević, D. Franke, J. Kreissl, H. Künzel, D. Bimberg, 1.55- μM mode-locked quantum-dot lasers with 300 mhz frequency tuning range, Appl. Phys. Lett. 106 (3) http://dx.doi.org/10.1063/1.4906451.

[224] T. Habruseva, D. Arsenijević, M. Kleinert, D. Bimberg, G. Huyet, S.P. Hegarty, Optimum phase noise reduction and repetition rate tuning in quantum-dot mode-locked lasers, Appl. Phys. Lett. 104 (2) (2014) 021112, http://dx.doi.org/10.1063/1.4861604, http://aip.scitation.org/doi/10.1063/1.4861604.

[225] T. Habruseva, S. O'Donoghue, N. Rebrova, D.A. Reid, L.P. Barry, D. Rachinskii, G. Huyet, S.P. Hegarty, S. Member, S.O. Donoghue, N. Rebrova, D.A. Reid, L.P. Barry, D. Rachinskii, G. Huyet, S.P. Hegarty, Quantum-dot mode-locked lasers with dual-mode optical injection, IEEE Photonics Technol. Lett. 22 (6) (2010) 359–361, http://dx.doi.org/10.1109/LPT.2009.2039347, http://ieeexplore.ieee.org/document/5378530.

[226] G. Fiol, M. Kleinert, D. Arsenijević, D. Bimberg, 1.3 μM range 40 GHz quantum-dot mode-locked laser under external continuous wave light injection or optical feedback, Semiconductor Sci. Technol. 26 (1) (2010) 014006, http://dx.doi.org/10.1088/0268-1242/26/1/014006.

[227] R.M. Arkhipov, T. Habruseva, A. Pimenov, M. Radziunas, S.P. Hegarty, G. Huyet, A.G. Vladimirov, Semiconductor mode-locked lasers with coherent dual-mode optical injection: simulations, analysis, and experiment, J. Opt. Soc. Am. B 33 (3) (2016) 351–359, http://dx.doi.org/10.1364/JOSAB.33.000351, http://josab.osa.org/abstract.cfm?URI=josab-33-3-351.

[228] H. Asghar, E. Sooudi, J.G. McInerney, Stabilization of self-mode-locked qdash lasers subject to simultaneous continuous-wave optical injection and optical feedback, Applied Optics 57 (22) (2018) E45, http://dx.doi.org/10.1364/AO.57.000E45, https://www.osapublishing.org/abstract.cfm?URI=ao-57-22-E45.

[229] D. Arsenijević, M. Kleinert, D. Bimberg, Phase noise and jitter reduction by optical feedback on passively mode-locked quantum-dot lasers, Appl. Phys. Lett. 103 (23) (2013) 231101, http://dx.doi.org/10.1063/1.4837716, http://aip.scitation.org/doi/10.1063/1.4837716.

[230] M.A. Shemis, A.M. Ragheb, M.T.A. Khan, H.A. Fathallah, S. Alshebeili, K.K. Qureshi, M.Z.M. Khan, L-band quantum-dash self-injection locked multiwavelength laser source for future wdm access networks, IEEE Photon. J. 9 (5) http://dx.doi.org/10.1109/JPHOT.2017.2733162.

[231] Z.G. Lu, J.R. Liu, P.J. Poole, C.Y. Song, S.D. Chang, Ultra-narrow linewidth quantum dot coherent comb lasers with self-injection feedback locking, Opt. Express 26 (9) (2018) 11909–11914, http://dx.doi.org/10.1364/OE.26.011909, http://www.opticsexpress.org/abstract.cfm?URI=oe-26-9-11909.

[232] S. Stutz, D. Auth, C. Weber, L. Drzewietzki, O. Nikiforov, R. Rosales, T. Walther, L.F. Lester, S. Breuer, Dynamic intermode beat frequency control of an optical frequency comb single section quantum dot laser by dual-cavity optical self-injection, IEEE Photonics J. 11 (5) (2019) 1–8, http://dx.doi.org/10.1109/JPHOT.2019.2932452, https://ieeexplore.ieee.org/document/8784221.

[233] B. Dong, X.C. d. Labriolle, S. Liu, M. Dumont, H. Huang, J. Duan, J.C. Norman, J.E. Bowers, F. Grillot, 1.3-μM passively mode-locked quantum dot lasers epitaxially grown on silicon: gain properties and optical feedback stabilization, J. Phys. Photonics 2 (4) (2020) 045006, http://dx.doi.org/10.1088/2515-7647/aba5a6, https://iopscience.iop.org/article/10.1088/2515-7647/aba5a6.

[234] H. Asghar, E. Sooudi, M. Aslam Baig, J.G. McInerney, Recent advances in stabilization of mode-locked quantum dash lasers at 1.55 μm by dual-loop optical feedback, Opt. Laser Technol. 122 (2020) 105884, http://dx.doi.org/10.1016/j.optlastec.2019.105884, https://www.sciencedirect.com/science/article/pii/S0030399219307960.

[235] Z.G. Lu, J.R. Liu, C.Y. Song, J. Weber, Y. Mao, S.D. Chang, H.P. Ding, P.J. Poole, P.J. Barrios, D. Poitras, S. Janz, M. O'Sullivan, High performance inas/inp quantum dot 34462-ghz c-band coherent comb laser module, Opt. Express 26 (2) (2018) 2160, http://dx.doi.org/10.1364/OE.26.002160, https://opg.optica.org/abstract.cfm?URI=oe-26-2-2160.

[236] J. Robertson, T. Ackemann, L.F. Lester, A. Hurtado, Externally-triggered activation and inhibition of optical pulsating regimes in quantum-dot mode-locked lasers, Sci. Rep. 8 (1) (2018) 12515, http://dx.doi.org/10.1038/s41598-018-30758-2.

[237] J.C. Norman, D. Jung, Y. Wan, J.E. Bowers, Perspective: the future of quantum dot photonic integrated circuits, APL Photonics 3 (3) http://dx.doi.org/10.1063/1.5021345.

[238] J.C. Norman, D. Jung, Z. Zhang, Y. Wan, S. Liu, C. Shang, R.W. Herrick, W.W. Chow, A.C. Gossard, J.E. Bowers, A review of high-performance quantum dot lasers on silicon, IEEE J. Quantum Electron. 55 (2) (2019) 1–11, http://dx.doi.org/10.1109/JQE.2019.2901508, https://ieeexplore.ieee.org/document/8653374.

[239] V. Cao, J.-S. Park, M. Tang, T. Zhou, A. Seeds, S. Chen, H. Liu, Recent progress of quantum dot lasers monolithically integrated on Si platform, Front. Phys. 10 (February) http://dx.doi.org/10.3389/fphy.2022.839953/full, https://www.frontiersin.org/articles/10.3389/fphy.2022.839953.

[240] S. Liu, D. Jung, J.C. Norman, M.J. Kennedy, A.C. Gossard, J.E. Bowers, 490 Fs pulse generation from passively mode-locked single section quantum dot laser directly grown on on-axis GaP/Si, Electron. Lett. 54 (7) (2018) 432–433, http://dx.doi.org/10.1049/el.2017.4639, https://digital-library.theiet.org/content/journals/10.1049/el.2017.4639.

[241] K. Van Gasse, S. Uvin, V. Moskalenko, S. Latkowski, G. Roelkens, E. Bente, B. Kuyken, Recent advances in the photonic integration of mode-locked laser diodes, IEEE Photonics Technol. Lett. 31 (23) (2019) 1870–1873, http://dx.doi.org/10.1109/LPT.2019.2945973, https://ieeexplore.ieee.org/document/8861364.

[242] Z.-H. Wang, W.-Q. Wei, Q. Feng, T. Wang, J.-J. Zhang, InAs/GaAs quantum dot single-section mode-locked lasers on Si (001) with optical self-injection feedback, Opt. Express 29 (2) (2021) 674, http://dx.doi.org/10.1364/OE.411551, https://opg.optica.org/abstract.cfm?URI=oe-29-2-674.

[243] J. Hauck, A. Zazzi, A. Garreau, F. Lelarge, A. Moscoso-Mártir, F. Merget, J. Witzens, Semiconductor laser mode locking stabilization with optical feedback from a silicon pic, J. Lightwave Technol. 37 (14) (2019) 3483–3494, http://dx.doi.org/10.1109/JLT.2019.2917321.

[244] B. Dong, H. Huang, J. Duan, G. Kurczveil, D. Liang, R.G. Beausoleil, F. Grillot, Frequency comb dynamics of a 13 μm hybrid-silicon quantum dot semiconductor laser with optical injection, Opt. Lett. 44 (23) (2019) 5755, http://dx.doi.org/10.1364/OL.44.005755, https://www.osapublishing.org/abstract.cfm?URI=ol-44-23-5755.

[245] J. Liu, Z. Lu, S. Raymond, P.J. Poole, P.J. Barrios, D. Poitras, Dual-wavelength 925 ghz self-mode-locked inp-based quantum dot laser, Opt. Lett. 33 (15) (2008) 1702, http://dx.doi.org/10.1364/OL.33.001702, https://www.osapublishing.org/abstract.cfm?URI=ol-33-15-1702.

[246] Z.G. Lu, J.R. Liu, P.J. Poole, P.J. Barrios, D. Poitras, S. Raymond, G. Pakulski, A passive mode-locked inas/inp quantum dot laser with pulse duration of less than 300 fs, in: K.G. Eyink, F. Szmulowicz, D.L. Huffaker (Eds.), Quantum Dots, Particles, and Nanoclusters VI, Vol. 7224, 2009, p. 722413, http://dx.doi.org/10.1117/12.809525, http://proceedings.spiedigitallibrary.org/proceeding.aspx?doi=10.1117/12.809525.

[247] M. Ruiz, N. Michel, M. Calligaro, Y. Robert, M. Krakowski, D.I. Nikitichev, M.A. Cataluna, D. Livshits, E.U. Rafailov, New tapered quantum-dot mode-locked laser diode with high peak power, low divergence and good beam quality, in: Conference Digest - IEEE International Semiconductor Laser Conference, 2010, pp. 170–171, http://dx.doi.org/10.1109/ISLC.2010.5642658.

[248] D.I. Nikitichev, Y. Ding, M. Ruiz, M. Calligaro, N. Michel, M. Krakowski, I. Krestnikov, D. Livshits, M.A. Cataluna, E.U. Rafailov, High-power passively mode-locked tapered InAs/GaAs quantum-dot lasers, Appl. Phys. B 103 (3) (2011) 609–613, http://dx.doi.org/10.1007/s00340-010-4290-5.

[249] F. Gao, S. Luo, H.-M. Ji, S.-T. Liu, D. Lu, C. Ji, T. Yang, Single-section mode-locked 1.55-μm InAs/InP quantum dot lasers grown by MOVPE, Opt. Commun. 370 (2016) 18–21, http://dx.doi.org/10.1016/j.optcom.2016.02.061, https://linkinghub.elsevier.com/retrieve/pii/S0030401816301535.

[250] M. Gaafar, D.A. Nakdali, C. Möller, K.A. Fedorova, M. Wichmann, M.K. Shakfa, F. Zhang, A. Rahimi-Iman, E.U. Rafailov, M. Koch, Self-mode-locked quantum-dot vertical-external-cavity surface-emitting laser, Opt. Lett. 39 (15) (2014) 4623, http://dx.doi.org/10.1364/OL.39.004623, https://www.osapublishing.org/abstract.cfm?URI=ol-39-15-4623.

[251] M. Laemmlin, G. Fiol, C. Meuer, M. Kuntz, F. Hopfer, A. Kovsh, N. Ledentsov, D. Bimberg, Distortion-free optical amplification of 20–80 GHz modelocked laser pulses at 1.3 [micro sign]m using quantum dots, Electron. Lett. 42 (12) (2006) 697, http://dx.doi.org/10.1049/el:20061256, https://digital-library.theiet.org/content/journals/10.1049/el_20061256.

[252] P. Adamiec, B. Bonilla, A. Consoli, J.M.G. Tijero, S. Aguilera, I. Esquivias, High-peak-power pulse generation from a monolithic master oscillator power amplifier at 15 μM, Appl. Opt. 51 (30) (2012) 7160, http://dx.doi.org/10.1364/AO.51.007160, https://www.osapublishing.org/abstract.cfm?URI=ao-51-30-7160.

[253] A. Alhazime, Y. Ding, D. Nikitichev, K. Fedorova, I. Krestnikov, M. Krakowski, E. Rafailov, Broadly tunable quantum-dot based ultra-short pulse laser system with different diffraction grating orders, Electron. Lett. 49 (5) (2013) 364–366, http://dx.doi.org/10.1049/el.2012.3761, https://onlinelibrary.wiley.com/doi/10.1049/el.2012.3761.